The Molecular Role of the *Saccharomyces cerevisiae* DNA Helicase Srs2 during Meiosis

Ta-Chung Chou

A thesis submitted for the degree of:

Doctor of Philosophy

December 2014

University of Sheffield

Department of Molecular Biology and Biotechnology

"Absence of evidence is not necessarily evidence of absence."

- Carl Sagan

Abstract

SRS2 gene in *S.cerevisiae* encodes a DNA helicase, which is an orthologue of bacterial UvrD helicase family. Srs2 plays important roles during meiosis as in the *srs2-101* mutant where helicase activity is defective has shown reduction in sporulation efficiency, spore viability and more rapid Spo11-induced DNA-double strand break (DSB) repair. To ask if the rapid DSB repair in *srs2-101* cells is due to the lack of anti-Rad51 recombinase activity that results in faster DSB turnover via sister chromatids as repair templates, we have used *hed1Δ*, *dmc1Δ* and *mek1Δ* which are proposed to be related to inter-sister recombination and a recombination assay system which differentiate recombination intermediates to specify repair templates. In addition, cytological approaches including Rad51 immunofluorescent staining and visualisation of Zip1, tubulin and spindle-pole body to effectively monitor the meiotic progression in *srs2-101* cells. Our results show that *srs2-101* does not necessarily increase inter-sister recombination even though it could potentially increase Rad51 level. In addition, a fraction of *srs2-101* cells seem to have delayed formation/dissolution of synaptonemal complex, and these cells show persistent Rad51 foci during meiosis. By monitoring spindle-pole body and tubulin during meiosis, we found a big population of *srs2-101* cells stalled at meiosis I with two spindle-pole bodies. Our studies shed light on various functions of Srs2 and emphasise on the balance of recombinases during meiosis.

Acknowledgements

Many thanks to all the people I met in Sheffield, including my colleagues Emad, who supported me in cytological work and writing my thesis; Emily, a very enthusiastic young scientist who always triggers me to think more about doing science; Laura, who is always there to help sort out ordering and all the big and small things in the lab; Tzu-Ling, who helped me a lot in solving experimental problems; and of course all the previous lab members including Adam, Slava, Thibaut and Yinka, all these people have helped me develop experimental skills during the last few years. In particular, I would like to thank my supervisor Alastair, as a very nice BOSS and a friend. I'll never forget all the memories with you in the lab, office or even in your house! My thesis would not be completed without all these peoples' unconditional support.

Further thanks to my lovely family especially my parents who have been financially supporting me since I started my PhD. I wouldn't be able to survive without their enormous effort and support. Also thanks to all my flatmates Bai-Hua, Bernard, Chi-Wei, Everth, Jia-Rui, Meng-Di, Ming-Lun, Renardo, Tang, Qi-Hong and Yoshihiro and my friends I met in the department Alison, Arthur, Asma, Eileen, Illiana, Jamey, Lina, Michael, Nico, Shler, Taib and Simon, whose patience and beloved characteristics always comfort and cheer me up. I won't be able to overcome all the difficulties I encountered without you during my harsh times. Thank you all!

Abbreviations

AE	Axial element
CE	Central element
CTAB	Hexadecyltrimethylammonium bromide
DAPI	4',6-diamidino-2-phenylindole
dAG	Diploid Alastair Goldman
dHJ	Double Holliday Junction
dH_2O	Deionised water
DNA	Deoxyribonucleic acid
dNTP	Deoxyribonucleotide triphosphate
DSB	Double strand break
DSBR	Double strand break repair
dsDNA	Double-stranded DNA
EDTA	Ethylenediaminetetraacetic acid
hAG	Haploid Alastair Goldman
HR	Homologous recombination
IR	Ionised radiation
IH	Interhomologue
IS	Intersister
JM	Joint molecule
LE	Lateral element
MI/MII	Meiosis I/Meiosis II
MRX	Mre11, Rad50 and Xrs2 complex

NHEJ	Non-homologous end joining
pAG	Plasmid Alastair Goldman
PCR	Polymerase chain reaction
SC	Synaptonemal complex
SDSA	Synthesis dependent strand annealing
SSA	Single strand annealing
ssDNA	Single-stranded DNA
UV	Ultraviolet light

Table of Contents

Chapter1

General Introduction

1.1 General Introduction of *Saccharomyces cerevisiae*

Saccharomyces cerevisiae (hereafter *S. cerevisiae*), also called budding yeast, has long been considered as a model organism for the study of eukaryotic molecular genetics due to many reasons. It harbours relatively smaller genome in comparison to other eukaryotic organisms (ranging from 12 to 14Mb), and the genome has been fully sequenced, which makes manipulation of DNA recombination techniques much easier than other eukaryotes. The yeast genome is just over 12 million base pairs in length and contains about 6000 genes. Surprisingly, about 20 per cent of human disease genes have counterparts in yeast. The *S. cerevisiae* genome was sequenced as a collaborative effort which involved a consortium of more than 600 scientists from over 100 laboratories. At the time this was considered to be the largest decentralised experiment in modern molecular biology. What follows are links to the original papers published as a result of this international effort to sequence the first eukaryotic genome. Despite it has a comparatively smaller genome, it retains conservation of metabolic, developmental and genetic pathways that mimic, for instance, some human disabilities, disorders or diseases which cannot be experimented due to ethical and technical issues.

S. cerevisiae can exist as either haploids or diploids. Diploid cells are larger than haploids because of harbouring twice as much genetic information as haploids, in which the diameter of a diploid cell is roughly 1.3 times bigger than a haploid cell. Also, diploid cells are more ovoid and round shaped than haploid cells, although mutation of genes may cause changes in morphology as well. *S. cerevisiae* cells reproduce asexually by forming buds. A cell which gives rise to a bud is called a mother cell and the bud is called a daughter cell. The budding pattern of diploid cells and haploid cells is also different. Haploid cells bud in an axial pattern whereas diploid cells bud in a polar pattern. Therefore *S. cerevisiae* earns its name of budding yeast because of its special way of reproduction.

1.2 General Overview of Meiosis

Meiosis is a specialised cell division process that takes place in most sexually reproducing organisms. Sexual organisms must halve their chromosome numbers during the process of sexual reproduction to produce haploid gametes. The goal of meiosis is achieved by undergoing a process mediated by a huge number of genes and proteins, in which a single round of DNA replication is followed by two successive rounds of chromosome segregation. Meiosis is not only essential for ensuring equal number of chromosomes segregated into each offspring, but also important for creating genetic diversity. In general, meiotic division can be divided into two parts, meiosis I (MI) and meiosis II (MII). The first division in meiosis, MI, also called reductional division, is the separation between homologous chromosomes that consist of two strands of identical sister chromatids. The second division, MII, is the stage where sister chromatids equationally segregate to form four haploid gametes that are essential for sexual reproduction. During mitosis, on the other hand, sister chromatids are intimately connected along their

lengths at centromere/kinetochore region to ensure their proper segregation. Once spindle fibres are attached to the kinetochore and the pull-force is established, sister chromatids are well oriented, and sister chromatid connections are subsequently released. This movement of sister chromatids is also in an equational fashion since genetic material is not halved like in meiosis (Figure 1.1). During the first division of meiosis, if a cell cannot accurately segregate homologues (meiosis I non-disjunction), gametes with extra or missing copies of chromosomes result in aneuploidy. In unicellular organisms such as *S. cerevisiae,* aneuploidy progeny is rarely seen, in which it only occurs 1 in 10,000 meiosis (Sears et al., 1992). However, any lack of a particular chromosome in haploid cells leads to inviability due to all essential genes are spread to each of the 16 chromosomes. Frequency of MI non-disjunction in multicellular organisms, on the other hand, varies between different species. For example, in fruit fly *Drosophila melongaster*, aneuploidy occurs at frequencies between 1 in 1,700 and 1 in 6,000 meioses (Koehler et al., 1996). The frequencies of aneuploidy in mouse is much higher, raging from 1~2% of fertilisation (Hassold and Hunt, 2001). In humans, despite the fact that the frequency of aneuploidy accounts for only 0.3% of live birth, up to 30% of fertilisations are estimated to have chromosomal abnormality, majority of which arises from chromosome missegregation during gamete formation. There are several common human disorders, which are cause by aneuploidy, including trisomy of chromosome 21 (Down Syndrome), trisomy of chromosome 13 (Patau's Syndrome), and a number of chromosome disorders (XXX syndrome in females XXY Klinefelter's Syndrome) and XYY syndrome in males. These examples provide strong evidence that genetic disorders are tightly correlated to aneuploidy.
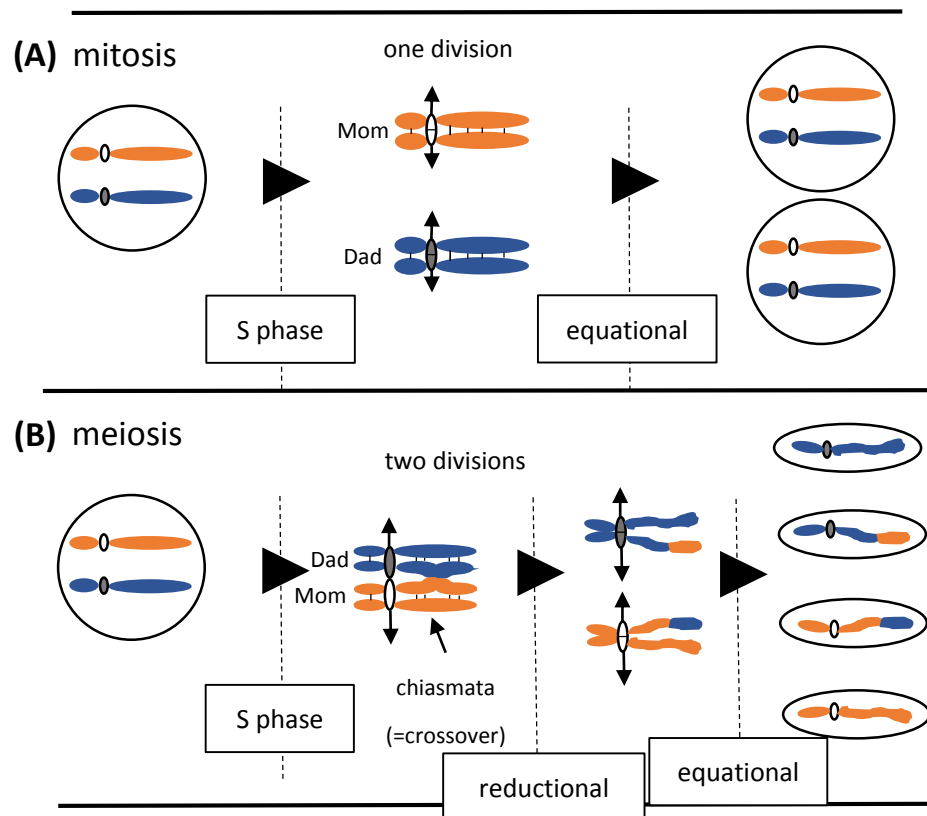
Figure 1.1. Comparison between mitotic and meiotic cell divisions. (A and B) Chromosomes are replicated during S phase before entering both mitosis and meiosis, forming identical copies of sister chromatids which are inter-connected along their whole length by sister chromatid cohesion proteins. (A) During mitosis, kinetochores of each sister chromatid are attached to the spindles and pulled from opposite poles after DNA replication. Then loss of sister cohesion allows sister chromatids to split equally, in which the number of chromosome remains unchanged (equational division). (B) Unlike mitosis where only one segregation occurs, two divisions take place during meiosis. During the first meiotic prophase, two homologues align and recombine, forming bridges which connect the homologous chromosomes (chiasmata). Kinetochores of each homologue are subsequently attached to spindle fibres and contracted to opposite poles. However premature homologue disjunction is prevented by interhomologue connection. Loss of sister chromatid cohesion in the arm region leads to release of interhomologue connection provided from chiasmata, and maintenance of sister chromatid cohesion at centromere region ensures that segregation takes place in a reductional manner. When cells enter the second meiotic division, sister chromatids are segregated by having each kinetochore attached to spindles and pulled to the opposite poles. Sister chromatids are then segregate equationally by losing sister chromatid cohesion in the centromeric region.

Before entering meiosis, cells undergo a series of steps that lead to meiosis:

G1 phase (gap1): Proteins for preparation of genetic material replication are synthesised during G1. Cells expand in size at this stage as well.

S phase (synthesis): Genetic material is replicated after cell cycle exiting the G1 phase. The major goal of S phase is DNA replication, in which each chromosome replicates and becomes a complex consists of two identical sister chromatids. In *S. cerevisiae*, the entry of meiosis is triggered by nitrogen limitation, which leads to sporulation (yeast gametogenesis). Despite the fact that meiotic progression is tightly linked and regulated by the mitotic cell cycle, it has fundamental difference from the mitotic counterpart. Firstly, it is not a "cycle" as it is a one-way process where diploids carry two copies of chromosomes are halved into one in haploids.

G2 phase: This phase is not seen in meiosis as in mitosis, where in mitosis the cells' chromatin condenses into chromosomes.

Meiosis can be divided into several stages in detail: Meiosis I (prophase I, metaphase I, anaphase I and telophase I) and Meiosis II (prophase II, metaphase II, anaphase II and telophase II). Prophase I, where a series of genetic events take place, such as homologue pairing, homologous chromosome synapsis and homologous recombination, is tightly regulated. The first stage of meiotic prophase is leptotene. In leptotene, each individual chromosome consisting of two identical sister chromatids starts to pack and condense into thin threads within nucleus, as what it means from the Greek word "leptonema". During the transition period leptotene to zygotene, chromosomes continue to condense and chromatin spatially arranged to form a linear array of loops, comprising the chromosome axis (Zickler and Kleckner, 1999). This axis element (AE) starts to form at leptotene, along with the formation of the lateral element (LE) at zygotene (Figure1.2).

5

The following stage zygotene (known as zygonema, meaning "paired threads" in Greek), where chromosomes are roughly lined up and paired. From early zygotene to the next stage pachytene (known as pachynema, meaning "thick threads"), chromosomes form a special arrangement called bouquet because the way of telomere clustered to one end of the nuclear periphery. Chromosomes continue condensing and becoming fully synapsed by the end of pachytene. At this stage, the meiosis specific proteinaceous structure, the synaptonemal complex (SC) is formed between each synapsed homologous chromosome. This proteinaceous structure is highly essential for establishing proper chromosome alignment and pairing and is dependent on the initiation of recombination in yeast. The requirement of DSB catalytic activity of Spo11 however varies between different species. In *S. cerevisiae*, SC fails to form successfully in the absence of Spo11 DSB catalytic activity (*spo11-Y135F*), supporting the idea that the SC formation requires recombination to occur (Neale et al., 2002). Other organisms such as *C.elegans* and drosophila, on the other hand, the maturation of SC is unaffected when Spo11 is mutated (Dernburg et al., 1998; McKim, 1998), suggesting that efficient and proper homologue pairing can therefore be carried out without SC.

At the subsequent stage of meiosis, diplotene, the SC breaks down which leads to chromosome separation. Importantly, at this stage, structures known as chiasmata become cytologiaclly visible. Chiasmata are cytological manifestation of reciprocal genetics exchange (crossover recombination). The fact is, crossover takes place throughout the leptotene-pachytene stages but chiasmata can only be seen during diplotene stage, in which chiasmata mark the sites where non-sister chromatid exchange between homologous chromosomes. The final stage of prophase I is diakinesis, where homologue kinetochores are attached to spindle
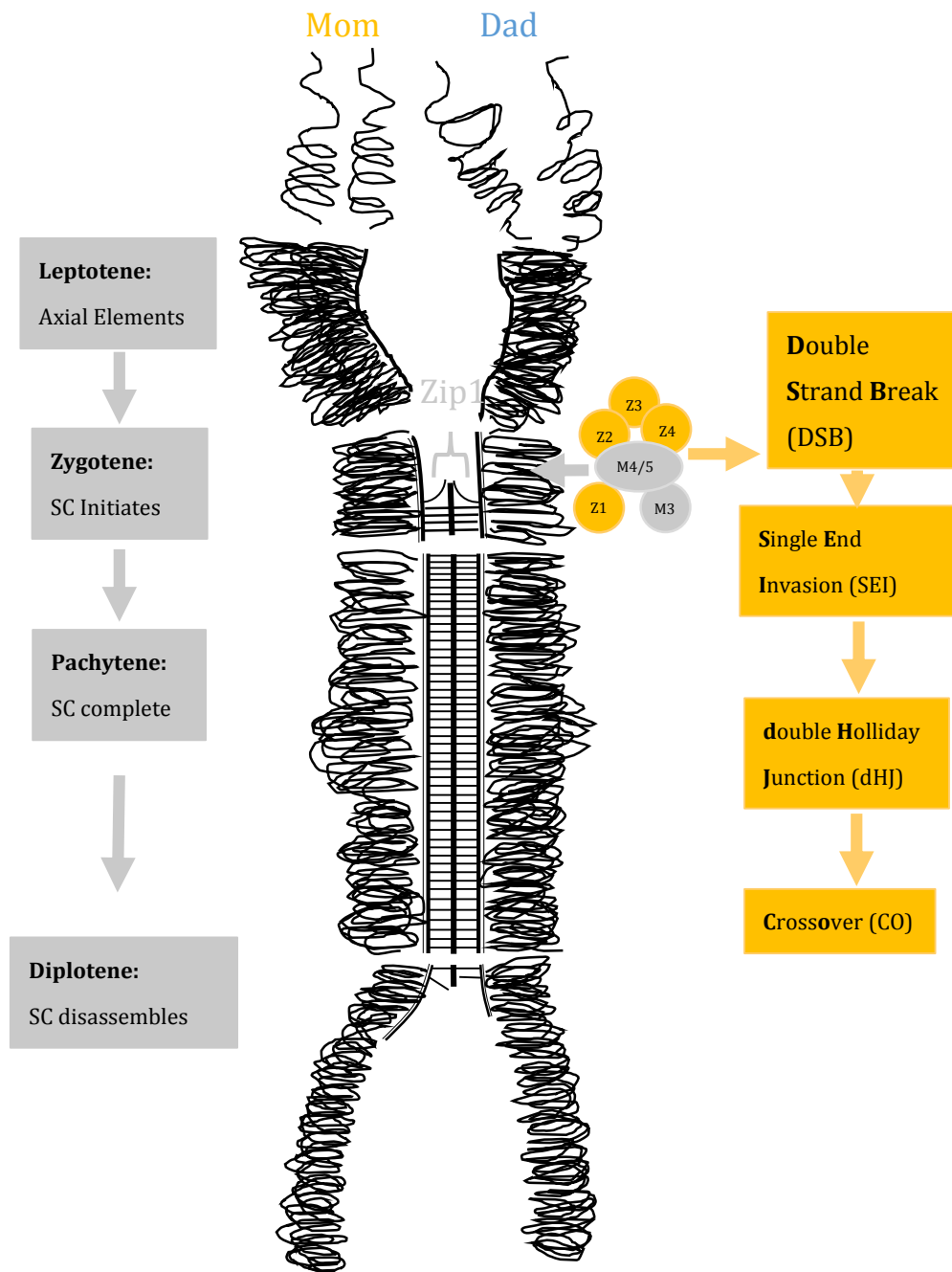
Figure 1.2. Stages of assembly of synaptonemal complex (SC) and DNA recombination events. On the left side, the cytological stages of meiotic prophase I are shown in green boxes. On the right side, homologous recombination events are depicted in orange boxes. ZMM proteins including Zip1 (Z1), Zip2 (Z2), Zip3 (Z3), Zip4 (Z4), Msh4/5 (M4/5), Mer3 (M3) are shown to refer to their functions for SC formation and recombination. Zip1 is specifically indicated as a transverse element of SC's central element.

fibres pulling from opposite poles. At this stage each bivalent are aligned properly on the metaphase plate. Chromosome disjunction is then achieved by two distinct events. First, homologous chromosomes are separated by spindle contraction from the opposite poles, and secondly, sister chromatid cohesion is lost in the chromosome arms. Subsequently, at the second meiotic division, kinetochores of sister chromatids are attached to spindle fibres and pulled from the opposite poles of the cell. Contraction of meiosis II spindle and loss of sister chromatid cohesion at the centromeric regions of sister chromatids help sister chromatids to segregate to opposite poles.

1.3 The Synaptonemal Complex (SC)

The synaptonemal complex (SC) is a meiosis-specific tripartite proteinaceous structure, which forms between homologous chromosomes in almost all species (reviewed by Moses, 1968; Zickler & Kleckner, 1999). The formation of SC begins with the development of proteinaceous structure of each chromosome, called the axial element (AE)(Zickler and Kleckner, 1999). AEs are formed and linearised by the integration of the base of each chromatin loop, and therefore depend on sister chromatid cohesion, which occur along with meiotic double-strand break formation (Padmore et al., 1991). In the following stage of meiosis, zygotene, a central element of the two homologous AEs is formed that associates the homologues to join together. These AEs are then referred to as lateral elements (LEs). The central space between the two parallel LEs consists of the central element (CE). The ladder-like CE consists of two components: two longitudinal components that are parallel to the LEs, and a number of equally spaced transverse CE components that connects the two longitudinal components. Tomographic analysis shows that the transverse filament (TF) stretches

continuous filaments that run from one LE, through the CE, to the other side of the LE. However there are some TFs don't pass through the CE, instead, they penetrate halfway and terminate at CE (Schmekel and Daneholt, 1995). Despite some variations in the structure of SCs were observed (e.g. the CE resembles a ladder in many insects but does not form distinct shape in mammals), most of the structures are highly conserved from simple unicellular to complex multicellular organisms. Furthermore, even the dimensions of the SC are conserved between most species. The distance between the two LEs approximately spans 100nm in nearly all SCs (Schmekel and Daneholt, 1995). The assembly of the SC has yet to be examined due to its size, complexity and variability in living cells until using electron microscopy (EM) and sectioning techniques. The SC is collapsed and disordered in chromosome spreads, which makes a reliable three-dimensional image of the SC a difficult task to handle with. Also, to observe the various components of the SC is yet another challenge, because various structures may appear in a superposition fashion and only a certain segment of a component is observed in a given time (Moses, 1968). In this regard, tomography of EM can reconstruct symmetric and asymmetric structures of the SC, which provides a reliable three-dimensional model of the SC (Figure 1.3).
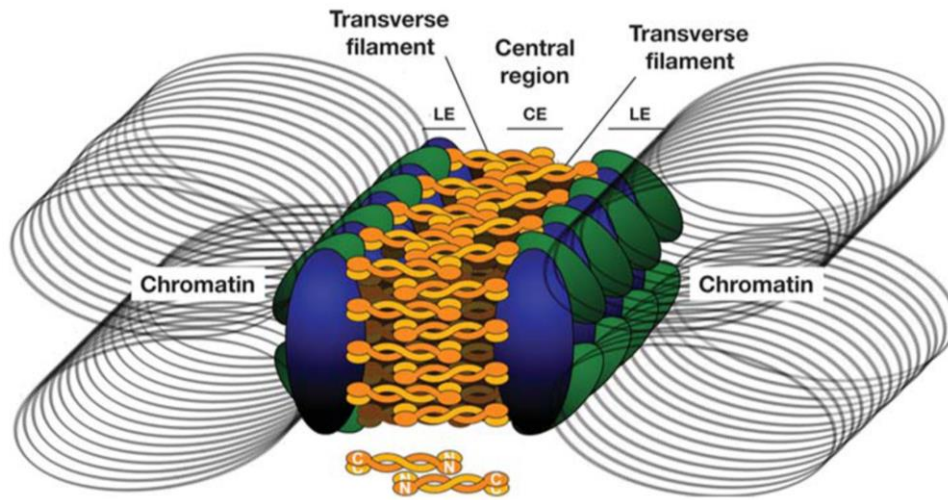
Figure 1.3. The three-dimensional model for a cross section of a segment of the SC with lateral elements (LE),transverse filaments (TF), central element(CE), and central region. The bottom of this figure shows the arrangement of transverse filament proteins, which consists of Zip1 and SCP1. On the other hand, the arrangement of cohesins/condensins (blue ovals) and other LE proteins (green ovals) are also shown (Page and Hawley, 2004).

Numerous protein components of the SC have been identified in yeast and mammalian cells; SCP1 of rat and its homologue in hamster (Schmekel and Daneholt, 1995) and Zip1 in *S. cerevisiae* (Sym et al., 1993). In *S. cerevisiae*, Zip1was demonstrated by immunoeletron microscopy that is localised to the central region of fully synapsed chromosomes but not the AEs, which are the precursors of LEs (Sym et al., 1993). Two additional mammalian proteins SC48 and SC65 along with SCP1 localised to the CE of SC (Chen et al., 1992; Smith and Benavente, 1992). Immuno-EM technique further revealed that the C-terminal region of Zip1/SCP1 associated with LEs, and the N-terminal region of Zip1/SCP1 is in CE and is interconnected with filaments from the other side of LE (Schmekel and Daneholt, 1995). In *zip1* mutant yeast cells, LEs form normally, but the CE does not form. Therefore in conclusion, Zip1/SCP1 is a central component of the SC (Mary Sym and G. S. Roeder, 1995).

Importantly, budding yeast Zip2 and Zip3 promote the assembly of the central region of the SC, in which assembly of Zip1 requires both Zip2 and Zip3, which localise with Zip1 (Fung et al., 2004). However Zip2 and Zip3 foci formation is independent of Zip1, as their foci form before Zip1. Furthermore, normal Zip2 and Zip3 foci are found in *zip1* cells, suggesting their roles in axial association. This is consistent with the idea which is proposed by Roeder and colleagues that Zip2 and Zip3 form a synaptic initiation complex (SIC) that are required for mature synapsis (Chua and Roeder, 1998). Zip2 localisation is dependent on Zip3, suggesting that Zip3 promotes synapsis by recruiting Zip2 to axial associations (Agarwal and Roeder, 2000). Both Zip2 and Zip3 foci are also dependent on DSB formation. Moreover, biochemical experiments indicate that these proteins are

associated with recombination proteins at DSB sites, supporting the idea that Zip2/3 promote SC initiation at recombination sites (Rockmill et al., 2003).

The components of the LEs are also identified, such as Hop1, Red1 and Mek1 (Hollingsworth et al., 1995; Niu et al., 2005, 2007, 2009) and mammalian SCP2 and SCP3 (Dobson et al., 1994). Hop1, Red1 and Mek1 are meiosis specific proteins that localise to AEs (Smith and Roeder, 1997), and mutations of these genes display different levels of defects in assembly of the SC. In the absence of Red1 or Hop1, no mature SC is formed (Hollingsworth and Byers, 1989; Loidl et al., 1994; Rockmill and Roeder, 1990). *red1* cells show failure to assemble the SC due to complete loss of AE formation; whereas *hop1* cells form fragmented AEs, which has milder phenotype than the *red1* (Hollingsworth and Byers, 1989). Recombination levels are also reduced in the triple mutant of *red1 hop1 mek1* (Hollingsworth and Byers, 1989; Rockmill and Roeder, 1990), suggesting that meiotic recombination events are tightly linked to these LE components. Hop1 and Red1 form a complex on to chromosomes prior to DSB formation, which composes of chromosome axes. At this stage, Red1 is already phosphorylated before DSBs are formed, whereas phosphorylation of Hop1 is dependent on DSB formation (Niu et al., 2007). Red1 is then further phosphorylated in response of DSB formation and becomes hyper-phosphorylated. Mek1 is a meiosis specific serine/threonine protein kinase, whose recruitment is via Hop1-phosopho T318 and its activation also requires DSB formation (Carballo et al. 2008). It is proposed that Mek1 dimerisation takes place after its recruitment to hyper-phosphorylated Red1 or Hop1 T318. This is promoted by phosphorylated Hop1 C domain, which enables Mek1 kinase activation by autophosphorylation that is also proposed to be important for proper localisation of Mek1 to Hop1/Red1 complexes (Niu et al.,

2007). The formation of Hop1/Red1/Mek1 complexes is to ensure efficient recombination between homologous chromosomes by establishing barriers to sister chromatid repair (BSCR), in which phosphorylation of these proteins plays a key role in assembly of these complexes that suppresses DSB repair between sister chromatids. More details about BSCR will be discussed in section 1.5.

The ZMM group comprises of seven proteins, Zip1/Zip2/Zip3/Zip4, Msh4/Msh5 and Mer3. These proteins were first identified in *S. cerevisiae* which function in SC assembly and meiotic recombination. Presumed orthologues of ZMM were also found in plants and animals, suggesting that these proteins are evolutionarily conserved between species (Lynn et al., 2007). In fact, ZMM proteins play important roles in providing a tight link between assembly of the SC and meiotic recombination, which represents the most distinctive feature of meiosis. The ZMM group proteins are functionally collaborating with each other in establishing crossover, but evolutionarily, these proteins are not related (Lynn et al., 2007). As ZMM proteins function in assembly of the SC, which provides intimate coordination with homologous recombination on DNA level, it is therefore important to look deeper into how SC assembly and homologous recombination are correlated (see Figure 1.2). Meiotic DSBs are induced at multiple sites during leptotene, where axial elements start to form along the sister chromatids base. Subsequently, DSBs are processed by multiple factors with nuclease- and/or helicase-activities from 5' ends, generating single-stranded 3' overhangs. At this stage, Zip1 protein starts to localise and form transverse filaments at the central region of the SC. Then Zip1 gradually pull the axial elements of the two homologues together. This is followed by single-end invasion (SEI) searching for homologues as repair templates (Bishop and Zickler, 2004; Börner et al., 2004;

Hunter and Kleckner, 2001). This transition occurs before proceeding from zygotene to pachytene (Lynn et al., 2007). During pachytene, the second end of a break associates with donor sequence, followed by re-ligation of the two ends of a DSB, a double Holliday junction is formed (Schwacha and Kleckner, 1995). Assembly of the SC is completed; homologues are juxtaposed by transverse filaments, flanked by two lateral elements (previously axial elements). Finally, double Holliday junctions are resolved into crossovers at or before pachytene exit, and the SC is disassembled by diplotene stage. At the final stage, connections established by the exchange of homologous chromosome arm (chiasmata) are formed and become cytologically visible (Neale and Keeney, 2006). At this point two homologous chromosomes physically exchange genetic material via crossover.

1.4 Meiotic Homologous Recombination

Recombination refers to a process of the exchange or transfer of genetic information between DNA molecules. Homologous recombination (HR) on the other hand, involves DNA sequences that are identical (or mostly identical) to each other. However, if recombination takes place between the two DNA molecules with little homology or even no sequence identity, it is referred to as non-homologous end joining (NHEJ). Two types of recombination events have been identified by the segregation of heterologous markers during meiosis: crossing over (CO) and gene conversion (GC). Studies in budding yeast have shown that CO and GC are closely associated with each other, but from different intermediates of meiotic recombination (Allers and Lichten, 2001). Several models have been proposed to elucidate the mechanisms of recombinational DSB repair, including double-strand repair (DSBR) model and synthesis-dependent strand annealing

(SDSA) model. These models share some molecular pathways including, (a) process initiated by a DNA DSB, (b) processing of the DSB by nucleolytic resection to form 3'-ssDNA overhangs, (c) formation of presynaptic filaments on the ssDNA ends, (d) strand invasion into a heteroduplex DNA to form a D-loop, (e) 3' end DNA extension by DNA polymerase. Details and proteins involved in these processes will be discussed below (also see Figure 1.4).

1.4.1 DSB formation

During meiosis, homologous recombination plays a vital role in proper chromosome segregation by establishing physical connections between homologous chromosomes, in which homologous chromosomes are properly aligned on the spindle and to segregate precisely. In *S. cerevisiae*, meiotic recombination is initiated by programmed DNA DSB (Keeney et al., 1997). DSBs are highly deleterious for genome integrity but occur in replication, meiosis and immune system development. In meiosis, DNA DSBs are catalysed by meiosis specific transesterase Spo11, which is highly conserved among most species(Keeney et al., 1997). Spo11 forms a dimer, which cleaves both strands of DNA. After the cleavage, 5' termini on both side of the DSB are covalently bound to Spo11, forming a Spo11-oligonucleotide hybrid structure. The explanation for the formation of this structure was elusive, as meiotic formation does not result from simple hydrolysis of phosphodiester backbone of DNA. The explanation lies in a model proposed by Scott Keeney that the active site of Spo11, a tyrosine side chain attacks DNA phosphodiester backbone, generating a covalent phosphodiester bond between Spo11 and the 5' termini of the DSB, releasing a free 3' OH (Keeney et al., 1997).
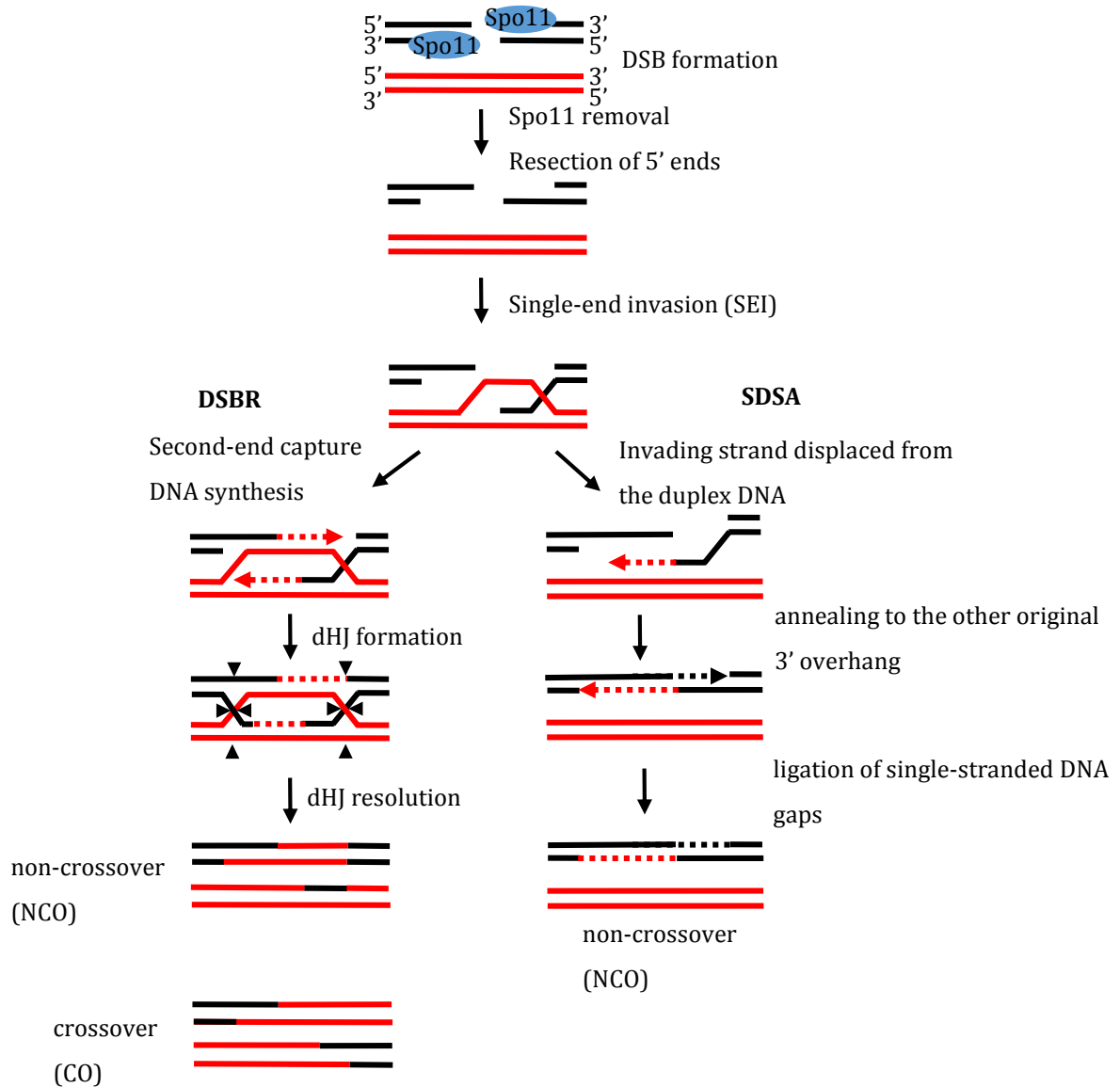
Figure 1.4. The double-strand break repair model (DSBR) and the synthesis-dependent strand annealing (SDSA) model of meiotic recombination. Homologues are depicted in black (paternal) and red (maternal). A DNA DSB is induced by Spo11 endonuclease activity on one of the homologue (paternal DNA in this case). After the break is made, DSB ends are resected to form 3'-ssDNA tails and one of the tails is capable of invading the duplex homologous DNA sequence (maternal). In DSBR model, capture of the second end of the DSB following by DNA synthesis forms a double-Holliday junction (dHJ), whose alternative resolution can generate crossover (CO) or non-crossover (NCO) products. However in SDSA model, the second end of the DSB is displaced from the donor sequence following by DNA synthesis, forming only NCO products.

1.4.2 DSB processing

Spo11 remains covalently bound to the 5'end of each side of the break after DSBs have been made (Neale et al., 2005; Mimitou & Symington, 2009). Processing and removal of this covalent structure is essential for DSB repair during recombination as this allows formation of 5' ssDNA overhangs that are required for strand exchange and homologue pairing. The removal of this covalent structure is catalysed by the formation of single strand DNA nick that is adjacent to the each side of the break, hence forming Spo11-oligonucleotide structure that is released from the break site(Neale et al., 2005). These Spo11-oligonucleotide complexes were found to have equal amount but differ in lengths (10-40 nucleotides), suggesting that the cleavage of Spo11 from the DSB sites occurs asymmetrically (Longhese et al., 2009). It has been shown that the removal of Spo11 from the DSB sites requires a number of proteins that involve in eliminating the Spo11-oligonucleotide structure for further processing of the DSB, including the Mre11/Rad50/Xrs2 (MRX) complex and Sae2 (Longhese et al., 2009).

Mre11 and Rad50 form an evolutionarily conserved complex, harbouring DNA binding, 3'-5' exonuclease and ssDNA endonuclease activities(Krogh and Symington, 2004; Mimitou and Symington, 2009a). In *S. cerevisiae*, Mre11 and Rad50 interact with Xrs2, whereas in human, Mre11 and Rad50 bind to NBS1 (Nijmegen breakage syndrome 1) to form a complex (MRN).

Mutations in members of the MRX complex causes increase sensitivity in ionizing radiation (IR), failure to induce meiotic DSBs and defects in mitotic recombination (Krogh and Symington, 2004; Mimitou and Symington, 2009a). The role of the MRX complex in DNA processing was characterised by the analysis of budding

yeast Rad50 mutant allele (*rad50s*), in which cells accumulate unprocessed DSBs during (Alani et al., 1990; Cao et al., 1990; Mimitou and Symington, 2009a). Moreover, defects in Mre11 nuclease activity and Sae2 mutants also cause accumulation of unprocessed DSBs during meiosis(Krogh and Symington, 2004; Longhese et al., 2009; Mimitou and Symington, 2009a) In the cases of mutants of Mre11 and Sae2, induction of DSB formation by Spo11 is made, but not Spo11 removal, which is similar to *rad50s*. This suggests that removal of Spo11 may occur by Mre11-mediated endonucleolytic cleavage cooperative with Sae2 participation. This suggestion is consistent with the findings that Sae2 possesses a ssDNA endonuclease activity independently of MRX complex and cooperates with MRX to process hairpin structure *in vitro* (Lengsfeld et al., 2007; Longhese et al., 2009; Mimitou and Symington, 2009a). These findings suggest that Sae2 may facilitate resection cooperatively with MRX complex by providing endonucleolytic cleavages, hence forming clean ends that serve as substrates for nucleases such as MRX complex and Exo1 to carry out further DNA break end processing. As mentioned above, resection of both ends of a DSB is initiated by the MRX complex combined with Sae2 activity, in which these factors remove 50 to 100 bases of DNA from the 5' end (Mimitou and Symington, 2009b) . This is then followed by a long 5' to 3' resection carried out by multiple enzymes such as Exo1, Sgs1 and Dna2(Mimitou and Symington, 2009b). Sgs1 function in DSB repair will be discussed separately in section 1.6.

Exo1 is a conserved member of Rad2 family of nucleases, which possesses 5'-3' dsDNA exonuclease and 5' flap endonuclease activities *in vitro* (Mimitou and Symington, 2009a; Tran et al., 2004). Exo1 also acts in mismatch repair, meiotic recombination (crossover control) and participates in processing the degradation

of stalled replication forks and uncapped telomeres (Krogh and Symington, 2004; Mimitou and Symington, 2009a). The *exo1Δmre11Δ* has severe defects in cell growth and IR resistance compared with *mre11Δ* (Mimitou and Symington, 2010). These defects can be partially suppressed by over-expressing Exo1 on plasmids, indicating Exo1 is able to carry out some DSB processing in the absence of MRX complex (Krogh and Symington, 2004; Lee et al., 2002; Moreau et al., 2001). This is consistence with the observation that Exo1 is the only nuclease with well-characterised role in DSB resection in the absence of MRX complex (Fiorentini et al., 1997). However the partial rescue of *exo1Δmre11Δ* phenotype by over dosed Exo1 is not observed in Mre11 nuclease defective (*mre11-nd*) mutants, suggesting that certain DSBs require specific initiation process by the MRX complex (e.g. Spo11 induced DSBs(Krogh and Symington, 2004; Mimitou and Symington, 2009a). In addition, high dosage of Exo1 is needed to suppress only limited defects resulting from deletion of Mre11, reflecting the fact that Exo1 is poorly required to the DSB in the absence of MRX complex. This may explain milder phenotypes observed in *mre11-nd* mutants, where MRX complex is formed, but severer phenotypes in *mre11Δ* and other mutants that MRX complex formation is inhibited (Krogh and Symington, 2004).

It is reported that helicase activity, in conjunction with a specific single-strand endo or exonuclease activity are involved in DSB end resection (Mimitou and Symington, 2009b). The *E.coli* RecQ helicase together with the RecJ 5'-3' exonuclease function in DSB resection, suggesting that the yeast RecQ helicase, Sgs1, may also be participating in DSB resection. Zhu et al showed that when expressing Sgs1 alleles with deletion or single amino acid substitution in the helicase domain in *sgs1Δ*, normal mitotic HO DSB end resection is lost, indicating

that helicase activity of Sgs1 is required for efficient DSB end resection (Zhu et al., 2008). In addition, these authors used a single-strand annealing (SSA) assay, in which extensive resection track is required to repair I-SceI or HO induced break. They found that deletion of Sgs1 resulted in a slight delay in repair with a resection track at 5-7kb long, but a severe defect in repair was observed with repeats located 25kb apart, implying Sgs1's role in processing of DSB ends (Zhu et al., 2008). Moreover, the *exo1Δ sgs1Δ* double mutant exhibited complete defects in the SSA assay, in which evidence of inefficient end processing was observed, consistence with the hypothesis that Sgs1 is involved in DSB end resection (Mimitou and Symington, 2009b; Zhu et al., 2008).

Dna2 is a conserved endonuclease/helicase involved in DSB and post-replicational repair pathways (Bae et al., 1998; Budd and Campbell, 2009; Mimitou and Symington, 2009b). Furthermore, Zhu et al. provided evidence that Dna2 nuclease activity acts cooperatively with Sgs1 in DSB processing (Zhu et al., 2008). Several findings of nuclease/helicase in DSB end resection have led Mimitou et al. to propose a two-step model for DSB end processing (Figure 1.5). In meiosis, the MRX complex along with Sae2 are required to endonucleolytically remove covalently bound Spo11, which generates intermediates with short 3' ssDNA tails that are quickly processed by Exo1 and/or Sgs1 nuclease activities. However, whether Sgs1 and Dna2 act together in meiotic DSB processing remains to be determined (Mimitou and Symington, 2009a).

Meiotic breaks

Exo1, Sgs1-Dna2 ⊣ Spo11

MRX MRX

Spo11

recruitment / activation of Sae2

Step 1

Sae2

Spo11

MRX MRX

Sae2

Spo11

Trimming of ends by MRX-Sae2
removes Spo11 leaving short 3'
overhangs

3'3'

Exo1, Sgs1-Dna2

processive resection by Exo1 or Sgs1-Dna2?

Step 2

Exo1

Sgs1/Rmi1/Top3

Dna2   ?
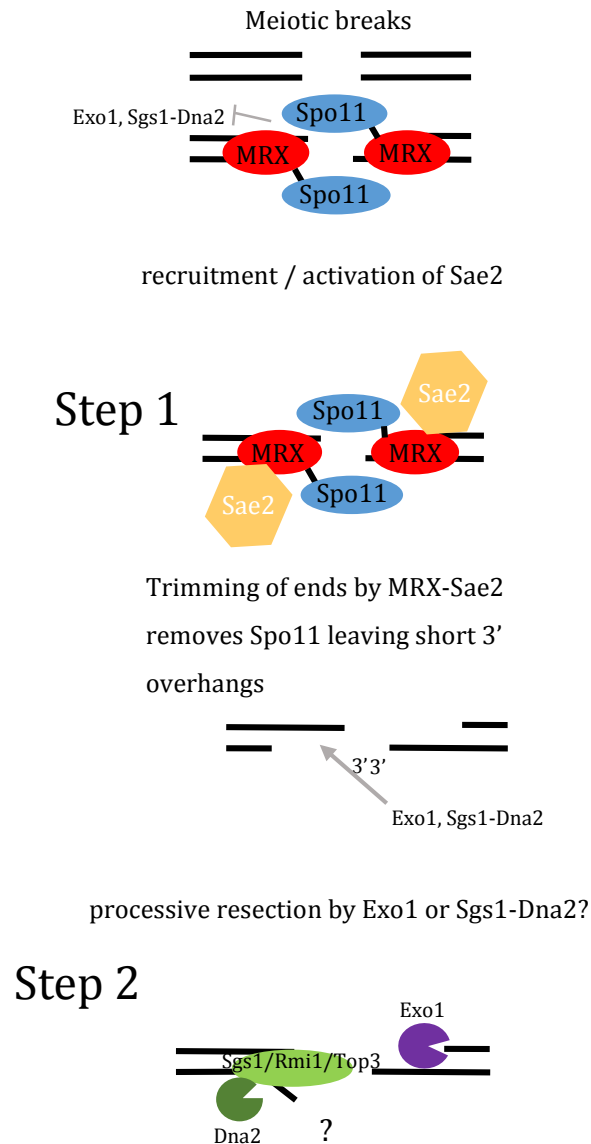
Figure 1.5. Two-step resection process which includes combined nuclease and helicase activities.

Meiotic DNA DSBs are induced by Spo11. After the breaks are made, Spo11 remains attached to the 5' ends the break and thus blocks further DNA processing because these ends are poor substrates for Exo1 and Sgs1/Dna2. Removal of Spo11 from meiotic DSB ends requires Sae2 and MRX complex endonucleolytic activity that releases Spo11 together with a Spo11-bound short (10-40nt) oligonucleotide. The MRX complex provides the Mre11 nuclease activity which acts cooperatively with Sae2 to carry out the first step in DSB processing, the removal of Spo11-oligonucleotide from the 5' end. Also, MRX complex is required to recruit other nucleases as well as helicases including Dna2, Exo1 and Sgs1 to the break sites. Further resection (step 2) is proposed to be processed by Exo1 or combined activities Sgs1/Rmi1/Top3 and Dna2. Whether Sgs1/Dna2 are involved in DNA processing remains to be determined (Mimitou and Symington, 2009a).

1.4.3 DNA strand invasion

Processing of the DSB ends gives rise to 3' ssDNA overhangs, which are substrates for recombinases required for homologous recombination. Recombinases are the enzymes that mediate pairing of DNA sequences between homologous chromosomes (San Filippo et al., 2008). Two recombinases Rad51 and Dmc1 are identifies in eukaryotes. Rad51 is involved in both mitotic DSB repair as well as meiotic homologous recombination. Dmc1 on the other hand, is specific to meiotic DSB repair. Both recombinases catalyse DNA joint (strand invasion) by forming presynaptic filament, in which monomers of these recombinases polymerise on 3' ssDNA derived from DSB end processing (Busygina et al., 2008; Neale and Keeney, 2006). Rad51 is a homologue of bacterial RecA protein involving in strand exchange and recombinational repair in both mitosis and meiosis. In the beginning of strand invasion, 3' overhangs are coated with replication protein A (RPA), which prevents ssDNA secondary structure formation (Krogh and Symington, 2004). Then Rad52 epistasis group proteins including Rad52, Rad54, Rad55 and Rad57 help facilitate Rad51 binding onto ssDNA tails (Figure 1.6). Rad52 directly interacts with both Rad51 and RPA and helps recruit Rad51 by displacing RPA and simultaneously sending Rad51 to ssDNA (Krogh and Symington, 2004; Song and Sung, 2000). Cytological data have revealed that Rad51 localisation to DSB sites is dependent on Rad52, consistent with biological data demonstrating Rad52 is required for Rad51 loading onto RPA coated ssDNA tails (Gasior et al., 1998; Krogh and Symington, 2004; Miyazaki et al., 2004). *RAD54* encodes a member of Snf2-family of SF2 helicase, however, instead of behaving like conventional DNA helicases, which are capable of separating strands of duplex DNA, the Snf2 proteins are more likely to act as motor proteins that remodel protein-DNA complexes (Heyer et al., 2006). Rad54 has been found to have several functions
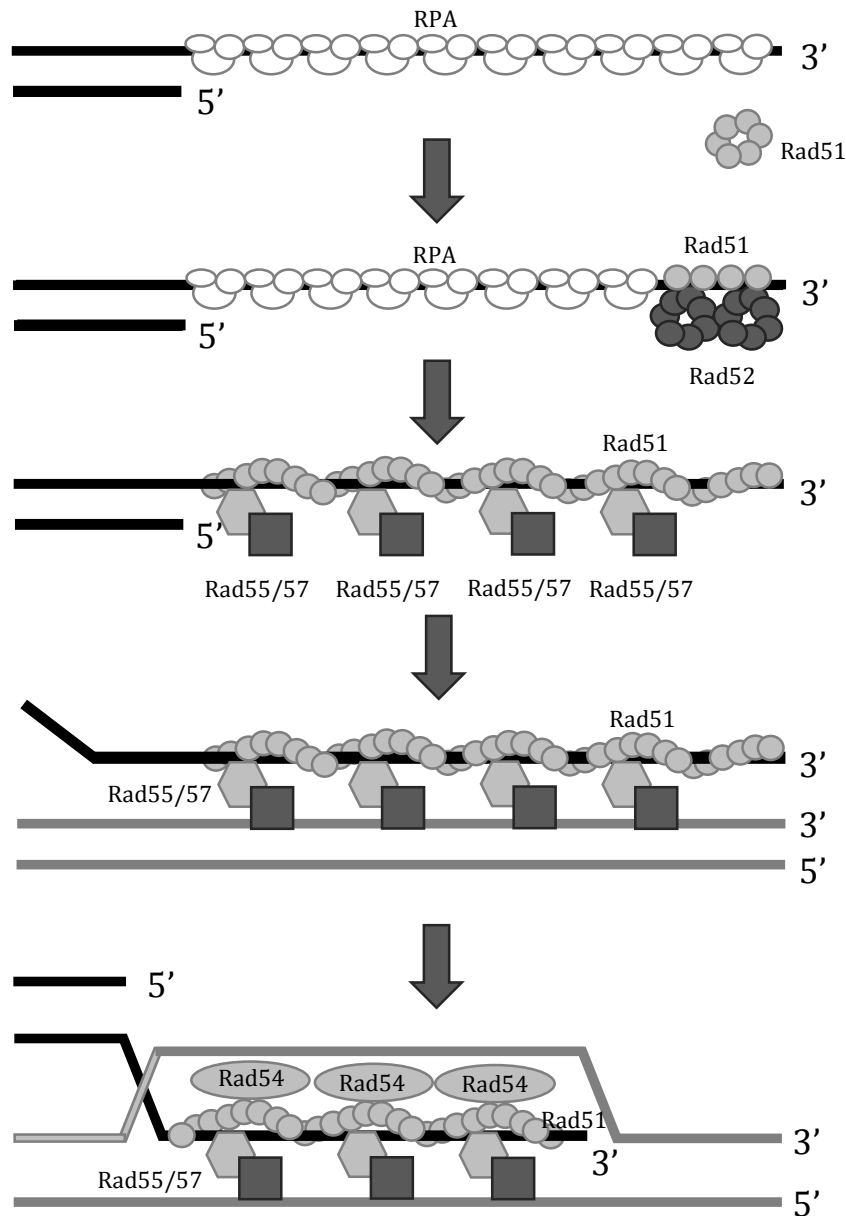
Figure 1.6. Model for Rad51-mediated strand invasion and its mediators Rad52, Rad54 and Rad55/57 (only one side of the DSB is shown). Rad52 helps Rad51 recruit to 3'-ssDNA tails which are initially bound by RPA. Subsequently, RPA is displaced and the Rad51 nucleofilament extends along the ssDNA mediated by Rad55/57. Rad55/57 complexes facilitate elongated Rad51 filament to strand invade homologous donor DNA sequence. Rad54 then interacts with Rad51 which promotes chromatin remodeling, DNA unwinding and strand annealing between homologous DNA and the Rad51 nucleofilament (adapted form Krogh and Symington, 2004).

during and after strand invasion, including 1. Rad54 promotes Rad51 nucleation onto RPA coated ssDNA, as Rad52 functions in facilitating Rad51 loading (Heyer et al., 2006; Hollingsworth, 2010), which reflects Rad54's role in stabilising Rad51 filament by establishing a co-complex with Rad51-ssDNA filament (Mazin et al., 2003; Solinger et al., 2002). 2. Rad54 helps clear off nucleosomes and promotes strand invasion by its ATP-dependent translocation on duplex DNA (Heyer et al., 2006). 3. Rad54 dissociates Rad51 from duplex DNA in a ATP-dependent fashion (Solinger et al., 2002). Note that Rad51 remains bound to heteroduplex DNA, and its release from heteroduplex DNA is significantly slower than its bacterial homologue RecA. Rad54 is responsible to dislodge Rad51 from heteroduplex DNA by its ATPase activity.

The Rad55 and Rad57 proteins are also implemented in formation of Rad51 presynaptic filament. These proteins are Rad51's paralogue as they only share 20-30% identity to Rad51. IR sensitivity of *rad55* or *rad57* mutants at low temperature is as much as *rad51* mutants, but this sensitivity is suppressed at 30°C, suggesting that the role of Rad55 and Rad57 in Rad51 nucleofilament stabilisation (Krogh and Symington, 2004). Moreover, Rad51 foci in meiotic cells are dependent on both Rad55 and Rad57 (Gasior et al., 2001; Miyazaki et al., 2004; Sugawara et al., 2003), consistent with the idea that Rad55 and Rad57 stabilise Rad51 filament. The Rad55 and Rad57 proteins form a heterodimer (see Figure 1.6) that binds to ssDNA, in which Rad51 protein is stably nucleated onto ssDNA in the present of RPA during strand invasion (Sung, 1997). However, Rad55 does not interact with RPA but with Rad51, exhibiting a possibility that this Rad55/Rad57 heterodimer's activity in mediating strand exchange is distinct from Rad52 (Johnson and Symington, 1995).

24

Little attention of how the Dmc1 presynaptic filament is assembled and maintained is received. The early steps in meiotic recombination are proposed to proceed through two pathways. One is solely dependent on Rad51, referred to as the Rad51-only pathway. The other pathway depends on both Rad51 and Dmc1, referred to as the Dmc1-dependent pathway (Tsubouchi and Roeder, 2004). There are at least two factors that are not involved in the Rad51-only pathway but in the Dmc1-dependent pathway. These are Hop2 and Mnd1, which are meiosis specific proteins that interact with each other (Leu et al., 1998; Tsubouchi and Roeder, 2004). *hop2* and *mnd1* mutants have shown failure to convert DSBs to subsequent intermediates, suggesting that Hop2/Mnd1 is required for Dmc1 to process meiotic strand exchange (Leu et al., 1998; Tsubouchi and Roeder, 2002, 2003). Furthermore, epistasis analysis by Tsubouchi and Roeder indicates that Hop2/Mnd1 acts downstream of Dmc1, regulating proper and accurate Dmc1-mediated homology searching in the Dmc1-dependent pathway (Tsubouchi and Roeder, 2004). Other two Dmc1 accessory factors, Mei5 and Sae3 are also required for cells undergoing proper meiosis. Unlike Hop2/Mnd1, Mei5/Sae3 and Dmc1 act in the same pathway, as meiotic phenotypes in *dmc1 mei5* and *dmc1 sae3* are literally the same (Tsubouchi and Roeder, 2004).

How Rad51 and Dmc1 are located onto DSB ends remain elusive. A current model proposed by Shinohara et al that Rad51 might load on one end of a DSB and Dmc1 loads on the other (Sheridan and Bishop, 2006; Shinohara et al., 2000), fits well with experimental works. Other configuration, in which Dmc1 is proposed to be supported by Rad51 to catalyse meiotic strand invasion between homologue, provides further insights into how strand invasion is regulated (Sheridan and Bishop, 2006). Sheridan and Bishop propose that in WT yeast cells, strand

invasion is biased towards inter-homologue chromosomes, in which Dmc1 is supported by a scaffold comprises of axial proteins and Rad51 (Sheridan and Bishop, 2006). Therefore in *rad51*, while Dmc1 is no longer directed by Rad51, tendency of invasion between sister chromatids is decreased (Sheridan and Bishop, 2006).

Finally, after strand invasion catalysed by recombinases, DNA synthesis is carried out at the invading end using donor sequence as genetic information repair template. After strand invasion and DNA synthesis, two types of recombinational repair pathways are proposed, according to where the DSB end goes to. If the second end of the DSB is captured to form an intermediate with two Holliday junction, the repair pathway is referred to the double-strand break repair (DSBR) pathway. Alternatively, the repair pathway proceeds to the synthesis-dependent strand annealing (SDSA) by strand displacement, following by annealing of the extended single strand end on the other break end (Figure 1.4).

1.4.4 DSBR model

Formation of semi-stable single end invasion intermediates results in most CO production, in which capture of Second DSB end to form a double Holliday junction (dHJ) intermediate (hereafter called joint molecules, JMs) is critically important (Hunter and Kleckner, 2001; Jessop et al., 2006). Alternate resolution of JMs gives rise to COs and NCOs. That is, most of resolution of dHJs is biased to form COs as main products of homologous recombination in wild type *S.cerivisiae* and many other organisms. However, proteins that are implemented to resolve JMs as COs are yet to be determined (Jessop and Lichten, 2008). Lichten et al suggest that coupled helicase and topoisomerase (Sgs1/Rmi1/Top3) activities disassemble

JMs in a process called dissolution, which contributes only NCO production; on the other hand, JMs can also be resolved by endonuclease activities including Mus81-Mms4/Yen1 and Slx1-Slx4. These authors also suggest that CO formation in DSBR requires stable SEI intermediates to proceed second end capture and opposite cleavage of JMs to form CO products. This requires ZMM proteins, which stabilises and protects the early SEI intermediates from disassembling by Sgs1 (De Muyt et al., 2012). Moreover, strand invasion intermediates that escape from both Sgs1 disassembly and ZMM protein protection and can form dHJs or multichromatid JMs (De Muyt et al., 2012; Jessop and Lichten, 2008). Finally, resolution of these JMs or multichromatid JMs by Mus81-Mms4 generates both COs and NCOs.

1.4.5 Synthesis-dependent strand annealing (SDSA) model

The SDSA pathway takes place when single end DNA is displaced and annealed with the other DSB end after DNS synthesis. Although the SDSA model was proposed to address mitotic DSB repair, there is evidence suggests that SDSA also plays important role in meiotic HR. SDSA accounts for a great majority of HR products in meiotic HR, in which NCO is the only outcome of the SDSA pathway. That is, not all meiotic DSBs result in CO formation, only a small fraction of meiotic DSBs does (San Filippo et al., 2008). Studies have suggested that helicases including Sgs1/BLM and Srs2 are implemented in regulating CO/NCO decision(De Muyt et al., 2012; Jessop and Lichten, 2008; Jessop et al., 2006). Apart from their roles in DNA replication, both Sgs1 and Srs2 are proposed to be involved in disassembly of D-loop formation mediated by Rad51 or Dmc1, which promotes strand displacement (De Muyt et al., 2012; Jessop et al., 2006). This drives events toward strand annealing with the other DSB end that leads to form NCO products.

1.5 Barrier to sister chromatid recombination (BSCR)

It is well known that homologous recombination is essential for DSB repair, and recombination creates proper homologue pairing during meiosis which promotes homologue segregation thereby gives rise to genetic diversity. For DSB repair, sister chromatids are the preferred repair template simply because they are close to each other. For meiosis on the other hand, all the important recombination event occurs between homologues. However, the biochemical process of strand exchange is unbiased to either sisters or homologues and the default partner choice is sisters because they are nearby. In budding yeast, there is a strong bias towards DSB repair using homologous chromosomes as repair templates in preference to sister chromatids (Terentyev et al., 2010). In other words, it is believed that recombination between homologues (interhomologue recombination, hereafter IH recombination) dominates over sister chromatid recombination (hereafter IS recombination) during meiosis (Goldfarb and Lichten, 2010). Note that there are two ways to establish bias of using homologous chromosomes to repair DSBs rather than sister chromatids. One possible way could be a mechanism, which promotes strand invasion and homologue searching towards homologues. Another way could be establishing a barrier to sister chromatid recombination (BSCR), in which strand invasion of sister chromatids is prevented and usage of homologue as repair templates becomes default (Terentyev et al., 2010).

As the mechanism of establishing BSCR in meiosis is still elusive, how partner choice is differentiated between normal DSB repair and meiosis is of particular interests. As meiotic recombination is initiated by programmed DSBs, two DSB

ends are therefore generated and assigned for different partner choice. One end of the DSB searches for homologue via a nascent D-loop. The other end may remain bound with its sister chromatid probably also in a nascent D-loop. As these events progress, a ~400nm bridge structure starts to form and link to chromosome axes, with each DSB end and its recombinosome components (Hong et al., 2013; Storlazzi et al., 2010). These structures are closely related to presynaptic alignment because the formation of these bridges along the chromosomes results in homologue pairing (Hong et al., 2013). Fates for the two DSB ends in many organisms may be decided by two RecA homologues: meiotic Dmc1 for the homologue-associated end and mitotic Rad51 for the sister-associated end (Hong et al., 2013; Shinohara et al., 2000). These bridges provide an important implication that the two DSB ends form a physical linkage for recombination. A differentiation step then takes place when recombination progresses, in which a subset of "ends-apart" bridge intermediates becomes IH COs, whereas the remainder becomes IH NCOs primarily. Importantly, only one of the two ends are assigned to proceed DNA synthesis, and in most of the cases, this extension initiates from the homologue-associated end rather than the sister-associated end, therefore leads to form double Holliday junctions between homologues, which then specifically tend to form IH COs. However in some minority cases, extension at the sister-associated end does occur, which presumably leads to form IS COs.

A meiosis specific gene HED1 (high-copy suppressor of *red1*) appears to provide a distinct mechanism that down regulates the Rad51-dependent pathway, thereby promotes Dmc1-mediated strand invasion between homologues to form IH COs (Busygina et al., 2008, 2012; Tsubouchi and Roeder, 2006). Hed1 directly interacts

with Rad51, which specifically prevents Rad54 facilitating Rad51 to strand invade, leaving Rad51-presynaptic filament assembly unaltered (Busygina et al., 2008). Also, biochemical experiments have revealed that Hed1 prevents Rad54 recruitment to the DSB and has no effects on the Rad52-dependent recruitment of Rad51 to the break (Busygina et al., 2008), indicating Hed1's role in specifically attenuating the assembly of Rad51-Rad54 complex, thereby down-regulates Rad51-only pathway. In *dmc1* mutants, meiotic DSBs are unrepaired even though Rad51 is still present and sister chromatids could be repair source. Deletion of the Rad51 inhibitor Hed1 rescues meiotic DSB repair and IH recombination defects in *dmc1Δ*, suggesting that repair between sister chromatids is inhibited and the inhibitory mechanism is established by Hed1 (Busygina et al., 2008; Tsubouchi & Roeder, 2003, 2006). Moreover, the meiotic defects result from the *dmc1* mutants can also be suppressed by over-expressing both Rad51 and Rad54, in which elevating the level of these two proteins promotes DSB repair via sister chromatids as templates, further suggesting that IS recombination is normally prevented unless the activity of Rad51 or its accessory protein Rad54 is experimentally increased (Bishop et al., 1999; Hollingsworth, 2010). The information of how the repair bias towards IH recombination is further established from the study of a meiosis specific kinase Mek1 (also known as Mer4). Mek1 forms a complex with Hop1 and Red1 and is required for a number of events including formation of AEs and SC and establishing a pachytene checkpoint to ensure all DSBs are properly repaired by pachytene stage (Bailis and Roeder, 1998; Hollingsworth and Ponte, 1997; Rockmill and Roeder, 1991; Xu et al., 1997).

It is thought that Rad54 is a key player in establishing BSCR during meiosis. Niu et al screened a number of purified proteins that are phosphorylated by Mek1 and

involved in Rad51-mediated recombination. They found that Rad54 is phosphorylated by Mek1 on threonine 132 both *in vitro* and *in vivo* (Hollingsworth, 2010; Niu et al., 2005). The phosphorylation on Rad54 reduces both the interaction with Rad51 and stimulation of Rad51 activity in strand invasion. Moreover, meiotic cells that are incapable of phosphorylating Rad54 can partially suppress the IH recombination defects result from *dmc1* (Hollingsworth, 2010). This suppression is proposed to be dependent on Mek1, in which Rad51 recombinase activity is decreased by reducing the Rad51-Rad54 association through Rad54 phosphorylation, thereby creating BSCR (see Figure 1.4). This inhibitory mechanism is based on the studies of meiosis checkpoint kinase Mec1 and Tel1 that are activated in response to meiotic DSB, which subsequently phosphorylate Hop1 (Niu et al., 2005; Wan et al., 2004). Phosphorylated Hop1 then binds and activates Mek1, which phosphorylates targets including the Rad51 accessory factors Tad54 and Rdh54 (Niu et al., 2007, 2009), thereby prevents interaction between Rad51 and these factors and supposedly to reduce IS recombination. The Mek1-dependent mechanism for preventing Rad51-Rad54 interaction seems to act in parallel with Hed1, in which both inhibitory mechanisms seek to exclude Rad54 to associate with Rad51 in different ways. The up-to-date data have indicated that recombination bias towards IH is established by suppression of Rad51 activity, which is created by Hed1 interruption and Rad54 phosphorylation mediated by Mek1 activity (Hollingsworth, 2010).

1.6 Sgs1

Sgs1 is a member of the RecQ helicase family expressed in *S. cerevisiae*. The RecQ helicase family is highly conserved from prokaryotes to eukaryotes, and a large number of family members also exist in vertebrates (e.g. BLM, WRN, RT/REC4,

RECQ1 and RECQ5) and in *S. cerevisiae* Sgs1 (Rockmill et al., 2003). In human, loss of BLM activity in Bloom's syndrome leads to cancer predisposition and a significant increase in sister chromatid recombination and genome instability (Jessop and Lichten, 2008). What's more, the BLM together with its partner proteins topoisomerase IIIα (top3α) and Rmi1 form a complex and can resolve synthetic dHJ to NCO products *in vitro* (Mankouri and Hickson, 2007). It has also been suggested that BLM complex disassembles dHJ to suppress DNA recombination, indicating BLM's helicase activity plays a vital role in directing CO/NCO decision and in maintaining genome stability.

Yeast Sgs1 also forms a complex with Top3 and Rmi1 as its human homologue does, and it has also been implicated in determining CO/NCO during homologous recombination. The absence of Sgs1 in budding yeast results in increase in mitotic recombination (sister chromatic exchange), chromosome rearrangement and reduction in spore viability/sporulation (Gangloff et al., 2000; Klein, 2001). These phenotypes reflect the fact that Sgs1/BLM helicases have direct anti-CO activity. The measurement of ectopic and allelic recombination during meiosis in budding yeast SK1 background shows that despite *sgs1* mutant cells show modest increase in CO formation (1.7 fold increase in the *sgs1* mutant than in WT), whereas NCO levels remain unchanged (Jessop et al., 2006). This is consistent with the idea that Sgs1/BLM can directly abolish some formation of COs without altering NCO products during meiosis. However, the impact on COs by the absence of Sgs1 is so much limited in meiosis than in mitosis, suggesting that during meiosis, an anti-CO function must be ensured to carry out NCO production and Sgs1's anti-CO activity is somehow hindered by meiosis-specific factors. Several reports have indicated that a set of yeast meiosis-specific proteins including Zip1, Zip2, Zip3,

Zip4, Mer3, Msh4 and Msh5 (ZMM proteins) are implicated in stabilising recombination intermediates, in which pre-CO intermediates are protected from Sgs1's anti-CO activity (De Muyt et al., 2012; Jessop and Lichten, 2008). This is evidenced by several genetic and cytological approaches. COs are severely reduced in *zmm* mutants, because ZMM proteins are core components for the formation of SC, a tripartite protein structure that is essential for proper homologue pairing and alignment at pachytene stage of meiosis. Mutation of Sgs1 partially suppresses CO defects observed in *zmm* mutants by increasing COs by 3-fold compared with *zmm* mutants (Jessop et al., 2006).

Yeast cells expressing *sgs1ΔC795*, in which only the first 652 amino acids are expressed, CO defects caused by *zmm* mutant background can be suppressed to different extents by the loss of both the helicase domain and HRDC domain, a region where BLM interacts with Holliday Junctions. For instance, CO defects in *zip1* can be suppressed by *sgs1ΔC795* by increasing COs by 3-fold, where NCO level is unaffected. In *zip2* cells, CO defects can also be suppressed by *sgs1ΔC795* by elevating CO levels. Despite the fact that NCOs are slightly affected in *zip2* cells expressing *sgs1ΔC795*, in general, loss of Sgs1 partially suppresses CO defects seen in *zmm* mutants. Consistent with cytology data that *sgs1ΔC795* increases Zip3 foci in SK1 background, which Zip3 foci are considered as accurate markers of CO sites (Jessop et al., 2006). This strengthens the idea that Sgs1 antagonises ZMM-mediated CO stabilisation.

1.7 Srs2

The SRS2 gene in *S. cerevisiae* encodes a DNA helicase, which has high homology with bacterial helicases such as UvrD, Rep and PcrA by having highly conserved

motifs which define as a DNA helicase family (Krejci et al., 2004; Marini and Krejci, 2010; Palladino and Klein, 1992). Different from these bacterial counterparts, Srs2 contains an additional region that mediates protein-protein interactions located at its C-terminal region (Papouli et al., 2005, Figure 1.7). As an effective DNA helicase equipped with Walker A motif, Srs2 is able to process DNA unwinding with 3'-5' polarity by its strong ssDNA dependent ATPase and helicase activity. Apart from preferred substrate such as 3' overhang DNA for its helicase activity, it is also able to unwind DNA substrates containing dsDNA, D-loops, forks, flaps and 5'-ssDNA (Van Komen et al., 2003). Importantly, Srs2 is capable of unwinding D-loop like recombination intermediates formed by Rad51 *in vitro* (Marini and Krejci, 2010), in which this activity is stimulated by Rad51-dsDNA complex (Dupaigne et al., 2008), suggesting that Srs2 destabilises Rad51-mediated formation of SEI structure during DNA recombination (Bernstein et al., 2011; Krejci et al., 2004; Marini and Krejci, 2010, Figure 1.8). Therefore, Srs2 has been described as an anti-recombinase protein as it antagonises Rad51 to form nucleoprotein filaments.

SRS2 (<u>s</u>uppressor of <u>rad6</u> <u>s</u>ensitivity) was first identified by screening for mutations that high UV sensitivity resulted from *rad6* strains was suppressed. The RAD6 gene is essential for many cellular functions. *rad6* mutant strains show increased sensitivity to DNA damaging agents such as UV, ionising radiation and chemically, alkylating agents. What's more, mutation of RAD6 results in meiotic recombination and sporulation, suggesting that RAD6 plays important roles in DNA damage sensing and DNA repair (Schiestl et al., 1990). All the suppressors of *rad6* mutants isolated and identified were alleles of one locus, which is SRS2. It was previously reported that SRS2 only acts as a suppressor of UV sensitivity of
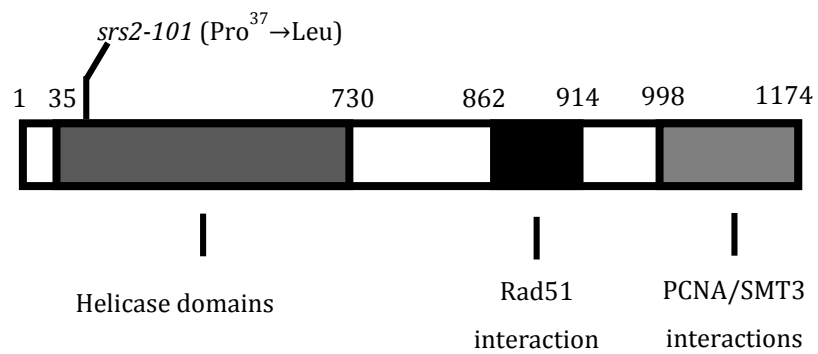
Figure 1.7. A schematic of helicase and protein-protein interaction domains in Srs2.

srs2-101 DNA helicase defective allele is indicated. This figure is adapted from P. Sung et al., 2009.
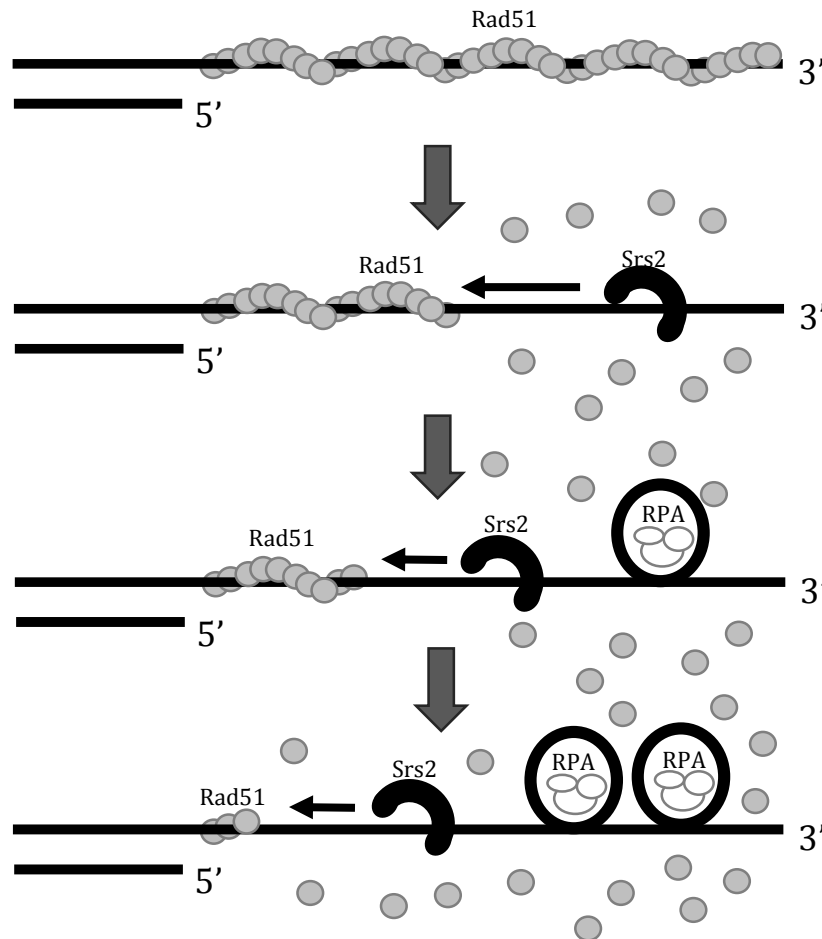
Figure 1.8. Model for Srs2 dismantling Rad51 presynaptic filament

Disruption of Rad51 presynaptic filament by Srs2. At the expenses of ATP hydrolysis, Srs2 dislodges Rad51 filament in the 3'→5' direction. The ssDNA is then available for ssDNA-binding replication protein A to prevent reloading of Rad51. This function of Srs2 inhibits D-loop formation and thus prevents second end capture during homologous recombination processes.

rad6. Srs2 can also suppress γ-ray sensitivity and growth defects of *rad6* in the later reports (Schiestl et al., 1990).Like *rad6* mutants, *rad18* is also highly sensitive to DNA damaging agents (Lawrence, C. W. 1982) and defective in post-replication repair of UV damaged DNA. Similarly, mutation of SRS2 suppresses these defects in *rad18* as in *rad6* mutants (Schiestl et al., 1990). In addition, this suppression by mutation of SRS2 in *rad6* mutants is semi-dominant for UV sensitivity but is dominant for γ-ray sensitivity respectively (Schiestl et al., 1990). Intriguingly, suppression by SRS2 mutation in *rad6* is completely lost when members of RAD52 epistasis group are absent or defective (Schiestl et al., 1990). Loss of suppression could result from *rad52 srs2* synergistically, but the fact that this double mutant is more UV sensitive than *srs2* single mutants, excluding the possibility that the loss of suppression by *srs2* in *rad6 rad52 srs2* is due to increased UV sensitivity in *rad52 srs2*. These results suggest that *SRS2* may be responsible for directing DNA lesions of *rad6* and *rad18* mutants to a Rad52 epistasis group-mediated homologous recombination pathway, in which sister chromatids may also be involved. Consistent with genetic evidence that mutations in *SRS2* frequently cause hyper-recombination phenotype, which substitutes post-replicative DNA repair defect results from *rad6* and *rad18* mutants (Schiestl et al., 1990; Sung and Klein, 2006).

How Srs2 is recruit to sites of DNA damage and dissociates Rad51 presynaptic filaments remains to be clarified, but biochemical data suggest that the anti-recombinogenic activity of Srs2 is possibly regulated and recruited by *CDK1*-mediated phosphorylation (Chiolo et al., 2005) or through a physical interaction with sumoylated PCNA (Papouli et al., 2005). In addition, Srs2 also has a direct physical interaction with Rad51 by its C-terminus region, which is not seen in the

bacterial homologue. However, whether this interaction is functionally important for anti-recombinogenic activity of Srs2 needs to be identified (Van Komen et al., 2003). This uncertainty was then elucidated and explained by a later report that the effects of Srs2 on mutated Rad51-mediated D-loop formation was examined, in conditions where Rad51 mutants were unable to interact with Srs2. Rad51 mutants such as *rad51-Y388H* and *rad51-G393D* retain their Rad51 catalytic activities faithfully but are unable to interact with Srs2, provide the best opportunity to identify if the functional significance of Srs2's anti-recombinogenic activity is tightly connected to the interaction with Rad51 (Seong et al., 2009). The result presented by these authors shows that the level of D-loop formation mediated by these Rad51 mutant alleles is not affected in comparison to the wild type when Srs2 is present, revealing the fact that the Srs2's anti-recombinase activity depends on itself to interact with Rad51.

The anti-recombinase activity of Srs2 is broadly evidenced by *in vitro* experiments, in which Srs2 acts to dislodge Rad51 nucleofilament from ssDNA. However, the role of Srs2 plays *in vivo* has been drawing more and more attention as deletion of Srs2 causes an increase in mitotic recombination and synthetic lethality when some other genes involved in homologous recombination including Swi2/Snf2 protein Rad54 and RecQ family helicase Sgs1 are also deleted, suggesting that its potential capability of avoiding toxic recombination intermediates to accumulate (Burgess et al., 2009).

Recruitment of Srs2 to DNA replication fork and damaged DNA was recently examined cytologically, where it was thought that sumoylated PCNA was important for Srs2 recruitment to replication fork (Papouli et al., 2005) and might

be affecting on recruiting to recombination foci. However, when Srs2 foci at replication forks examined in a non-sumoylated PCNA background or a Srs2 mutant that lacks SUMO-interaction motif, Srs2 foci at replication forks are significantly reduced but the Srs2 foci at recombination sites are unaffected, suggesting that recruitment of Srs2 to DNA replication forks or recombination sites occurred independently (Burgess et al., 2009).

Intriguingly, despite the fact that Srs2 dislodges by a direct interaction with Rad51 during recombination, the recruitment of Srs2 is not dependent on Rad51 as Srs2 localises to HR foci in the absence of Rad51 (Van Komen et al., 2003). What's more, Rad51 and Rad54 foci are significantly increased in the absence of Srs2, where Rad54 colocalises with Rad51 over 95% of the time (Burgess et al., 2009). Because removal of Rad51 nucleofilament is dependent on Srs2 helicase activity *in vitro* (Van Komen et al., 2003), it is of interest that whether the increase of the Rad54 foci also results from mutations in the conserved helicase domain or the absence of Srs2. In this regard, *srs2Δ* and Srs2 helicase-defective alleles were tested for Rad54 foci during recombination. Cytological data indicate that both *srs2Δ* and Srs2 helicase-defective mutants lead to increase in Rad54 foci, providing evidence that Srs2 is required to suppress the accumulation of recombination foci (Burgess et al., 2009).

The helicase and translocase (anti-recombinase) activities of Srs2 are both driven by ATP-fuelled ATP binding pocket, which is a highly conserved motif in many organisms. Mutation in the ATP binding motif of SRS2 results in loss of helicase and translocase activities and further causes hyper-recombination phenotype (Palladino and Klein, 1992). In addition, loss of translocase activity leads to

changes in remodelling Rad51 nucleofilament *in vivo* (Sasanuma et al., 2013). Therefore, the ATP binding motif is essential for Srs2 to function normally in DNA replication forks and DNA homologous recombination. It has been reported that different mutations in the conserved ATP binding motifs cause various phenotypes. The *srs2* mutant allele used in this study, *srs2-101*, was previously experimented that a base pair change in the conserved ATP binding domain results in the loss of helicase activity and further causes increase in UV sensitivity and hyper-recombination (Palladino and Klein, 1992). However, it is also reported that the level of hyper-recombination varies among mutations in the helicase consensus domains, suggesting that helicase activity is tightly correlated with recombination (Palladino and Klein, 1992). Furthermore, consistent with this suggestion, the most hyper-recombination allele is also the most UV-sensitive, providing stronger evidence that the helicase activity is closely linked to these mitotic phenotypes (Palladino and Klein, 1992).

The study of Srs2's role in mitosis is widely investigated, while its role in meiosis is however much less attended. Hannah L. Klein et al have shown that mutations in Srs2's helicase consensus sequence not only affect mitotic repair and recombination, but also lead to defects in meiosis, which reflect on reduced sporulation and spore viability, suggesting that Srs2 has a role in meiosis apart from mitosis. Accordingly, the helicases activity of Srs2 is required to maintain normal meiotic progression. Therefore the helicase deficient allele *srs2-101* diploid was examined for meiotic phenotype, as it is the most sensitive to UV among other helicase mutants. The *srs2-101* diploid attains 75% of WT sporulation and 60% spore viability that of WT (Palladino and Klein, 1992). What's more, it is also reported that only 16% of the tetrad dissected are full viable,

indicating a significant reduction in spore viability in this background compared to WT (81%). These data further evidence that Srs2, as a DNA helicase, is essential for normal meiotic progression.

1.8 Helicases in DNA recombination

Helicases are proteins known to catalyse duplex nucleic acids unwinding. This reaction is dependent on these helicases' ATP hydrolysis activity. Helicases participate not only in DNA replication, but also in DNA recombination, DNA repair, RNA splicing and translation initiation(Palladino and Klein, 1992). Although they are essentially important in both DNA and RNA metabolism, little attention has been paid to helicase in meiosis. In this study, we aim to address the importance of the DNA helicase Srs2 specifically during meiosis, which has been shown that the helicase activity is necessary for mitotic DNA repair and meiotic spore viability (Palladino and Klein, 1992). Srs2 is a 3' to 5' DNA helicase, which has been proposed to regulate HR negatively by a reduction in recombination efficiency and is important in completion of the noncrossover (SDSA) pathway in a way that is different from the crossover pathway (Ira et al., 2003). Srs2 has also been proposed to be capable of dismantling Rad51 presynaptic filament by ATPase activity in order to eliminate untimely and abnormally formed strand invasion events. Intriguingly, however, when A-box ATP binding domain of Srs2 is mutated, hyper-recombination in mitosis, increased UV sensitivity, delay in commitment to meiosis and reduced spore viability are observed (Palladino and Klein, 1992). Srs2's probable orthologue in human is hFBH1, whose helicase domain shows functional similarities to Srs2, can substitute for Srs2 function (Chiolo et al., 2007). Srs2 co-localises with Rad51, and when it is absent, there is an increase in the frequencies of recombination foci (Burgess et al., 2009) and HR

(Chanet et al., 1996; Colavito et al., 2009; Milne et al., 1995). Mutations in Srs2's DNA helicase consensus domain or deletion of Srs2 both result in increasing recombination frequencies (hyper-recombination) in mitosis (Palladino and Klein, 1992). The hyper-recombination phenotype of Srs2 helicase defective and deletion is likely due to the lack of translocase activity as there is no (or reduced) negative regulation for Rad51 presynaptic filament. Rad52 epistasis group proteins are required for recruitment of Rad51 to ssDNA, which helps Rad51 to compete with RPA for binding. Importantly, when Srs2 is absent, the requirement of Rad51 for Rad52 epistasis group proteins is reduced, hence reiterating that Srs2 negatively regulates Rad51 binding to ssDNA (Burgess et al., 2009; Colavito et al., 2009; Liu et al., 2011; Seong et al., 2009). This inhibitory mechanism may prevent second end capture, thus directing DSB repair towards NCO via SDSA pathway (Ira et al., 2003, Figure 1.8).

Srs2 might also be important for meiosis as the absence of its orthologue in *S. pombe* results in severe meiotic defects. Accordingly, these defects are associated with the observations that Rad51 foci are persistent and chromosomes are segregated poorly (Colavito et al., 2009; Sun et al., 2011). In *S. cerevisiae*, both the *srs2-101* mutant allele (mutated at the ATP binding pocket) and *srs2* severely reduces spore viability and delays meiotic progression (Palladino and Klein, 1992).

Unlike in mitosis, meiosis is complicated by the fact that proper segregation between homologous chromosomes are ensured by establishing COs mediated by a second RecA orthologue Dmc1, whereas only NCOs are produced in mitosis. In addition, the majority of COs are generated by ZMM proteins with some minor ZMM independent pathway (Jessop et al., 2006). Therefore how Srs2 regulates the

balance between RecA proteins during strand invasion in this complicated mechanism remains to be determined.

Another helicase Sgs1, which belongs to RecQ family of DNA helicases including BLM, WRN, RT/REC4, RECQ1, RECQ5, and RECQ1 in vertebrates, plays an important role in maintaining the genome integrity by their activity of anti-HR (Ira et al., 2003). Loss of BLM activity increases exchange between sister chromatids and the risk of cancer (Bernstein et al., 2010). Similarly in *S. pombe* and *S. cerevisiae*, Sgs1 is required for full spore viability, and among the viable spores in budding yeast, an increase in CO is observed in the absence of Sgs1. Interestingly, the absence of both helicases of Srs2 and Sgs1 results in synthetic lethality, suggesting that helicase activity is required to prevent accumulation of toxic intermediates when undergoing meiosis.

1.9 Initial aim of this study

Our previous data indicate that *srs2-101* cells processed meiotic DSBs more quickly than wild-type cells based on both steady-state and cumulative DSB levels (L. Hulme et al. 2008, unpublished data, also see Figure 3.2 and 3.4). The first aim of this study is to find out the cause of the rapid meiotic repair by which cells undergo meiosis without functional helicase/translocase activity. We hypothesised that strand invasion between sister chromatids would be a more preferable option when helicase/translocase activity of Srs2 is absent because Srs2 is proposed to antagonise Rad51, which is essential for intersister recombination process. Furthermore, the up-to-date data have not fully addressed meiotic defects of *srs2-101* cells (e.g. delayed meiosis progression, elongated lifespan of the SC and reduced spore viability). We therefore aim to find out the

answers for these using cytological approaches, including surveillance of SC formation/dissolution, spindle pole body (SPB)/ tubulin (TUB) and most importantly, Rad51 localisation in nucleus.

Chapter 2

Materials and Methods

2.1 Materials

All media was made up with deionised water (dH$_2$O) and autoclaved with the standard program, which includes 15 minutes of sterilisation. All solutions were also made up with dH$_2$O using the same autoclave program as stated above. Percentages used in this thesis are w/v for solid chemicals and v/v for liquid solutions.

2.1.1 Media

YEPD

Standard yeast growth media: 1% yeast extract (Difco), 2% peptone (Difco), 2% D-glucose (Fisher Chemical), 40 mg/l adenine. Solid YPD medium contains 2% agar (Difco).

Yeast strains express antibiotic resistant genes were selected on YPD plates with specific concentration of antibiotics as followed:

200 µg/ml of G418 sulfate (MELFORD) for *KanMX* strains

200 µg/ml of hygromycin B (Duchefa Biochemie) for *HPMX* strains

200 µg/ml of nourseothricin- sulfate (Duchefa Biochemie) for *NatMX* strains

Antibiotics were added to autoclaved YPD medium when cooled down to 55°C

YPG

Yeast growth medium for selection against petite mutants: 15% glycerol (BDH), 1% yeast extracts (Difco), 2% peptone (Difco), 2% agar (Difco).

Minimal medium

Minimal plates contains 0.67% yeast nitrogen base without amino acids (Difco), 2% D-glucose (Fisher Chemical), 2% agar (Difco).

Synthetic Complete (SC) medium

The components of SC medium are exactly the same as minimal medium, except for 0.85 g/l of dropout mastermix and 1 μl/ml of 2M NaOH. Complete mastermix contains the ingredients as shown below:

0.8g adenine, 0.8g arginine, 4.0g aspartic acid, 0.8g histidine, 2.4g leucine, 1.2g lycine, 0.8g methionine, 2.0g phenylalanine, 8.0g threonine, 0.8g tryptophan, 1.2g tyrosine, 0.8g uracil. Dropout medium is basically the same as SC medium but one or more supplements are excluded.

Potassium acetate (K-acetate) medium

K-acetate liquid was used to initiate yeast sporulation contains 1% potassium acetate (J.T. Backer) and is supplemented with appropriate amino acids (Sigma) at specific concentrations for auxotrophies of the strains used in this study. The concentrations for each amino acid are as followed: 0.2g adenine, 0.2g arginine, 1.0g aspartic acid, 0.2g histidine, 0.6g leucine, 0.3g lycine, 0.2g methionine, 0.5g phenylalanine, 2.0g threonine, 0.2g tryptophan, 0.3g tyrosine, 0.2g uracil. Solid K-acetate plate includes 2% agar (Difco) and 0.1% D-glucose (Fisher Chemical).

PSP2 medium (presporulation medium)

0.67% yeast nitrogen base without amino acids (Difco), 0.2% yeast extract (Difco), 1% potassium acetate (J.T. Backer), 50mM potassium phthalate, pH5.0.

2TY

Bacterial growth medium: 1.1% tryptone (Difco), 1% yeast extract (Difco), 0.5% NaCl. Solid medium contains 1.5% agar (Difco), pH7.4.

Ampicillin 2TY medium: 50 µg/ml ampicillin (Sigma) was added to autoclaved and cooled to 55°C 2TY broth. This medium was used to select DH5α strains containing plasmids expressing β-lactamase.

2.1.2 General solutions

50x TAE: 2M Tris-acetate, 50mM EDTA, pH8.0

20x SSPE: 3.6M NaCl, 200mM NaH_2PO_4, 20mM EDTA, ph7.4

10xTE: 100mM Tris-HCl, 10mM EDTA, pH8.0

RNaseA: 10 mg/ml RNaseA in 10mM Tris-HCl (pH7.5), 22.5mM NaCl. Heated in heating blocks at 100°C for 15 minutes, and slowly cooled down to room temperature. Stored at -20°C.

6x DNA loading buffer (2-dye front): Xylene cyanol (BDH), Bromopfenol Blue (Sigma), 10% SDS (Fisher), Glycerol (Fisher), H_2O

2.1.3 CTAB DNA extraction solutions

CTAB dilution solution: 1% CTAB (Sigma), 50mM Tris-HCl (pH 7.5), 10mM EDTA (pH 8.0); filter sterilised.

CTAB extraction solution: 3% CTAB (Sigma), 100mM Tris-HCl (pH 7.5), 25mM EDTA (pH 8.0), 2M NaCl, 2% PVP40.

CTAB spheroplasting solution: 1M Sorbitol (Sigma), 50mM KPO$_4$ Buffer (pH 7.5), 10mM EDTA (pH 7.5).

Proteinase K: 10mM Tris-HCl, 2mM CaCl2, 50% glycerol, solution was filter sterilised prior to the addition of Proteinase K to a final concentration of 20mg/ml.

Sorbitol solution: 0.9 M Sorbitol (Sigma), 100 mM Tris-HCl, 100 mM EDTA (pH 8.0).

Meiotic time course spheroplasting solution: 20% Glycerol, 1 M Sorbitol, 50 mM KPO$_4$ Buffer (pH 7.5), 10 mM EDTA (pH 7.5).

2.1.4 Solutions for plug DNA preparation

SCE solution: 1M sorbitol, 0.1M sodium citrate, 0.06M EDTA, pH7.0, filter-sterilised.

1% low melting point (LMP) agarose mix: 1% LMP, 0.125M EDTA, pH7.5. Microwaved and equilibrated at 40°C. This solution has to be made freshly on the day of experiment to avoid agarose hydrolysis.

Solution 1: SCE solution plus 5% β-mercaptoethanol and 1mg/ml zymolyase 100T. This solution must be made freshly and kept on ice until use.

Solution 2: 0.45M EDTA pH7.5, 0.01M Tris-HCL pH7.5, 7.5% β-mercaptoethanol, 10 µg/ml RNase A. This solution also needs to be freshly made on the day of use.

Solution 3: 0.25M EDTA pH7.5, 0.01M Tris-HCl pH 7.5, 1% sarkosyl (from 10% sarkosyl solution, filter-sterilised), 1mg/ml proteinase K (directly added as a powder). This solution can be prepared without the addition of proteinase K, filter-sterilised and kept at room temperature. Add proteinase K before use.

Plug storage solution: 0.05M EDTA pH7.5, 50% (w/v) glycerol. Filter-sterilise and keep at room temperature.

Running buffer: 2L 0.5X TBE

Running gel: 1.3% LMP (1.95g of LMP in 150ml of 0.5X TBE)

2.1.5 Solutions for chromosome spreading

Zymolyase solution: 10mg/ml zymolyase

Digestion solution: 0.8M sorbitol, 10mM dithiothreitol (prepared from 1M stock)

Stop solution: 0.1M MES, 1mM EDTA, 0.5mM $MgCl_2$ and 1M sorbitol, pH 6.4

Fixation solution: 4% paraformaldehyde in PBS pH7.4

Detergent: 1% Lipsol

2.1.6 Yeast strains used in this study

All experiments were carried out using diploid *S. cerevisiae* strains in SK1 background. *srs2-101* mutant strains were derivatives of hAG1500, which is a *srs2-101* transformant from hAG5 by Lydia Hulme. *srs2Δ* mutants were made available from hAG1379 (a gift from Rita Cha). The genotypes of all the haploids and diploids are listed in Table 2.1 and 2.2, respectively.

Table 2.1 Haploid *S. cerevisiae* strains

Name	Genotype	Source
hAG4	*MATa ura3 lys2 ho::LYS2 leu2⁻(Xho1-Cla1) trp1::hisG*	S58, M. Lichten
hAG5	*MATα ura3 lys2 ho::LYS2 leu2⁻(Xho1-Cla1) trp1::hisG*	S60, M. Lichten
hAG1379	*MATa ura3 ho::hisG leu2::hisG,his4X arg4N, srs2Δ::KanMX4*	Rita Cha
hAG1500	*MATα ura3 lys2 ho::LYS2 leu2⁻(Xho1-Cla1) trp1::hisG srs2-101*	L. Hulme
hAG1689	*MATa lys2 ho::LYS2 ura3Δ(hindIII-smaI) arg4Δ(eco47III-hpaI) leu2::Ura3-rev-tel-arg4-ecPal9 ndt80Δ(Eco47III-BseRI)::KanMX6*	S3652, M.Lichten
hAG1695	*MATa ura3 lys2 ho::LYS2 leu2⁻(Xho1-Cla1) trp1::hisG srs2-101*	This study
hAG1742	*MATa ura3 lys2 ho::LYS2 leu2⁻(Xho1-Cla1) trp1::hisG ZIP1-GFP*	This study
hAG1743	*MATα ura3 lys2 ho::LYS2 leu2⁻(Xho1-Cla1) trp1::hisG ZIP1-GFP*	This study
hAG1746	*MATα lys2 ho::LYS2 ura3 arg4-nsp dmc1Δ::ARG4 leu2-R smo1-1*	This study
hAG1747	*MATa lys2 ho::LYS2 ura3 arg4-nsp dmc1Δ::ARG4 leu2-R smo1-1*	This study
hAG1770	*MATα ho::lys2 lys2 ura3 leu2- nuc1D::LEU2 trp1::hisG hed1::HPMX*	This study
hAG1771	*MATa ho::lys2 lys2 ura3 leu2- nuc1D::LEU2 trp1::hisG hed1::HPMX*	This study
hAG1808	*Matα lys2 ho::LYS2 leu2- arg4-nsp/arg4-nsp,bgl ura3::URA3-[arg4-vde] SPO11+ ADE2::pLW21mek1-as mek1Δ::LEU2*	This study
hAG1844	*MATα ho::LYS2 ura3 leu2::hisG trp1::hisG his3::HIS3p-GFP-TUB1-HIS3*	A. Marston
hAG1845	*MATα ho::LYS2 lys2 ura3 leu2::hisG his3-hisG trp1::hisG his3::HIS3p-GFP-TUB1-HIS3 CNM67-3mCherry-NatMX4*	A. Marston
hAG1847	*MATα ho::LYS2/ho::hisG leu2::hisG/leu2⁻(Xho1-Cla1) srs2Δ::KanMX4*	This study
hAG1886	*MATa ho::LYS2 TRP1 ura3 (VMA-201?)*	E.Strong
hAG1887	*MATα ho::LYS2 TRP1 ura3 (VMA-201?)*	E.Strong
hAG1898	*MATa ho::LYS2 ura3 leu2- trp1::hisG his3::HIS3p-GFP-TUB1-HIS3*	This study

Chapter 2
Materials and Methods

hAG1899	*MATa ho::LYS2 ura3 leu2- trp1::hisG his3::HIS3p-GFP-TUB1-HIS3 CNM67-3mCherry-NatMX4*	This study

Table 2.2 Diploid *S. cerevisiae* strains

Name	Genotype	Source
dAG1534	*MATα ura3 lys2 ho::LYS2 leu2⁻(Xho1-Cla1) trp1::hisG ZIP1-GFP* ———— —— ———— ————————— ——— ————— *MATa ura3 lys2 ho::LYS2 leu2⁻(Xho1-Cla1) trp1::hisG ZIP1-GFP*	L. Hulme
dAG1627	*MATa lys2 ho::LYS2 ura3Δ(hindIII-smaI) arg4Δ(eco47III-hpaI)* ———— —————————— ———————————— ——————————— *MATα lys2 ho::LYS2 ura3Δ(hindIII-smaI) arg4Δ(eco47III-hpaI)* *leu2::URA3-rev-tel-arg4-ecPal9* ———————————————————— *LEU2* *HIS4* ———————————————————— *his4Δ(SalI-ClaI)::URA3-rev-tel-arg4-ecPal9* *trp1::hisG srs2-101* ———————— ———————— *trp1::hisG srs2-101* *ZIP1-GFP ndt80Δ(Eco47III-BseRI)::KanMX6* ———————— —————————————————————— *ZIP1-GFP ndt80Δ(Eco47III-BseRI)::KanMX6*	M. Lichten
dAG1631	*MATα lys2 ho::LYS2 ura3Δ(hindIII-smaI) arg4Δ(eco47III-hpaI)* ———— ————————— ———————————— ——————————— *MATa lys2 ho::LYS2 ura3Δ(hindIII-smaI) arg4Δ(eco47III-hpaI)* *LEU2* ———————————————————— *leu2::Ura3-rev-tel-arg4-ecPal9* *his4Δ(SalI-ClaI)::URA3-rev-tel-arg4-ecPal9* ———————————————————— *HIS4* *ndt80Δ(Eco47III-BseRI)::KanMX6 trp1::hisG Zip1-GFP*	This study

51

	ndt80Δ(Eco47III-BseRI)::KanMX6 trp1::hisG Zip1-GFP	
dAG1633	*MATα lys2 ho::LYS2 ura3 arg4-nsp dmc1Δ::ARG4 leu2-R smo1-1* ―――― ―― ―――― ―― ―――― ――――― ―――― ―――― *MATa lys2 ho::LYS2 ura3 arg4-nsp dmc1Δ::ARG4 leu2-R smo1-1*	This study
dAG1634	*MATa lys2 ho::LYS2 ura3 arg4-nsp dmc1Δ::ARG4 leu2-* ―――― ―― ―――― ―― ―――― ――――― ―― *MATα lys2 ho::LYS2 ura3 arg4-nsp dmc1Δ::ARG4 leu2-* *trp1::hisG smo1-1 srs2-101* ――――― ―――― ―――― *trp1::hisG smo1-1 srs2-101*	This study
dAG1637	*MATa ho::lys2 lys2 ura3 leu2- trp1::hisG hed1::HPMX arg4-nsp* ――― ―――― ―― ―― ―― ―――― ―――――― ―――― *MATα ho::lys2 lys2 ura3 leu2- trp1::hisG hed1::HPMX arg4-nsp* *srs2-101* ―――― *srs2-101*	This study
dAG1640	*MATα ho::lys2 lys2 ura3 leu2- nuc1D::LEU2 trp1::hisG* ――― ―――― ―― ―― ―― ――――― ―――― *MATa ho::lys2 lys2 ura3 leu2- nuc1D::LEU2 trp1::hisG* *hed1::HPMX* ―――――― *hed1::HPMX*	This study
dAG1642	*MATα lys2 ho::LYS2 ura3 arg4-nsp/arg4-nsp,bgl leu2-* ――― ―― ―――― ―― ―――――――――― ―― *MATa lys2 ho::LYS2 ura3 arg4-nsp/arg4-nsp,bgl leu2-* *smo1-1 dmc1Δ::ARG4 hed1::HPMX nuc1D::LEU2* ―――― ―――――― ―――――― ―――――― *SMO1 dmc1Δ::ARG4 hed1::HPMX NUC1*	This study
dAG1647	*MATa ho::LYS2 lys2 ura3 arg4-nsp/arg4-nsp,bgl leu2- smo1-1* ―――― ―――― ―― ―― ――――――――― ―― ―――― *MATα ho::LYS2 lys2 ura3 arg4-nsp/arg4-nsp,bgl leu2- SMO1* *dmc1Δ::ARG4 hed1::HPMX srs2-101 nuc1D::LEU2* ――――――― ―――――― ――――― ―――――― *dmc1Δ::ARG4 hed1::HPMX srs2-101 NUC1*	This study
dAG1659	*MATα ho::LYS2/ho::hisG ura3 leu2-R/leu2::hisG arg4-nsp/arg4N* ――― ――――――――――― ―― ――――――――― ――――――― *MATa ho:: LYS2/ho::hisG ura3 leu2-R/leu2::hisG arg4-nsp/arg4N*	This study

	srs2Δ::KanMX4 dmc1Δ::ARG4 smo1-1 ————————— ————————— —————— *srs2Δ::KanMX4 dmc1Δ::ARG4 smo1-1*	
dAG1660	*MATα ho::LYS2/ho::hisG ura3 leu2- arg4-nsp,bgl/arg4N his4X* ———— ———————————— ——— ——— ———————————— —————— *MATa ho::LYS2/ho::hisG ura3 leu2- arg4-nsp,bgl/arg4N his4X* *srs2Δ::KanMX4 dmc1Δ::ARG4 hed1::HPMX* ———————————————————— —————————— *srs2Δ::KanMX4 dmc1Δ::ARG4 hed1::HPMX*	This study
dAG1661	*MATa ho::LYS2/ho::hisG ura3 leu2- arg4N nuc1D::LEU2* ———— ———————————— ——— ——— ——————— —————— *MATα ho::LYS2/ho::hisG ura3 leu2- arg4N NUC1* *trp1::hisG srs2Δ::KanMX4 hed1::HPMX* —————————————————— —————————— *trp1::hisG srs2Δ::KanMX4 hed1::HPMX*	This study
dAG1666	*MATa ho::LYS2 lys2 ura3 leu2- arg4-bgl/arg4-nsp,bgl ade2* ———— ———————— ——— ——— ——— —————————————————— ——— *MATα ho::LYS2 lys2 ura3 leu2- arg4-bgl/arg4-nsp,bgl ade2* *TRP1 srs2-101 ADE2::pLW21mek1as mek1Δ::LEU2* ———————— ———————— ———————————————— —————————— *trp1::hisG srs2-101 ADE2:: pLW21mek1as mek1Δ::LEU2*	This study
dAG1667	*MATα lys2 ho::LYS2 ura3 leu2- arg4-nsp/arg4-nsp,bgl* ————— ——— ———————— ——— ——— ———————————————————— *MATa lys2 ho:: LYS2 ura3 leu2- arg4-nsp/arg4-nsp,bgl* *dmc1Δ::ARG4 smo1-1 srs2-101 ade2 ADE2::pLW21mek1as* —————————— —————— ———————— ——— ———————————————— *dmc1Δ::ARG4 smo1-1 srs2-101 ade2 ADE2::pLW21mek1as* *mek1Δ::LEU2 trp1::hisG* —————————— ———————— *mek1Δ::LEU2 trp1::hisG*	This study
dAG1673	*MATa ho::LYS2 lys2 ura3 leu2- arg4-nsp,bgl dmc1Δ::ARG4* ————— ———————— ——— ——— ——— —————————— —————————— *MATαho::LYS2 lys2 ura3 leu2- arg4-nsp,bgl dmc1Δ::ARG4* *smo1-1 ade2 ADE2::pLW21mek1as mek1Δ::LEU2 trp1::hisG* —————— ——— ———————————————— —————————— ———————— *smo1-1 ade2 ADE2::pLW21mek1as mek1Δ::LEU2 trp1::hisG*	This study
dAG1674	*MATα ho::lys2 ura3 leu2- arg4-nsp,bgl dmc1Δ::ARG4 srs2-101*	This study

	MATa ho::lys2 ura3 leu2- arg4-nsp,bgl dmc1Δ::ARG4 srs2-101 *ade2 ADE2::pLW21mek1as mek1Δ::LEU2 trp1::hisG hed1::HPMX* ——— ————————— ——————— ———— ————————— *ade2 ADE2::pLW21mek1as mek1Δ::LEU2 trp1::hisG hed1::HPMX*	
dAG1675	*MATa ho::lys2 ura3 leu2- arg4-nsp,bgl trp1::hisG hed1::HPMX* ———————— ——— ——— ————————— ———————— ————————— *MATα ho::lys2 ura3 leu2- arg4-nsp,bgl trp1::hisG hed1::HPMX* *dmc1Δ::ARG4 ade2 ADE2::pLW21mek1as mek1Δ::LEU2* —————————— ——— ————————————————— ———————— *dmc1Δ::ARG4 ade2 ADE2::pLW21mek1as mek1Δ::LEU2*	This study
dAG1676	*MATa ho::lys2 ura3 leu2- arg4-nsp dmc1Δ::ARG4 trp1::hisG* ——— ———————— ——— ——— ——————— ——————————— ———————— *MATα ho::lys2 ura3 leu2- arg4-nsp dmc1Δ::ARG4 trp1::hisG* *srs2-101 ZIP1-GFP* ———————— ————————— *srs2-101 ZIP1-GFP*	This study
dAG1677	*MATa ho::LYS2 lys2 ura3 arg4-nsp/arg4-nsp,bgl leu2-* ——— ———————— ——— ——— ———————————————————— ——— *MATα ho::LYS2 lys2 ura3 arg4-nsp/arg4-nsp,bgl leu2-* *dmc1Δ::ARG4 hed1::HPMX srs2-101 trp1::hisG ZIP1-GFP* —————————— ——————————————— ———————— ———————— ————————— *dmc1Δ::ARG4 hed1::HPMX srs2-101 trp1::hisG ZIP1-GFP*	This study
dAG1678	*MATα ho::LYS2/ho::hisG lys2 ura3 leu2::hisG/leu2-K arg4N* ——— ———————————————— ——— ——— ———————————————— ———————— *MATa ho::LYS2/ho: :hisG lys2 ura3 leu2::hisG/leu2-K arg4N* *sae2::KanMX6 srs2Δ::KanMX4* ————————————— —————————————— *sae2::KanMX6 srs2Δ::KanMX4*	This study
dAG1679	*MATα ho::LYS2 lys2 ura3 leu2⁻(Xho1-Cla1)/leu2-K trp1::hisG* ——— ———————— ——— ——— ———————————————————— ———————— *MATa ho::LYS2 lys2 ura3 leu2⁻(Xho1-Cla1)/leu2-K trp1::hisG* *srs2-101 sae2::KanMX6* ———————— ————————————— *srs2-101 sae2::KanMX6*	This study
dAG1680	*MATa ho::LYS2 TRP1 ura3 (VMA-201?)*	This study

54

	MATα ho::LYS2 TRP1 ura3 (VMA-201?)	
dAG1681	*MATα ura3 lys2 ho::LYS2 leu2⁻(Xho1-Cla1) trp1::hisG srs2-101* ———— ——— ——— ———— —————— ———— ———— *MATa ura3 lys2 ho::LYS2 leu2⁻(Xho1-Cla1) trp1::hisG srs2-101*	This study
dAG1682	*MATa ura3 lys2 ho::LYS2 leu2⁻(Xho1-Cla1) trp1::hisG ZIP1-GFP* ———— ——— ——— ———— —————— ———— ———— *MATα ura3 lys2 ho::LYS2 leu2⁻(Xho1-Cla1) trp1::hisG ZIP1-GFP* *srs2-101* ———— *srs2-101*	This study
dAG1683	*MATa ho::LYS2/ho::hisG ura3 leu2::hisG/leu2⁻(Xho1-Cla1)* ———— —————— ——— ————————— *MATα ho::LYS2/ho::hisG ura3 leu2::hisG/leu2⁻(Xho1-Cla1)* *ZIP1-GFP srs2Δ::KanMX4* ———— ————— *ZIP1-GFP srs2Δ::KanMX4*	This study
dAG689	*MATα ho::LYS2 lys2 ura3 leu2⁻(Xho1-Cla1)/leu2-K trp1::hisG* ———— ———— ——— ——— —————————— ———— *MATa ho:: LYS2 lys2 ura3 leu2⁻(Xho1-Cla1)/leu2-K trp1::hisG* *sae2::KanMX6* ———— *sae2::KanMX6*	This study
dAG1691	*MATa ho::LYS2 ura3 leu2- trp1::hisG his3::HIS3p-GFP-TUB1-HIS3* ———— ———— ——— ——— ———— ———————————— *MATα ho::LYS2 ura3 leu2- trp1::hisG his3::HIS3p-GFP-TUB1-HIS3*	This study
dAG1692	*MATa ho::LYS2 ura3 leu2- trp1::hisG his3::HIS3p-GFP-TUB1-HIS3* ———— ———— ——— ——— ———— ———————————— *MATα ho:: LYS2 ura3 leu2- trp1::hisG his3::HIS3p-GFP-TUB1-HIS3* *CNM67-3mCherry-NatMX4* ———————— *CNM67-3mCherry-NatMX4*	This study

2.2 Growth and culture of *Saccharomyces cerevisiae*

2.2.1 General methods of isolating strains with desired genotype

Haploids strains used to make diploids were generally made by two different methods. Haploids were transformed by lithium acetate transformation or electroporation with desired genes directly in the situation where these genes were deleted or disrupted. Transformation methods will be indicated later in this chapter. In a more routine way, diploid strains with desired genotypes were sporulated and dissected, where desired genes were segregated to tetrad spores. The genotypes of spores were determined based on nutrient marker. In most cases, these manipulated genes were required in amino acids biosynthesis pathways that were essential for vegetative growth, and thus can be selected by growth on SC-medium lacking specific supplements. On the other hand, haploids that harbour antibiotic resistance genes marked with KanMX, HPMX, or NatMX were identified by growth on YPD containing 200μg/ml of G418, hygromycin or nourseothricin- sulfate respectively. For strains with no prototrophic or antibiotic resistance phenotypes (for e.g. VDE insertion at *TFP1* generating *TFP1::VDE*, or point mutation at *SRS2* creating *srs2-101*), diagnostic PCR with primers specific to the genes were designed to identify them. For identifying *TFP1* and *TFP1::VDE*, different product sizes indicated the relevant genotype. In the case of identifying *srs2-101*, where PCR product sizes were exactly the same, was differentiated from *AvaII* digestion, which *SRS2* digests contained 2 distinct bands, whereas *srs2-101* remained uncut. In this study, all the *srs2-101* derivatives were made from the original *srs2-101* strain hAG1500, which was hAG5 transformed with a *srs2-101* mutated gene fragment in SK1 background. All *srs2-101* diploids were checked by *AvaII* restriction digest. The base pair change in cells expressing *srs2-101*results in loss of an *AvaII* restriction site.

2.2.2 Haploid mating

Haploids of opposite mating type (MAT a or MAT α) were streaked out onto solid YPD plates prior to mating. Fresh single colonies of opposite mating type were picked by sterile plastic loops and mixed evenly onto the surface of a YPD plate in a small patch. The plate with the mating patch was incubated at 30°C for 24 to 48 hours. After incubation, the patch of cells was streaked out onto a fresh YPD plate and incubated for 2 days to allow single colonies to form. Colonies were patched onto a fresh YPD plate and crossed with mating testers hAG55 (MAT_a) and hAG56 (MAT_α). The patches were replica-plated onto a solid minimal media plate after 1 day of 30°C incubation. The mating type testers were wild type genotypes apart from having a mutation in *ura2*. In addition, wild type *S.cerevisiae* strains are able to grow on minimal media. Therefore, if mating of the two strains took place between the mating type tester strains and one of the strains used in this study (all *URA2*), then the strains were able to grow on minimal media due to all nutritional mutations in strains used in this study were complemented. Thus, growth with hAG55 (MAT a) represents a MAT α colony, and growth with hAG56 (MAT α) represents a MAT a colony. On the other hand, absence of growth with either mating type testers on minimal media showed that the original colony was diploid.

2.2.3 Standard 5ml cultures

Standard yeast 5ml cultures were made from freshly streaked single colonies and incubated at 30°C on a rotor drum overnight. These cultures were used for: yeast genomic DNA extraction, -80°C stock cells, starter culture for lithium-acetate transformation, protein extraction and starter culture for synchronous sporulation.

2.2.4 Diploid strains sporulation on solid potassium-acetate media

Sporulation of diploid strains on solid media was utilised for sporulation prior to tetrad dissection in strain-making strategies, genetic assays of recombination and random spore analysis (this technique will be introduced later in this chapter). A single colony of a diploid strain was streaked out from -80°C stock cells onto a YPD plate prior to sporulating. The single colony was patched onto a YPD plate, incubated overnight and replica-plated onto a potassium-acetate plate at 30°C. After incubation for 2 to 3 days, diploid cells were induced to undergo meiosis due to nutritional devastation. Almost 100% sporulation was obtained after incubation in the most of the strains used in this study.

2.2.5 Yeast lithium acetate transformation

Haploid yeast strains were transformed with linear or plasmid DNA molecules by the lithium-acetate method. A haploid strain that needs to be transformed was streaked onto a fresh YPD plate. When single colonies formed after incubation, standard 5ml culture was made from one of these colonies. The overnight culture was diluted into 50ml of YPD broth in a 250ml conical flask to an OD_{600} of 0.2, followed by growing at 30°C for 3 to 4 hours to allow at least 2 cell divisions to take place. Cell growth to an OD_{600} of 0.8 must be achieved. Cells were transferred to 50ml falcon tubes and pelleted at 3000rpm for 5 minutes. Cells were washed in 25ml sterile water twice, pelleted and resuspended in 50% PEG4000 with 100mM lithium-acetate, 278μg/ml denatured salmon sperm DNA. Chemicals were added in this order to reduce lithium-acetate to induce damage to cells. 1μg of transforming DNA was added to the competent cells and mixed thoroughly. Cells were mixed well by vortexing and incubated at 30°C for 30 minutes, followed by

heat shock incubation at 42°C for 30minutes. Cells were washed in 1ml sterile water and plated onto selective media and incubated for at least 3 days to allow transformants to grow.

2.2.6 Synchronous sporulation of *S.cerevisiae*

15ml of liquid YPD broth was inoculated with a fresh single colony. The culture was grown in a 250ml conical flask at 30°C for 20 hours, 270rpm. The culture was multiple diluted and inoculated into 250ml 30°C pre-warmed PSP2 pre-sporulation starter media in a 2 litre conical flask. Normal dilutions for the original YPD culture into pre-sporulation media ranged between 1:125 to 1:500, depending on the optical density at 600nm after 22-24 hours of incubation at 30°C, 270rpm. Cultures with values of OD_{600} between 0.7 and 0.8 (actual 1.4 to 1.6) were used for synchronous sporulation. Cultures were poured into 250ml centrifuge tubes and pelleted at 4,500rpm for 2 minutes. Cells were then vigorously washed in 250ml of 1% potassium-acetate, which was also pre-warmed to 30°C. Cells were pelleted and resuspended in 250ml of 1% potassium-acetate with various supplements that were needed for different strains. Cells were then quickly transferred 2.8 litre baffle flasks (pre-warmed to 30°C), and incubated at 30°C, 270rpm for the rest of the time course. Samples of time point 0 were then taken immediately when baffle flasks were placed in the incubators.

2.2.7 Yeast random spore analysis

Yeast strains to be analysed by random spore analysis were streaked out onto fresh YPD plates and incubated at 30°C for 2 days. A fresh diploid colony was sporulated on solid potassium-acetate media. Tetrads formed after a few days of incubation, and harvested by sterile plastic loops and incubated in 50μl of β-

glucuronidase (9,880U/ml, Sigma) on a rotor drum at 30°C for 4 hours. Following

by the addition of 950μl of 0.1% tween20, tetrads were separated by intensive

sonication (amplitude 5.5 microns) for at least 3 times, plus 1 minute on ice

between each sonication. More sonication pulses were needed if too many non-

single spores were observed. Numbers of single, double, triple, quadruple and

diploid cells were counted on a haemocytometer. The numbers obtained from the

haemocytometer were used to calculate the dilution and volume required for

roughly 300 cells on each YPD plate. A serial dilution to 10^{-4} was used for sonicated

cells. Dilutions of 10^{-3} and 10^{-4} were plated onto YPD plates with calculated

volume that was needed to get about 300 cells each plate. Recombination

frequency was calculated from the frequencies of arginine prototrophic colonies

relatives to viable colony forming units (CFU). Corrections were made for the

presence of non-single spores.

2.3 Molecular Biology Techniques

2.3.1 Yeast genomic DNA mini-prep (chemical method)

To extract the genomic DNA (gDNA) from yeast cells for PCR amplification or

enzyme digestion, 1.5ml of yeast liquid culture was used and gDNA was extracted

by the mini-prep extraction methods. Firstly, yeast cells were streaked out from -

80°C stock on YEPD plates and incubated in 30°C culture room overnight. Single

colonies were picked up by sterilized plastic loops and inoculated into a 5ml of

YPD broth in test tubes and incubated on the wheel in 30°C constant temperature

room overnight. 1.5ml of liquid culture was transferred to a clean eppendorf tube,

and centrifuged at full speed (13200rpm) for 30 seconds. Most of the supernatant

was poured off, and resuspended carefully by pipetting mixture up and down.

250μl of Zymolyase was added and mixed with the cell suspension, 30 minutes of

37°C water bath was then applied for zymolyase reaction. To confirm the yeast cell wall was degraded after the treatment of zymolyase, cells were observed under the light microscope (Canon). Cells that were already treated well with zymolyase appeared to be round and dark. Additionally, 200μl of lysis buffer and 100μl of 1M potassium acetate were added to the eppendorf tube, and the suspension was mix by inverting the tubes a few times. This would make a thick sticky mass. This was then followed by 10 minutes of full speed (13,200rpm) centrifugation at 4°C. This could pull some impurities such as proteins down to the bottom of the tube. The supernatant was poured into a new tube and the old one was discarded. 700μl of isopropanol was added and mixed by flipping the tube. The tube was centrifuged at full speed for 2 minutes. Supernatant was then removed, and 300μl of TE buffer and 2μl of DNA free RNase were added. The tube was incubated in 37°C water bath for 30 minutes and checked if the pellet was dissolved from time to time. 300μl of isopropanol and 30μl of sodium acetate were added, then centrifugation at full speed for 2 minutes. Discarded the supernatant and add 700μl of 70% ethanol to wash the pellet. Finally supernatant was removed and 30μl of TE buffer was added to dissolve the pellet. The gDNA was stored in -20°C if necessary.

2.3.2 Yeast genomic DNA mini-prep (MasterPure™ Yeast DNA purification Kit)

Yeast cells saturated from 1.5ml YPD culture were transferred to an eppendorf tube and pelleted in a microcentrifuge at 13,200rpm for 2 minutes. Most of the supernatant was discarded and the cell pellet was resuspended by the rest of the supernatant. 300μl of Yeast Cell Lysis Solution was added to the cell pellet collected from the saturated culture. The cell pallet was then treated with 1μl of 5

μg/μl RNase A (included in the kit, thermostable RNase A). To mix the cell pellet and RNase A, vortex mixing and pipetting the cells repeatedly with 1 ml pipette tip were applied. The cells were then incubated in 65°C incubator for 15 minutes to allow RNase A to digest unrequired RNA in the yeast cells. The eppendorf tube was transferred on ice for 5 minutes after the incubation, following by the addition of 150μl of MPC Protein Precipitation reagent and vortex mixed for 10 seconds. Cellular debris was pelleted by centrifugation in a microcentrifuge at 13,200rpm for 10 minutes. Cell debris and genomic DNA were separated at this stage. The supernatant was transferred to a clean eppendorf tube. 500μl of isopropanol was added to the tube, following by inversion of the eppendorf tube to mix the solution thoroughly. The DNA in the solution was pelleted by centrifugation at 13,200rpm for another 10 minutes. The supernatant was removed by pipetting and discarded. 0.5ml of 70% ethanol was added to the eppendorf tube to wash the DNA pellet, this was done by inverting the tube carefully for a few times.   Ethanol was carefully removed by pipetting and discarded. Additional centrifugation was applied to remove the remaining ethanol in the tube. The DNA pellet was air-dried and became transparent, and resuspended in 35-50μl of 1x TE buffer depending on the size of the DNA pellet.

2.3.3 Yeast Cell Preparation for CTAB Genomic DNA extraction

25 ml of yeast cells were harvested from meiotic time courses hourly into falcon tubes containing 6ml of 50% glycerol and 300μl of 10% sodium azide. Volumes of harvested cells from meiotic culture may be adjusted for different cell densities. Cells were pelleted by centrifugation at 4,000rpm, room temperature for 5 minutes. Supernatant was removed by pipetting and the cell pellets were resuspended in 1ml of spheroplasting solution plus 20% glycerol. Pelleted cells

again by centrifugation at 4,000rpm at room temperature for 5 minutes. Supernatant was removed thoroughly, and cells were frozen and stored at -80°C freezer.

2.3.4 CTAB High Efficiency Genomic DNA Extraction

To acquire high purity and concentration of genomic DNA (gDNA), CTAB gDNA extraction was implemented for special experiment such as Southern Blot. 25ml of yeast cells harvested from meiotic cultures hourly (from 0h~8h) were thawed on ice and washed in 1ml of ice-cold spheroplasting buffer, resuspended and transferred into clean eppendorfs. Cells were then pelleted by 4,000rpm centrifugation for 1 minute. Most of the supernatant was removed by pipetting and the pellet was resuspended in 100μl of spheroplasting buffer with 100T zymolyase and 1% mercaptoethanol (50μl). The cells were then incubated in 37°C water bath for 5 minutes. Mixing was applied by inverting the tubes. These processes were repeated three times in total. The extent of spheroplasting of the cells was checked by visual inspection in a microscope. 37°C of pre-heated CTAB extraction solution was added when more than 80% of the cells were spheroplasted, following by addition of 5μl proteinase K and mixed gently. The cell suspension was incubated in 37°C water bath for 15 minutes with gentle mixing and inverting in every 5 minutes. 100μl of IAA (isoamylalcohol): chloroform mixture (1:24) was added to extract the DNA complex. The mixture was incubated in room temperature for 2 minutes, subsequently the mixture was vortexed for a few seconds and centrifuged at full speed for 15 minutes. The aqueous phase was transferred to clean eppendorfs and 2μl of RNase was added. The mixture was incubated in 37°C water bath for 30 minutes for Rnase digestion. CTAB solution was layered to the mixture carefully. The mixture was then incubated in room

temperature for 10 minutes to allow further DNA precipitation. After the incubation, the precipitate became visible; the supernatant was removed carefully without discarding the precipitate. Then the precipitate was washed in 1ml of ice-cold 0.4M NaCl in TE twice and 300μl of ice-cold 1.42M NaCl in TE to resuspend the precipitate the DNA. The DNA was precipitated by addition of 600μl of 70% ethanol then centrifuged at full speed for 1 min. Finally 70~100μl of ice-cold TE buffer was added to the pellets depending on the sizes of the pellets. Overnight incubation at 4°C was applied to completely dissolve the DNA pellet in TE buffer.

2.3.5 DNA restriction digests

Purified DNA was digested with restriction enzymes under the conditions provided by the manufacturers. All digests were made up with Milli-Q H_2O and incubated in the 37°C water bath. Digests of yeast gDNA for Southern analysis were reacted for 3~4 hours or overnight for larger amount of gDNA. For analytical digests, 1 hour was applied for the incubation.

2.3.6 Native DNA electrophoresis

For routine DNA sizes analysis, purified DNA was added with 6x DNA loading dye and fragmented in 1% agarose gel in 1x TAE buffer at 80V for an hour. For DNA preparations of Southern blot analysis, DNA was also added with 6x DNA loading dye before loading, and DNA samples were separated in 250ml of 0.5% 25cm x 15cm TAE gel, applying 65V with buffer circulation overnight. Ethidium Bromide (200μg/l) was added to running buffer prior to electrophoresis.

2.3.7 Pulse-field gel electrophoresis (PFGE)

2.3.7.1 Making DNA Plugs

15~30ml of sporulating cultures at each time point of meiotic culture were harvested in 50ml falcon tubes. Cell cultures were pelleted for 4 minutes at 3200g. Cells were then resuspended in 5ml of 50mM EDTA pH7.5. This wash process was repeated once to remove sporulation medium completely. During the washes, the following mix was made: 0.83ml of 1% LMP agarose plus 0.17ml of Solution 1. The agarose and Solution 1 mixture was then vortexed and kept at 40°C. The supernatant of cell pellets was then discarded. After the last wash, 100μl of 50mM EDTA was added to resuspend the cell pellets. The pellets were transferred to Eppendorf tubes, equilibrated 30 seconds at 40°C. After the short equilibration, pre-warmed 200μl of LMP/Solution1 mix was added to the cell suspension, vortex briefly. The mixtures were promptly pipetted into plug mold. This step has to be carried out quickly as LMP solidifies in a short time. The plugs were cooled down for 10 minutes at 4°C. Small spatulas were used to express the plugs out from the plug mold into 3ml of Solution 2. The plugs were incubated in Solution2 for an hour at 37°C. Solution 2 was subsequently replaced with 3ml of Solution 3. The plugs were incubated overnight at 50°C. Solution 3 was then poured off and the plugs were washed twice with 3ml of 50mM EDTA for 15 minutes on a rotating wheel. 50mM EDTA was then replaced with 3ml storage buffer. The plugs were stored in storage buffer at -20°C.

2.3.7.2 Pulse-field gel electrophoresis gel running

2.2L of 0.5X TBE was prepared and 150ml of the TBE buffer was used for making 1.3% LMP agarose gel. The agarose gel was melted by heating in a microwave and kept at 55°C. The rest of the buffer was poured into the apparatus tank, the

circulating pump as well as the cooling system were switched on to cool down the running buffer. The temperature was set to 14°C. The plugs were cut into one-third using a clean razor blade. The plugs were washed in filter-sterilised 50mM EDTA and laid on the tooth of the comb. The plugs were then sealed on the comb with a few drops of LMP agarose. Set the comb vertically on the gel cast and slowly pour the agarose into the cast. Let the gel to solidify for 30 minutes at room temperature. The comb was slowly removed from the gel. The extruding bit of the plugs were then eliminated using a clean razor blade. The gel cast was dismantled and the gel was put into the apparatus properly with pre-cooled running buffer. The gel was equilibrated in the gel tank apparatus for 15 minutes. Then began electrophoresis. In this study, to separate Chromosome III efficiently 15 seconds for initial and final switch time, 120° switch angle, 6V/cm and 36-hour run time were applied.

2.3.8 Gel purification of DNA fragments

Required DNA fragments from purified DNA molecules such as plasmid DNA, genomic DNA or PCR products were separated by electrophoresis. The specific bands of DNA were excised from the agarose gel on the UV illuminator (UVP Inc.). DNA fragment of interested was extracted by using QIAGEN QIAquick® Spin kit. Gel-DNA slice was weighed and put in a clean eppendorf tube. Three volumes of Buffer QG were added to one volume of the gel slice. The gel-solution mixture was incubated at 50°C for 10 minutes with intermittent mixing (every 2~3 minutes) during incubation to help dissolve the gel. Incubation time may vary depending on percentage of the gel. After the gel slice was dissolved completely, the solution was added with one gel volume of isopropanol to increase yield of DNA fragments between 4kb and 500bp. The mixture was added to QIAquick® Spin Column, which

was placed in a provided 2ml collection tube. Centrifugation was applied at full speed (13200rpm) for 1 minute. The flow-through was discarded. To remove agarose thoroughly, 0.5ml of buffer QG was added to the sample and spun at full speed for 1 minute. The flow-through was then discarded again. To wash the sample, 0.5ml of Buffer PE was added to the sample, centrifugation was applied at full speed for 1 minute. The flow-through was removed. The spin column was spun for additional 1 minute to remove the rest of ethanol in the column. The spin column was placed onto a new eppendorf tube. To elute the DNA in the column, 50µl of Buffer EB was added to the centre of the membrane in the column and incubated for 1 minute at room temperature. 1 minute of centrifugation was applied to elute the DNA from the membrane. DNA sample was stored at -20°C for further use.

2.3.9 Ethanol precipitation of DNA

DNA from PCR products or gel purification was further precipitated by ethanol precipitation processes. 3M sodium acetate was added to the DNA sample at one tenth of the volume of the sample. The sample was mixed by inverting the tube for a couple of times. 2 volumes ice cold 100% ethanol was added to the solution to aid precipitation. DNA was further precipitated by occasional mixing and the samples were stored at -20°C overnight. Precipitated DNA was collected by full speed centrifugation (13200rpm) for 10 minutes. DNA pellets were washed in 1ml of 70% ethanol at room temperature. Extra centrifugation was then applied to remove the rest of ethanol left in the tubes, and the pellets were air-dried until the pellets became semi-transparent. 1x TE buffer was added to dissolve DNA pellets. Samples that were added with 1x TE buffer were incubated at room temperature for at least 1 hour to allow DNA to dissolve completely.

2.3.10 Polymerase chain reaction (PCR)

To amplify the gene of interested, polymerase chain reaction (PCR) was used. To begin with, DNA template was prepared by methods indicated above. For routine DNA amplification, DNA template (genomic DNA or plasmid DNA) was mixed with 10x PCR buffer (Bioline), 50mM $MgCl_2$, 10mM dNTP, forward and reverse primers (10mM each), and DNA Taq polymerase. The sample underwent a general PCR program: 95°C initialisation for 2 minutes, 95°C denaturation for 30 seconds, X°C annealing for 30 seconds, 72°C extension/elongation for Y minutes, where X is the primer-specific annealing temperature, and Y corresponds to product size and DNA polymerase efficiencies (e.g. MangoTaq 1kb/30sec). The cycle started from denaturing to extension for 30 times in general. PCR reaction was attenuated with a final extension for 10 minutes.

2.3.11 Yeast colony PCR

Yeast crude cell extract was prepared from a fresh single colony in the following way. A single colony was grown to a certain size (>1mm in diameter) and harvested by a sterilised loop. Cells were then mixed with 30μl 0.5% NaOH and heated in heating blocks at 100°C for 15 minutes. 5μl of crude extract was then used for PCR DNA template.

2.3.12 Southern Blotting

2.3.12.1 Electrophoresis of Southern gels

0.5 to 1μg of Sample DNA (from time-coursing) was digested by restriction enzyme for 3 to 4 hours in 37°C water bath or 37°C room for overnight. The 0.5% TAE agarose gel was then prepared by adding 1.25g of agarose in 250ml TAE buffer and microwave for a few minutes. The molten agarose was poured in a gel tray (25cm x 15cm) after it cooled down in 65°C water bath for 30 min. 10μl of

ethidium bromide was added to the buffer in the tank. The power pack was applied to run the gel at 65V with buffer circulation overnight.

2.3.12.2 Gel washing

The gel was rinsed in dH_2O for 15 min twice on a shaker at slowest speed. The gel was then washed in 0.25M of HCl for 15 minutes. This was followed by twice 15 min of dH_2O to remove HCl completely. Subsequently, the gel was rinsed in 1L of 0.4M NaOH for 45 minutes. The high concentration of NaOH denatures double-stranded DNA to become single-stranded that is compatible to be hybridised with specifically designed probes.

2.3.12.3 Blotting (vacuum)

The blotting apparatus was set up in the order of supporter screen, tube, Whatman blotting paper (20 x 28 cm), Hybond N^+ membrane (15 x 25 cm) and gasket (the Hybond N^+ membrane must be overlapped by the gasket, Figure 2.1). The agarose gel was placed on the gasket and overlapped the gasket on all sides. For vacuum blotting, 1L of NaOH was poured into the blotting apparatus, and vacuuming was applied (50-100mbar) for 2hr. The pressure was checked intermittently.

2.3.12.4 Blotting (capillary)

A stack of dry paper towels >5cm was prepared to bolster the whole transfer apparatus. Then a series of 3mm Whatman blotting papers were cut as follows: 5 pieces 20 x 28.5 cm (wet one piece in 1.5M NaCl, 0.5M NaOH), 3 pieces 20 x 24 cm; wet in 1.5M NaCl, 0.5M NaOH, 2 pieces 20 x 57 cm; wet in 1.5M NaCl, 0.5M NaOH. Prepare Hybond N^+ membrane (15 x 25 cm). The capillary transfer apparatus was set up as shown in Figure 2.2. 4 dry pieces of 20 x 28.5 cm blotting papers were

placed onto the stack of towels and the wet one was then placed on top of them. The Hybond N$^+$ membrane was placed on top and the bubbles were removed by rolling a stripette over the surface. Subsequently, the gasket and the gel was placed onto the membrane and 3 wet pieces 20 x 24 cm and 2 wet pieces 20 x 57 cm of blotting papers were put on top of the stack. Note that ~0.5cm margin of the gasket is covered by the gel. Two glass trays filled up with 1.5M NaCl and 0.5M NaOH were prepared and 2 wet pieces 20 x 57 cm were dipped into the two trays to form a transfer bridge. The surface of the bridge and the glass trays were covered with cling films to avoid buffer evaporation. Finally a gel tray was placed with an object weighed <500g, and blot for 16 hours.

2.3.12.5 Post-transfer

The gel was removed from the blotting apparatus and discarded, and the Hybond N$^+$ membrane was rinsed in 200ml of 2xSSPE briefly. The membrane was then placed on blotting paper and dried in the hood. DNA was UV cross-linked onto the Hybond N$^+$ membrane at optimal mode.
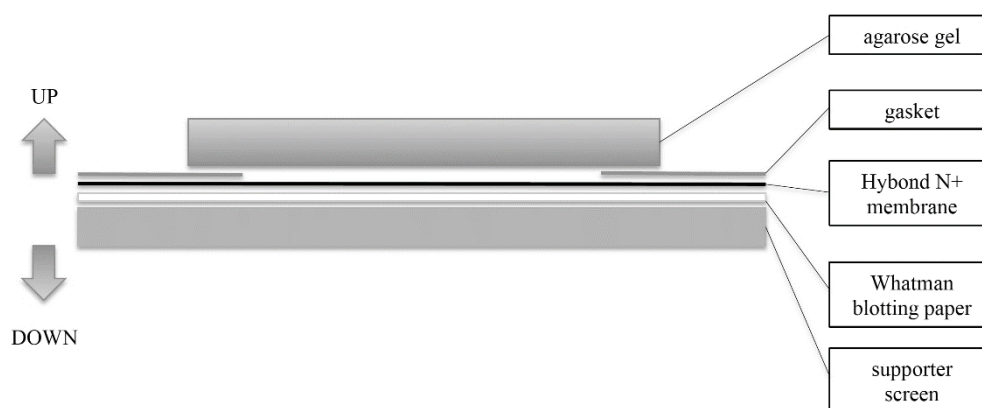
Figure 2.1. Vacuum transfer apparatus

The blotting apparatus was set up in the order of (from the bottom to the top) supporter screen, Whatman blotting paper (20 x 28 cm), Hybond N$^+$ membrane (15 x 25 cm), gasket and the agarose gel. The vacuuming was applied from the bottom of the apparatus so that the DNA on the agarose gel can be transferred to the Hybond N$^+$ membrane.
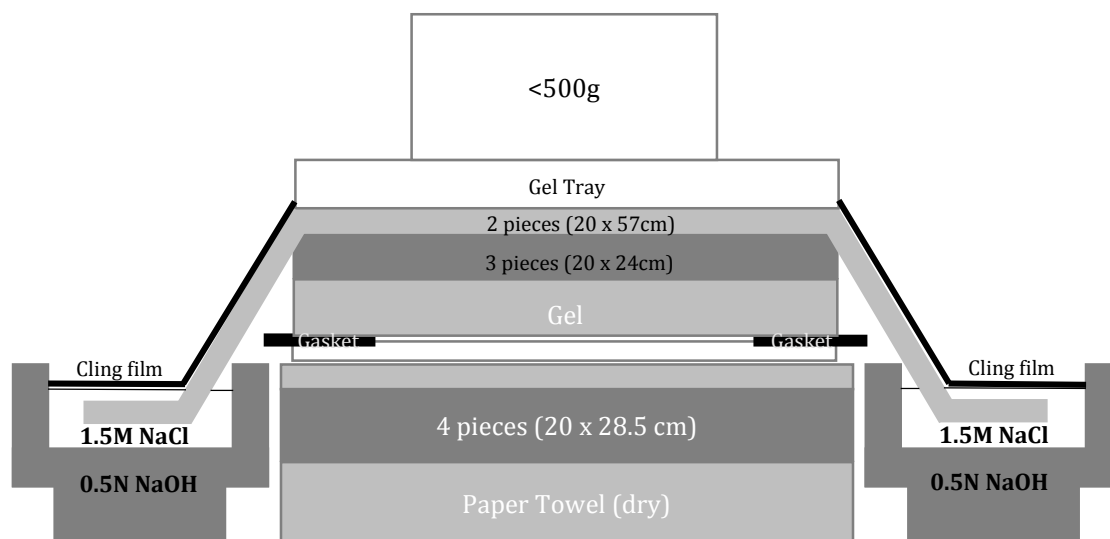
Figure 2.2. Capillary transfer apparatus

The capillary transfer apparatus was set up in the order shown above. Certain sizes of Whatman blotting papers were cut and placed onto the apparatus. The agarose electrophoresis gel containing fractionated restriction fragment DNA and the N^+-membrane were placed properly in between the blotting papers. The gasket was used to ensure that only the certain area of the gel was transferred to the membrane. A <500g object was placed on top of the stack to weight to the apparatus. Capillary action results in the buffer soaking through the transfer bridges. As the buffer flows through the gel the DNA fragments are transferred into the membrane, where DNA is bound to the N^+-membrane.

2.3.12.6 Generating ^{32}P-labelled DNA probes

To avoid contamination from genomic DNA when making DNA probes, PCR product of specific probes was gel purified. Gel purification products were used as template in random priming using ^{32}P-labelled dCTP. The template (10~20ng) was mixed with 5μl of random primer mix (HighPrime, Roche), including 1U/μl Klenow polymerase (labeling grade), 0.125mM dATP, 0.125mM dGTP, 0.125mM dTTP in 50% glycerol, and the mixture was denatured in heating blocks at 100°C for 5 minutes. The mixture was ice-chilled prior to addition of 5μl of ^{32}P-labelled dCTP. The radioactive mixture was incubated at 30°C for 30 minutes for random priming reaction to take place. Radioactive labeled probes were purified by using Bio-Spin columns (Bio-Rad), which are size-exclusion columns that remove unincorporated ^{32}P-labelled nucleotides.

2.3.12.7 Scanning densitometry and quantification

A Personal FX phosphorimager was implemented to scan the density of radiation emitted from the hybridised membranes. Quantification of emitted signals was assessed by Quantity One® software (BioRad). In brief, boundaries and numbers of lanes on the membrane were assigned by the lane tool, and lane background utility was used to eliminate background signals so that signals from background hybridisation were not included in the quantification. Bands to be quantified were assigned manually and adjusted to suitable range according to the peak areas. The quantity of each band was calculated automatically by integrating the peak area of the band with deduction of the background signals.

2.4 Methods in Biochemistry

2.4.1 Preparation of mitotic cells for protein extraction

A standard 5ml culture was made, and cells were pelleted at 4,000rpm for 5 minutes. Cell pellets were washed in 1ml of dH_2O to remove media thoroughly and transferred to clean eppendorf tubes. Centrifugation at full speed (13,200rpm) was applied subsequently to pellet cells. Cells were then frozen in liquid nitrogen and stored at -80°C ready for protein extraction.

2.4.2 Protein extraction (bead method)

Frozen cell pellets stored at -80°C were thawed on ice and resuspended in 1ml of lysis buffer (ice cold), which contained 50mM tris-HCl pH8.0, 1% NP40, 1x protease inhibitor tablet (Roche), and 2mM PMSF/ethanol. Cells were transferred to screw-capped tubes, pelleted at full speed centrifugation and washed in 1ml of lysis buffer again. 400µl of lysis buffer was added to the cell pellets with acid-washed glass beads (Sigma). Cells were broken on a Mini-Beadbeater (BIOSPEC PRODUCT) in 4°C room for 45 seconds 3 times, with cooling on ice for 1 minute between each pulses. The screw-capped tubes with broken cells were pinned holes at the bottom, fin in new eppendorf tubes and spin shortly. Glass beads were retained in the screw-capped tubes but the cell debris flowed through glass beads to new tubes. Cell debris was pelleted by additional centrifugation at 4°C for 30 minutes, full speed. The supernatant was transferred to new tubes and stored at -20°C.

2.4.3 Trichloroacetic acid (TCA) protein precipitation method

3~5ml of sporulating cell culture was harvested at each time point and subsequently washed with 1ml ice-cold dH_2O to remove sporulation medium.

After the wash, cells were resuspended in 1ml ice-cold dH$_2$O. Cells were mixed with 150µl of freshly prepared buffer D (1.85M NaOH, 7.5% β-mercaptoethanol) and incubated on ice for 15 minutes. 150µl of 55% TCA was added to the mixture and a 10-minute incubation on ice was applied. The cell suspension was then centrifuged at 14,000 rpm for 10 minutes, the supernatant was then discarded after the centrifugation. The protein pellets were resuspended with 250µl of buffer H (200mM Tris-HCl pH6.5, 8M urea, 5% SDS, 1mM EDTA, 0.02% bromophenol blue and 5% β-mercaptoethanol). Finally the protein pellets were denatured for 10 minutes at 65°C.

2.4.4 Bradford assay for protein quantification

Protein concentration of samples was determined by Bradford assay. Briefly, the standard curve was made from a known protein concentration (BSA, New England Biolabs). To measure a protein concentration of cell lysates, 3µl of 1 in 20 diluted cell lysate was added to 1ml of Bradford reagent (BioRad). The mixture was incubated at room temperature for 5 minutes. Optical density of samples was measured at 595nm and compared to the standard curve, which corresponded to protein concentrations of BSA.

2.5 Methods in cytology

2.5.1 DAPI nucleus staining

750µl of cell cultures were harvested hourly from synchronous sporulation cultures (in this case, 25ml of cell cultures were also taken out from sporulation media for DNA extraction). Cells were fixed in 750µl of 100% ethanol and stored at -20°C. All samples were nucleolus stained with 1µl of DAPI (4',6-Diamidino-2-Phenylindole, Dihydrochloride, final conc. 0.5µg/µl) in the dark, following by

incubation at room temperature for 1 minute. Cells were lelleted at full speed (13,200rpm) for 1 minute. The supernatant was removed. Cells were then resuspended in 150μl of 50% glycerol. To dismantle the formation of cell clumps and to facilitate microscopic examination of individual cells, amplitude of 4 of sonication for 10 seconds was applied to each sample. 5μl of each sample was transferred to a slide and observed under fluorescent microscope (Leica) with a standard DAPI filter. 100 cells of each sample were scored for monitoring meiotic progression by counting the number of DAPI-staining body present in each cell.

2.5.2 Chromosome spreading

3~5ml of meiotic cultures were taken from time points at 3~8 hour for chromosome spreading. Cells were pelleted at 3,500 rpm for 5 minutes and resuspended in 500μl of 1M ice-cold sorbitol. Cells were spheroplasted with 7μl of zymolyase (10mg/ml) and 10μl of 1M DTT, incubated at 42°C for 25 minutes to digest cell wall. Samples were gently vortexed every 10 minutes. After incubation, spheroplasting was stopped by addition of 3.5ml of ice-cold stop solution (1M sorbitol) to each sample. Samples were spun down at 3,500 rpm for 5 minutes and resuspended in 100μl of stop solution. Each sample was spread onto 4 clean slides, then one drop of fixation solution was added to each slide. 100μl of 2% Lipsol were added to the slides, the mixtures were then slightly spread on the slides. 100μl of fixation solution were subsequently added to the slides. Samples were spread thoroughly over the slides and allowed to dry overnight.

2.5.3 Immunofluoresence staining

Samples were prepared as slides from chromosome spreading. Slides for immunofluorescence staining were specifically selected from chromosome

spreading to ensure good quality of staining. Slides with cover slips were removed before the experiments started. The slides were washed twice with 200μl of H_2O and Tween20 for 5 minutes and slides were left and stood in a staining jar. Subsequently, the slides were washed twice in 1X PBS for 5 minutes each, 0.025% Triton X -100 in ddH2O for 10 minutes, and once in 1X PBS for 5 minutes. The slides were then incubated in 5% milk in PBS at 37°C for 20 minutes. Another incubation of 1% milk in PBS at 30°C for an hour for primary antibody was carried out. The slides were moved to 4°C to incubate overnight. After the overnight incubation, the slides were washed twice in 1X PBS for 5 minutes each. For secondary antibody binding, the slides were added with secondary antibody in 1% milk in PBS and incubated at 37°C for an hour. The slides were then washed three times in 1X PBS for 5 minutes each. The slides were ready for counterstain with DAPI (Vectashield) or scoring under fluorescent microscope.

Chapter 3

Srs2 is required for normal meiotic progression

Introduction

Srs2 prevents formation of Rad51 presynaptic filament by its translocase activity at the expense of ATP hydrolysis, which dislodges Rad51 from ssDNA (Sung and Klein, 2006) We suggest that Srs2 could act in controlling the amount of Rad51 forming a presynaptic filament, and thus influencing the proportion of DSB repaired via CO pathway versus NCO pathway (SDSA). Also, when Srs2 is absent, other pathways may compensate for restraining Rad51 binding to ssDNA (such as Hed1, see below), but non-functional alleles may block the pathway without catalysing their functions, poisoning HR machinery. Therefore, to test our ideas about Srs2, we analysed two alleles whose functions are separated, *srs2-101* and *srs2Δ*, which have lost ATPase activity and all seven helicase domains, respectively.

Results

3.1 The *srs2* mutant phenotype in meiosis

The mutation site of the mutant allele *srs2-101* is at the helicase consensus domain I (see Figure 1.7), in which a base pair change in this domain causes a leucine substitution for the original proline (Pro^{37}-Leu). This base pair change results in a loss of an *AvaII* site that can be used to determine whether the allele is mutated when making new strains in *srs2-101* mutant background by PCR. The *srs2-101* homozygous strain (hereafter *srs2-101*) is chosen to be our target of this study,

because it has been shown to have pronounced effects on mitotic recombination and UV sensitivity (Palladino and Klein, 1992). What's more, unlike other mutations at some other sites of the SRS2 sequences, the mutation site of *srs2-101* is at a helicase consensus domain which, when any defects occur in recombination or repair in this mutant, can be directly linked to the deficiency of the helicase activity or ATP binding activity. It has been reported that Rad51 nucleofilament is disassembled by Srs2 translocase activity, in which ATP-hydrolysis activity is required (Van Komen et al., 2003). We therefore also suggest that the *srs2-101* mutant would have lost the translocase activity and is unable to remove Rad51 efficiently (Sasanuma et al., 2013). The *srs2* null mutant (hereafter *srs2Δ*) was also investigated, because it is possible that when the Srs2 containing structure/complex is missing some other proteins may compensate for the function of Srs2.

To investigate the role of Srs2 in meiosis, we began with examining the nuclear division by DAPI staining, and scored spore viability for the *srs2-101* and the *srs2Δ* mutant. We further conclude nuclear division efficiency and spore viability of each strain in Table 3.1. All the nuclear division and spore viability of other mutants in this thesis would be referred to the contents of this table. We found that by DAPI staining (Figure 3.1 A-D, uninucleate, dinucleate, trinucleate and tetranucleate cells are shown), the commitment to meiosis of the *srs2* strains (Figure 3.1 E) was delayed compared to the wild-type, as the formation of trinucleate and tetranucleate cells was delayed. Fewer cells completing meiosis may result in the formation of immature spores and may also be associated with reduced spore viability. We therefore examined the spore viability in the wild-type, *srs2-101* and

srs2Δ mutants by tetrad dissection. Wild-type yeast cells that successfully complete two rounds of segregation in meiosis should give four viable spores (Figure 3.1 F). The spore viability in both *srs2* mutant strains was severely reduced to ~53% (Figure 3.1 G, H). We also analysed the pattern of spore viability of each strain, which allows us to better understand whether mutation or deletion of Srs2 can cause defects in segregation specifically during meiosis I or meiosis II (i.e. 0-2 viable spore indicates MI non-disjunction, 3-4 viable spore indicates MII non-disjunction). As shown in Figure 3.1 I, most of the wild-type tetrads are four-spore viable (blue bar), however, random patterns of viable spores were observed in both *srs2-101* and *srs2Δ*, suggesting that loss of helicase function or the entire *SRS2* gene severely affect chromosome segregation during both meiosis I and meiosis II. These results, in consistent with previous studies, indicate that mutations at helicase domain or deletion of *SRS2* have major impacts on meiosis.

Table 3.1

		Spore Viability					
Strain	**Viability[a]**	**4 spore viable**	**3 spore viable**	**2 spore viable**	**1 spore viable**	**0 spore viable**	**% Nuclear division**
WT	99.38%	97.44%	2.56%	0.00%	0.00%	0.00%	98%
srs2-101	53.13%	27.50%	5.00%	35.00%	17.50%	15.00%	63%
hed1Δ	99.58%	98.33%	1.67%	0.00%	0.00%	0.00%	93%
srs2Δ	53.75%	25.00%	27.50%	10.00%	12.50%	25.00%	52%
hed1Δ/srs2-101	51.25%	18.33%	21.67%	23.33%	20.00%	16.67%	37%
dmc1Δ	ND[b]	0.00%	0.00%	0.00%	0.00%	100%	<0.5%
dmc1Δ/hed1Δ	79.90%	62.92%	13.75%	12.92%	0.83%	9.58%	83%
dmc1Δ/srs2-101	ND	0.00%	0.00%	0.00%	0.00%	100%	<0.5%
dmc1Δ/hed1Δ/srs2-101	ND	0.00%	0.00%	0.00%	0.00%	0.00%	14%
hed1Δ srs2Δ	50.25%	29.00%	11.00%	22.00%	8.00%	30.00%	44%
hed1Δ/dmc1Δ/srs2Δ	ND	0.00%	0.00%	0.00%	0.00%	0.00%	15%
dmc1Δ/srs2Δ	ND	0.00%	0.00%	0.00%	0.00%	0.00%	<0.5%

[a]At least 160 spores were scored

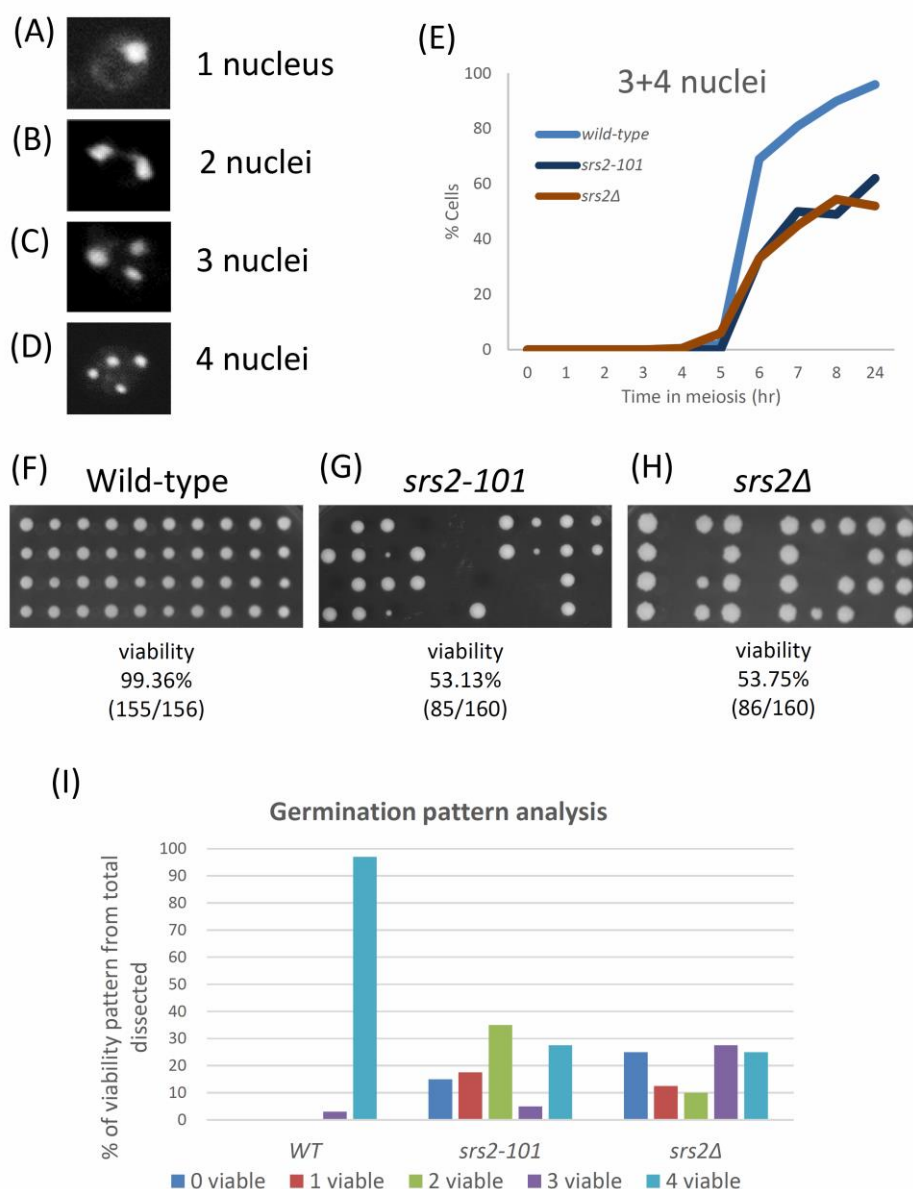[b]Not determined because strains failed to sporulate

Figure 3.1. Meiotic progression and spore viability are reduced in *srs2-101* and *srs2Δ* strains

(A-D) DAPI nuclear staining body of wild-type yeast cells (dAG1680) undergoing meiosis. DAPI staining body with one nucleus (A), two nuclei (B), three nuclei (C) and four nuclei (D) are shown. (E) Meiotic progression of wild-type, *srs2-101* and *srs2Δ* strains. Meiotic progression was measured by scoring the amount of cells that underwent meiosis I and meiosis II in 100 cells which subsequently generated trinucleates and tetranucleates. Spore viability test on wild-type (F) *srs2-101* (G) and *srs2Δ* (H) strains. Cells were sporulated on K-ace agar and treated with β-glucuronidase to be dissected onto YPD agar plates. Viable spores and total number of dissected spores are indicated. Viability was calculated by the proportion of viable spores to total dissected spores. (I) Viability patterns of wild-type, *srs2-101* and *srs2Δ* strains are categorised from 0~4 viable spores. Percentage represents the contribution from each category.

3.2 Rapid DNA-Double Strand Break repair in the *srs2-101* mutant

Defects in meiosis in the *srs2* mutants may be due to various possibilities such as delay in chromosome pairing or defects in DSB repair. To ask whether these meiotic phenotypes were due to defects in meiotic DNA-double strand break repair, an assay for DSB detection at a natural Spo11 hotspot *ARE1* promoter (Gerton et al., 2000) by meiotic time course was conducted. Spo11-DSBs can be distinguished from chromosomal DNA by both Spo11 excision and restriction enzyme digestion at both sides of the break, generating a ~8Kb fragment which can then be hybridised by a specifically designed probe for Southern blotting (Figure 3.2 A). The repaired DSBs or chromosomal DNA which is not cut by Spo11 are the parental bands sizing ~20Kb (Figure 3.2 A). In this assay, some bands that are slightly larger in size than DSBs may be a result of Spo11-induced uneven cuts or some cross-reacting bands. DSB levels in the wild-type and the *srs2-101* mutant both peaked at 4hr of the meiotic time course (Figure 3.2 D), however, reduced DSB levels were detected in *srs2-101* cells. DSB levels in the *srs2Δ* mutant were at the wild-type levels (Figure 3.3 C). These results suggest that either the *srs2-101* allele causes the cells to be less capable of producing DSBs, or meiotic DSBs were more rapidly repaired in *srs2-101* than the wild-type cells.

3.3 The frequency of DSB formation in *srs2-101* cells is normal

To distinguish between the possibilities of less DSBs being produced and the DSBs are more rapidly repaired, we examined the meiotic DSB frequencies of the wild-type and the mutants in *sae2Δ* background. Sae2 together with the MRX complex are required to remove covalently bound Spo11 after the breaks are made (Krogh and Symington, 2004). This process is essential for initiation of resection because
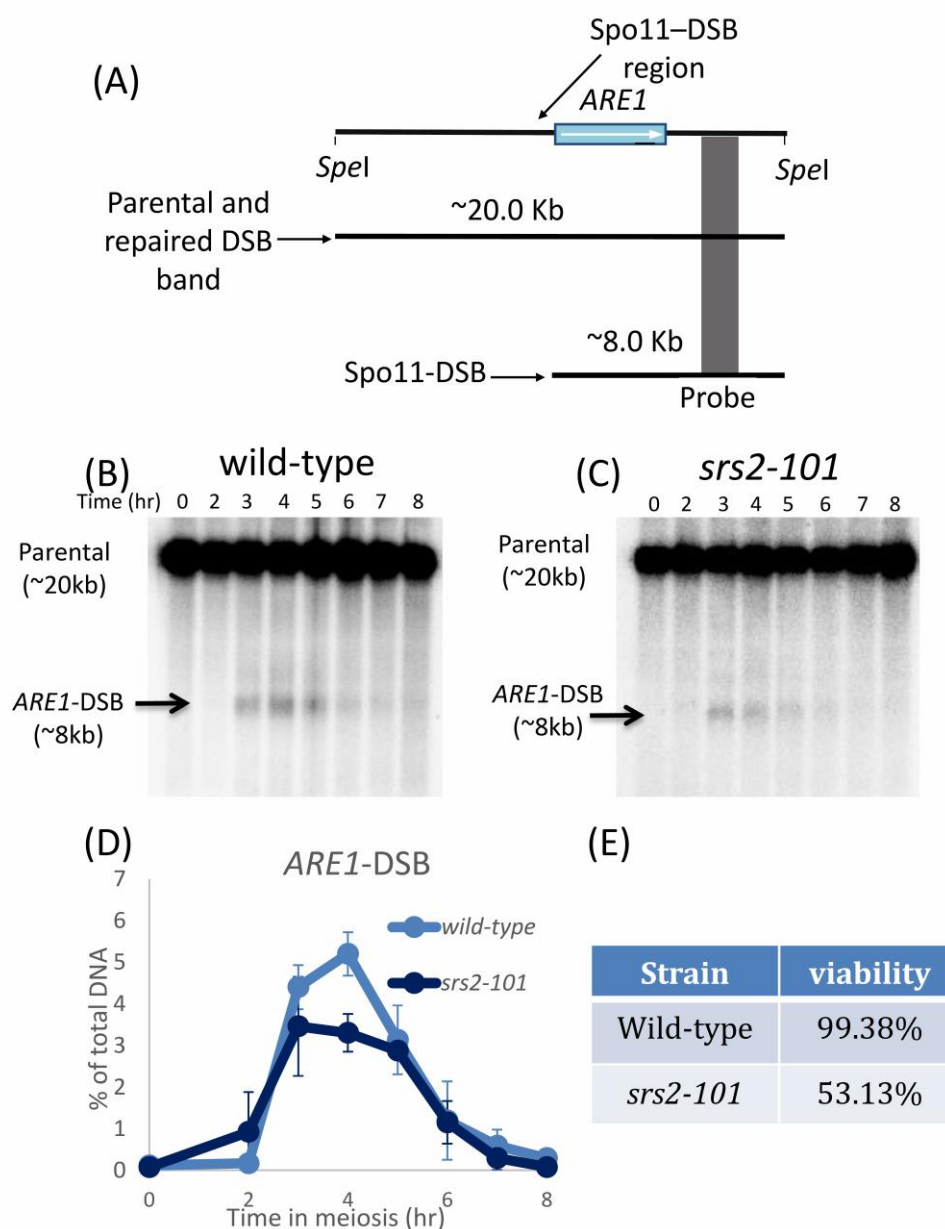
Figure 3.2. Analysis of steady-state Spo11-DSB levels at *ARE1* hotspot

(A) Schematic illustration of Spo11-DSB frequency assay at *ARE1-DSB* hotspot. Restriction endonuclease digest with *SpeI* and programmed meiotic Spo11 cleavage, following by hybridisation of a specifically designed probe create two distinctive bands: Parental and repaired DSB (~20Kb) and Spo11-DSB (~8Kb). Visualised DNA from wild-type (B) and *srs2-101* mutant (C) by Southern blots. Arrows indicate where Spo11-DSBs are. (D) Quantification of synchronised DNA from wild-type (light blue) and *srs2-101* mutant (dark blue) are indicated. Three independent experiments were used in both strains, error bars indicate standard deviation. Percentage of DSBs is calculated by dividing the Spo11-DSB signal by the sum of Spo11-DSB and parental and repaired DSBs signals.
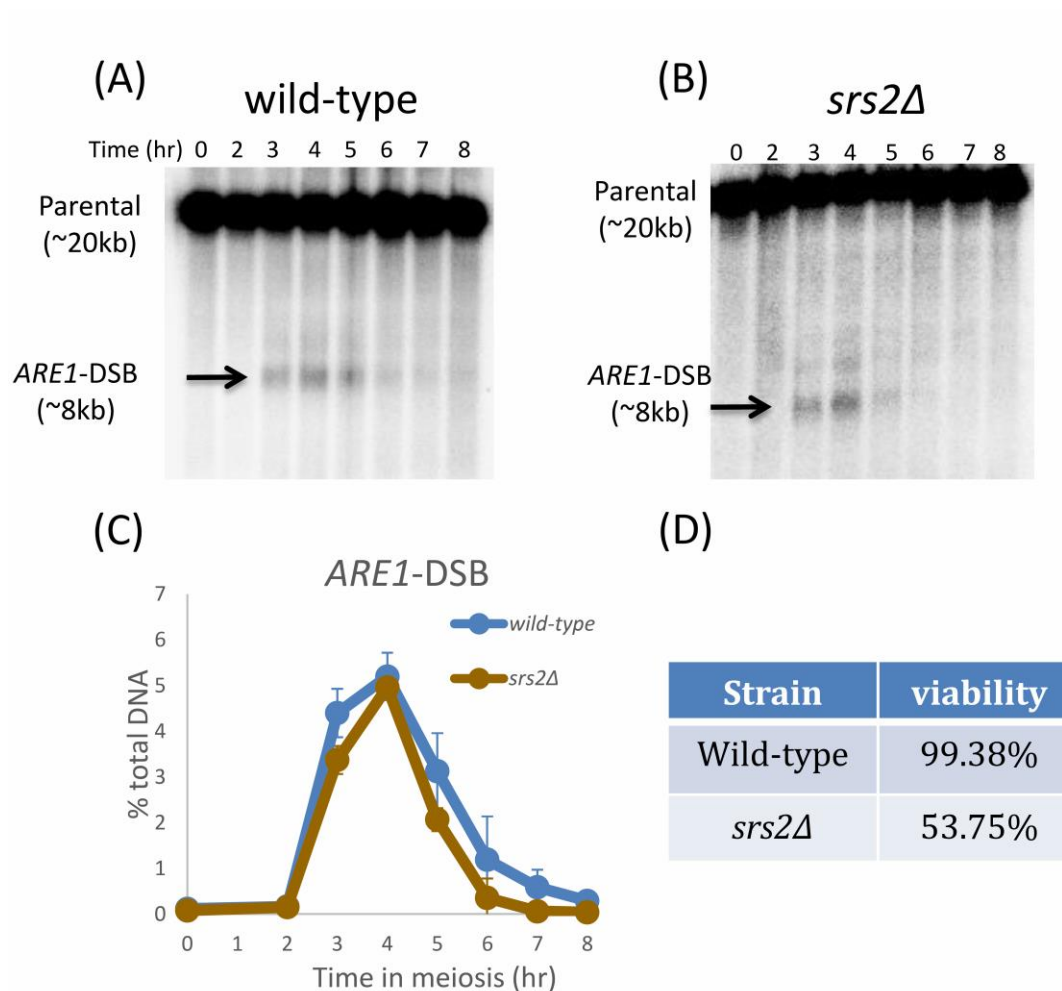
Figure 3.3. MeioticDSB levels in *srs2Δ*

(A-B) Representative Southern blots of DNA from wild-type and *srs2Δ*. Arrows indicate Spo11-DSB.

(C) Meiotic DSB levels (two independent experiments of each strain, error bars indicate standard deviation, light blue: wild-type, light brown: *srs2Δ*) are indicated during meiosis. *srs2Δ* mutant shows very similar steady-state DSB levels to the wild-type.
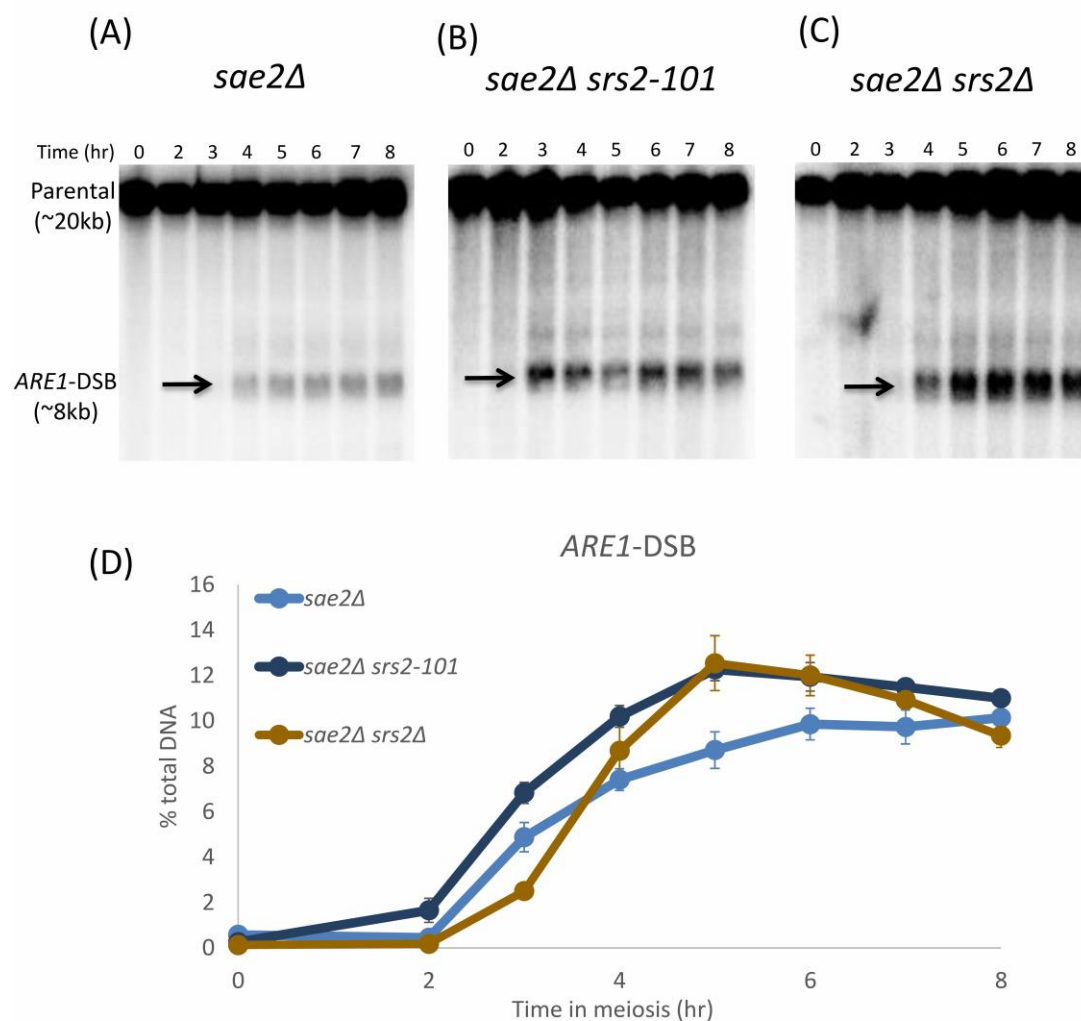
Figure 3.4. *ARE1*-DSB accumulates in *sae2Δ srs2-101* and *sae2Δ srs2Δ* mutants

Cumulative-DSB levels were assayed at *ARE1-DSB* hot spot in the absence of Sae2, a protein that is required for proper DSB processing after meiotic DSBs are made by Spo11 activity. Meiotic DSB accumulates due to failure of removal of Spo11 when Sae2 is absent, therefore, meiotic DSB frequencies of different mutants can easily be identified. (A-C) Visualisation of cumulative-DSB (arrows) in *sae2Δ*, *sae2Δ srs2-101* and *sae2Δ srs2Δ*, respectively. (D) Quantitative analyses of cumulative-DSB level of the three mutants shown in (A-C). Frequencies (two independent experiments, error bars indicate standard deviation) of meiotic DSB (light blue: *sae2Δ*, dark blue: *sae2Δ srs2-101* and light brown: *sae2Δ srs2Δ*) are indicated. Neither *sae2Δ srs2-101* nor *sae2Δ srs2Δ* show reduced or delayed DSB accumulation during meiosis, suggesting that mutation or deletion of Srs2 does not alter meiotic DSB frequencies.

DSB ends are unable to be processed until Spo11-oligonucleotide covalent structure has been removed from the break ends. Failure of DSB repair causes DSBs to accumulate throughout meiosis in *sae2Δ* mutants. We found that DSBs accumulated to a similar level both in the *srs2* mutants and in wild-type when Sae2 was absent (Figure 3.4), confirming that the mutants are capable of producing wild-type meiotic DSB levels. Therefore, from these results we conclude that lower DSB levels detected is due to an increased DSB turnover rate in the *srs2-101* mutant. The increased DSB repair efficiency was not observed in the *srs2Δ*, implying that there may be mechanisms that compensate when Srs2 is absent, but non-functional alleles (e.g. *srs2-101*) may form complexes that affect normal DSB repair.

3.4 Discussion

Helicases are involved in many DNA metabolisms such as replication, repair and recombination. During meiosis, programmed DNA DSBs are generated by meiosis-specific topoisomerase Spo11, which initiates crossovers that are required for accurate chromosome segregation. In these processes, helicases are potentially important for unwinding duplex DNA so that the broken DNA molecules can be repaired by the recombination machinery. The DNA helicase Srs2 is a strong candidate for meiosis because meiotic progression and spore viability are significantly reduced in the absence of Srs2 (Palladino and Klein, 1992). Our studies indicate that the helicase/translocase defective mutant *srs2-101* shows a significant reduction in sporulation efficiency (Figure 3.1 E) as well as spore viability (Figure 3.1 G). We also examined cells without expressing Srs2 protein, which showed similar sporulation efficiency (Figure 3.1 E) and reduced spore viability (Figure 3.1 H) as seen in *srs2-101* diploids. Despite the fact that a previous

study suggests that the deletion of Srs2 has no impact on chromosome pairing, in which chromosome pairing is essential for proper meiosis progression (Lui et al., 2006), a significant delay in meiotic progression was observed in *srs2Δ* mutant in our study. The spore viability profile analyses further suggest that both *srs2-101* and *srs2Δ* mutants confer severer meiotic defects especially in chromosome segregation (Figure 3.1 I, also see Table 3.1). Srs2 is a helicase that belongs to the SF-1 superfamily, which has been suggested to translocate proteins on ssDNA (Ira et al., 2003). In other words, Srs2 is potentially capable of removing target proteins such as Rad51 that are located on ssDNA forming presynaptic filaments during an early stage of recombination pathways. In mitosis, Srs2 has been suggested to dismantle Rad51 filament by its translocase activity, which reduces the efficiency of strand invasion catalysed by Rad51. Therefore it is expected that an increase in recombination should be observed when the Srs2 function is lost. A previous report has shown that *srs2-101* cells have a hyper-recombination phenotype in mitosis (Palladino and Klein, 1992), implying that recombination efficiency is increased due to lack of Srs2 function which is required to remove excess Rad51 from ssDNA. In meiosis, the *ARE1*-DSB kinetics profile of *srs2-101* cells generally shows lower DSB levels than both wild-type (Figure 3.2 D) and *srs2Δ* (Figure 3.3 C), which can be due to fewer DSB production or increased DSB repair efficiency. Using *sae2Δ,* which confers DSB accumulation during meiosis, we were able to find that the DSB frequencies in *srs2-101* and *srs2Δ* were at wild-type level, which roles out the possibility that *srs2* mutants have fewer DSB produced in meiosis and indicates that the DSB turnover is accelerated in *srs2-101* mutant. However, these results are based on a single DSB hot spot which do not fully show how *srs2* mutants affect DSB repair globally. Targeting Rad51 and/or Dmc1 in *srs2* mutant background using ChIP-sequencing (ChIP-Seq or Next-Gen Sequencing)

could examine genome-wide DSB repair events and exclude the possibility that these results are hot spot-specific. Another technique could be used to examine global DSB repair events is pulse field gel electrophoresis (PFGE). Using this method, we could literally visualise all DSBs of each chromosome so that the overall DSB repair kinetics of the *srs2* mutants could be compared with wild-type.

Recombination events in meiosis are different from mitosis, in which Dmc1, a meiosis specific recombinase that also involves in strand invasion in meiosis. Since Srs2 potentially removes Rad51 from ssDNA, the balance between the two recombinases becomes critically important.

We next set out to find if the increased DSB turnover rate in *srs2-101* is correlated to excessive formation of Rad51 filament using *hed1Δ*, in which deletion of *HED1* also reported to reduce the inhibition of Rad51 repair.

Chapter 4

Epistasis analysis of Srs2 and Hed1

Introduction

We hypothesised that the loss of Srs2 function would reduce the inhibition of repair by Rad51 because Srs2 is proposed to antagonise Rad51 from forming strand invasion filaments (Sasanuma et al., 2013). The inhibition of Rad51 is also known to be regulated by Hed1, a meiosis specific protein, which directly associates with Rad51 and prevents the interaction between Rad51 and Rad51-accessory protein Rad54, restrains Rad51-mediated strand invasion during meiosis (Busygina et al., 2008; Tsubouchi and Roeder, 2003, 2006). We interpreted part of the *hed1Δ* phenotype to be similar phenotypes to *srs2-101*, such as more rapid DSB repair (Tsubouchi and Roeder, 2006). Because both Hed1 and Srs2 interaction with Rad51 and both influence the timing of meiotic DBS repair, we then undertook an epistasis analysis to determine whether Srs2 and Hed1 act in different pathways to regulate Rad51 and to see if the double mutant of *hed1 srs2* had more severe phenotype.

Results

4.1 Confirmation that deletion of *HED1* promotes more rapid repair of the *ARE1* DSB

Before undertaking and epsitatis analysis with *hed1* and *srs2*, we confirmed that *hed1Δ* in our hands gives published phenotypes (although the issue of more rapid

repair was not discussed by Tsubouchi and Roeder, 2006). As shown previously, deletion of *HED1* barely influenced sporulation efficiency and spore viability compared to the wild-type (Tsubouchi and Roeder, 2006, Table 3.1, spore viability is 99.58%). We measured the DSB frequency and turnover in the *hed1Δ* single mutant (Figure 4.1). Compared to wild-type cells, the visible DSB frequency at *ARE1* in *hed1Δ* cells was substantially reduced up to 5 h, but the DSB repair was completed by 8h as observed in wild-type (Figure 4.1 C). This is consistent with published data (Tsubouchi and Roeder, 2006).

4.2 The more rapid DSB turnover is separable from spore viability in *srs2-101* cells

As Srs2 presumably removes Rad51 from ssDNA during strand invasion (Van Komen et al., 2003), it could be that in the absence of anti-recombinase activity of Srs2, Rad51 binding to DNA is elevated and this results in more Rad51 catalytic activity and rapid repair. We carried out an epistasis analysis to determine whether the rapid repair of *srs2-101* could be due to an increase in Rad51 activity as seen in *hed1Δ* cells and if Hed1 and Srs2 are in the same or different pathways in regulating Rad51 during meiosis.

When both Srs2 and Hed1 were both removed from cells, the DSB levels appeared to be lower than the single mutants (Figure 4.2 D, grey curve). This implies that in *hed1Δ srs2Δ* there is a synergistic increase in the speed of DSB-repair, possibly because Rad51 activation has been promoted through two different routes.

In the *hed1Δ srs2-101* double mutant cells, the DSB frequencies were not significantly altered compared to its single mutant counterparts (Figure 4.2 C,
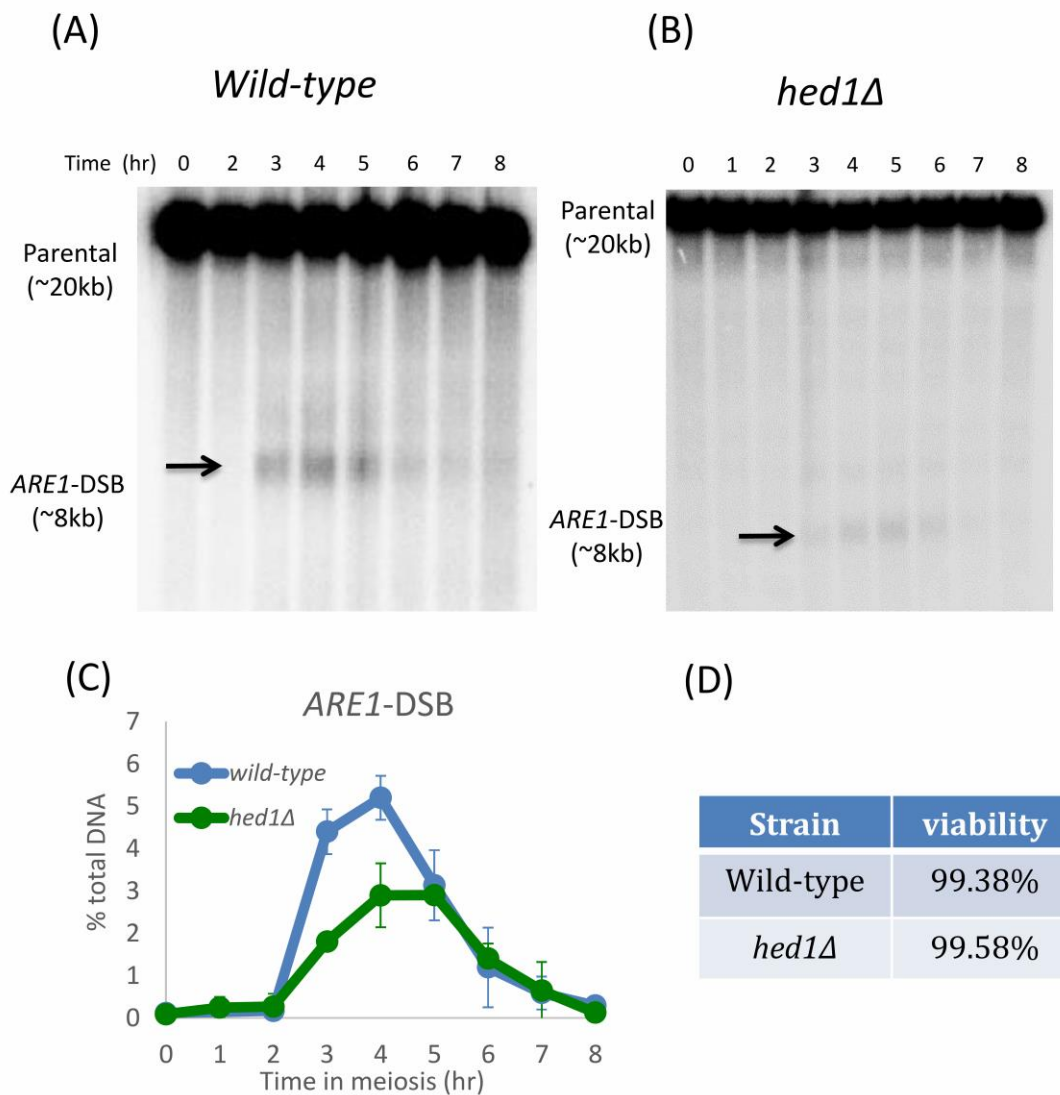
Figure 4.1. Deletion of *HED1* accelerates DSB turnover

Southern blots of synchronous DNA from wild-type (A) and *hed1Δ* (B). DNA DSBs of both strains were examined at the *ARE1-DSB* hot spot. Parental DNA, DSB DNA (arrows) and the time during meiotic time course are indicated. (C) Steady-state DSB frequencies (three independent experiments for wild-type and two experiments for *hed1Δ* were used, error bars indicate standard deviation, light blue: wild-type, green: *hed1Δ*) are represented in the graph. *hed1Δ* shows reduced DSB levels compared with wild-type, indicating its faster DSB turnover than the wild-type. (D) Spore viability of wild-type and *hed1Δ* is shown in the table.
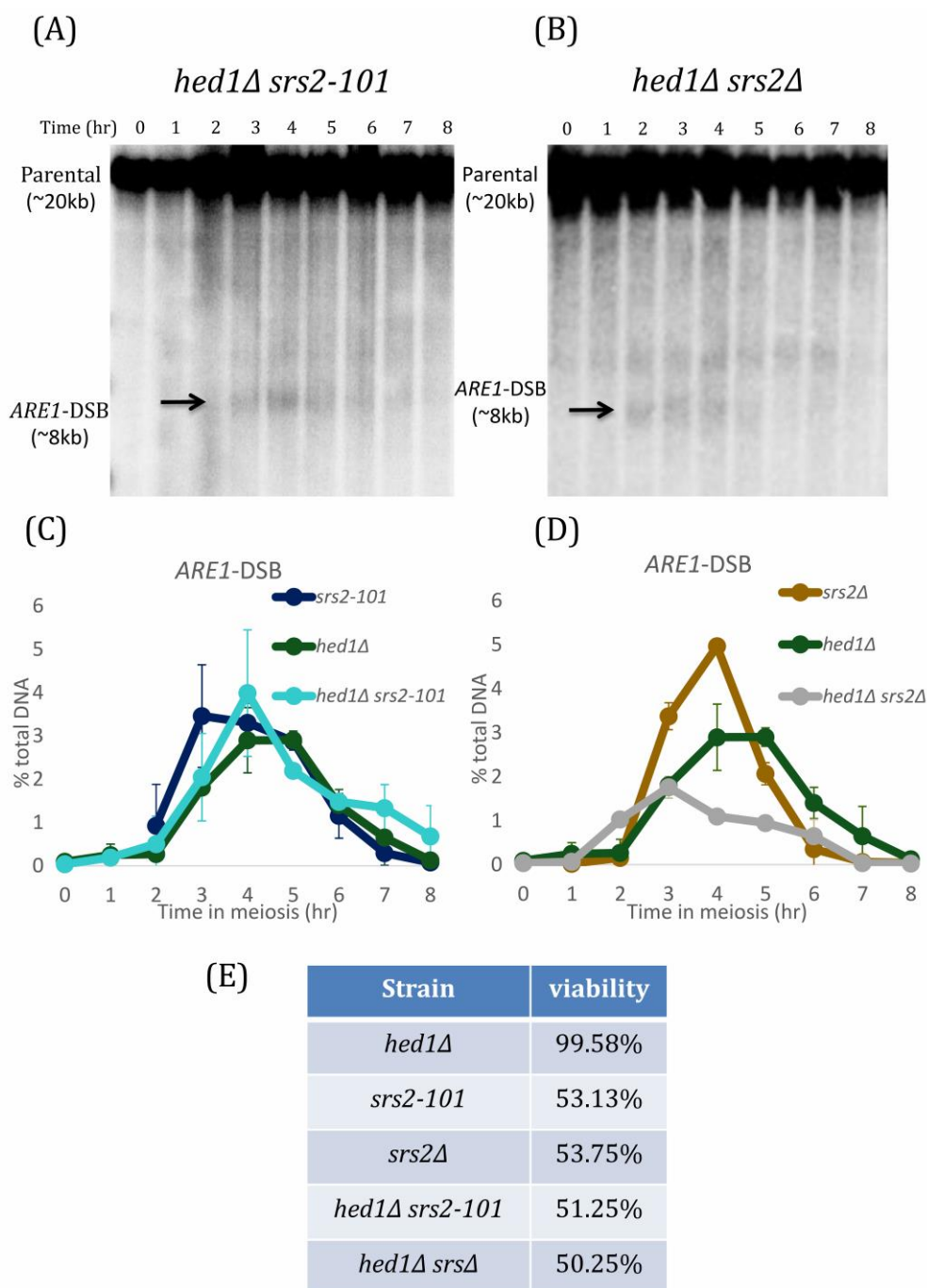
Figure 4.2. Deletion and mutation on *SRS2* in the absence of *HED1* lead to a significant reduction in spore viability but the effect on DSB turnover is limited

Southern blots of synchronous DNA from *hed1Δ srs2-101* (A) and *hed1Δ srs2Δ* (B), arrows indicate Spo11-DSBs. (C-D) Epistatic analyses were examined by *ARE1-DSB* frequencies in the strains indicated in the graph. Three independent experiments for *srs2-101* (dark blue) and two independent experiments for *srs2Δ* (brown), *hed1Δ srs2-101* (cyan), *hed1Δ* (dark green) and *hed1Δ srs2Δ* (grey), error bars indicate standard deviation. (E) Spore viability of each strain is shown in the table. *srs2-101* and *srs2Δ* significantly reduce spore viability in cells lack of *HED1*.

cyan curve). These results suggest that even if there is more Rad51 protein available for strand invasion in the *hed1Δ srs2-101* mutant, Rad51-mediated repair efficiency is restricted to some extent.

Spore viability was substantially reduced from near wild-type level (99.58%) in *hed1Δ*, to 51.25% and 50.25% in *hed1Δ srs2Δ* and *hed1Δ srs2-101* cells, respectively. This suggests that Srs2 is required for full spore viability when Hed1 is absent.

Taken together, these data imply that the phenotypes of more rapid DSB-turnover and spore viability are separable. With respect to the rate of DSB repair, Srs2 appears to be epistatic to Hed1 with respect to its influence on spore viability.

It has been reported that *hed1Δ* rescues *dmc1Δ* meiotic phenotypes including DSB repair and sporulation (Tsubouchi and Roeder, 2006) and we think that it is because intersister repair becomes more preferable in *hed1Δ*. We next set out to confirm if *hed1Δ* could rescue *dmc1Δ* on our own and to see if *srs2* alleles could also do the same.

4.3 Confirmation that deletion of *HED1* activates Rad51 and allows meiotic DSB repair and meiosis progression in the absence of Dmc1

In *SK1* strain background, *dmc1* mutants arrest in meiotic prophase due to failure of repair DSBs with significant defects in homologue pairing and SC formation, in which the conversion of DSBs into recombination intermediates is blocked. This is due to the establishment of barrier to sister chromatid recombination (BSCR),

which allows only Dmc1 triggered recombination between homologues and prevents Rad51 mediated inter-sister recombination (Shinohara et al., 1992, 1997). It has previously been shown that in *SK1* strain background, the defect in sporulation in *dmc1* cells is suppressed when Hed1 is eliminated, raising the possibility that meiotic DSBs are efficiently repaired in the *dmc1Δ hed1Δ* mutants (Tsubouchi and Roeder, 2006). Also, previous studies have shown that activation of Rad51 strand exchange activity allows meiotic DSB repair to progress in the absence of Dmc1, effectively generating viable spores (Tsubouchi and Roeder, 2003, 2006). To confirm if meiotic DSB repair is processed by activation of Rad51 in the absence of *DMC1*, meiotic DSB repair at the *ARE1* hot spot was examined in *dmc1Δ hed1Δ* doubly mutant cells. Consistent with previous studies, *dmc1Δ* single mutant accumulated unrepaired DSBs to a very high level over synchronous meiosis (Figure4.3 A and C), whereas in *dmc1Δ hed1Δ* cells, DSB signals peaked at 4h and disappeared at 8h of meiosis (Figure 4.3 C) (Lao et al., 2013; Tsubouchi and Roeder, 2006). Restored meiotic DSB repair is also associated with high spore viability in the *dmc1Δ hed1Δ* cells. Deletion of *HED1* substantially rescues the spore viability in the *dmc1Δ* background and also nuclear division (see Table 3.1, spore viability of *dmc1Δ hed1Δ* is 79.90%). Previous studies have shown that in comparison to *dmc1Δ hed1Δ,* no DSB repair was observed in the *dmc1Δ hed1Δ rad51Δ* mutant, suggesting that suppression of DSB repair defects by Hed1 in *dmc1Δ* background is dependent on Rad51 activity (Tsubouchi and Roeder, 2006). These results raise the possibilities that Rad51 activity plays a crucial role in DNA recombination during meiosis when Dmc1 is absent.
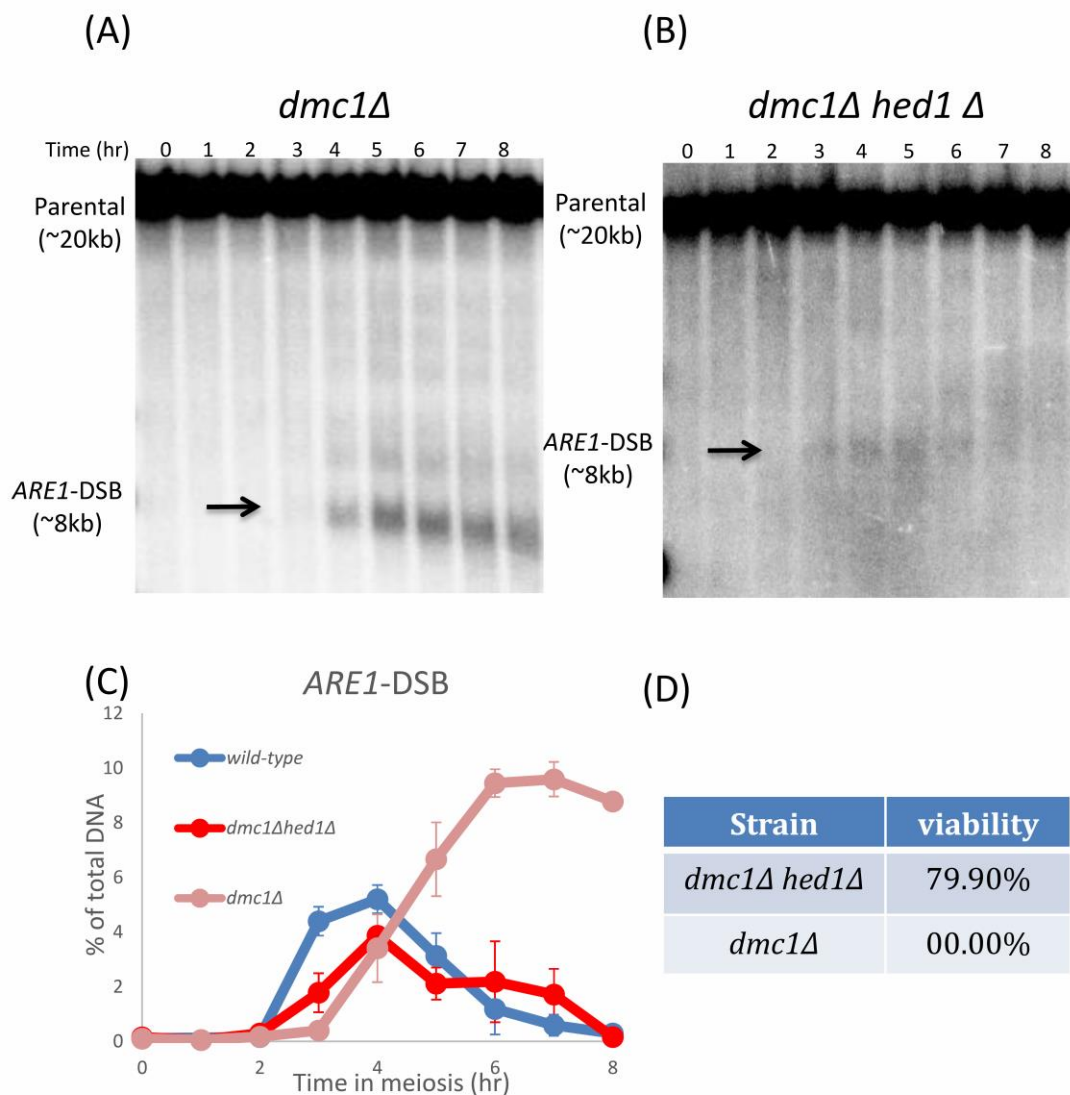
Figure 4.3. Deletion of *HED1* suppresses *dmc1* defect in meiotic DSB repair

Southern blots for DSB kinetics in *dmc1Δ* (A) and in *dmc1Δ hed1Δ* (B). Parental DNA, meiotic DSB DNA (arrows) and time during meiosis are indicated. (C) Quantification of meiotic DSB from (A) and (B).Wild-type (light blue), *dmc1Δ hed1Δ* (red) and *dmc1Δ* (pink) are displayed. (D) Spore viability of *dmc1Δ hed1Δ* and *dmc1Δ.*Three independent experiments were used for wild-type and two independent experiments for *dmc1Δ* and *dmc1Δ hed1Δ* strains. Error bars indicate standard deviation.

4.4 The *srs2-101* allele but not *srs2Δ* exacerbates the meiotic defects of *dmc1Δ*

Meiotic defects of *dmc1Δ* cells are suppressed by deletion of *HED1* because Rad51 is released from Hed1 inhibition and is able to act in place of Dmc1 for strand invasion. Since Srs2 is responsible for dismantling Rad51 presynaptic filament, it is of interest to know whether mutation or deletion of *SRS2* could activate Rad51 activity and phenocopy the *hed1Δ* in *dmc1Δ* cells. This would raise the possibility that Srs2 also deactivates Rad51-mediated strand invasion function like Hed1 does. To test this possibility, we assayed *ARE1*-DSB repair for *srs2-101* and *srs2Δ* mutants in *dmc1Δ* background. In *dmc1Δ srs2-101* cells, unrepaired DSBs accumulated to levels higher than that of *dmc1Δ* single mutant (Figure 4.4 C), whereas *srs2Δ* did not have the same impact on meiotic DSB repair in *dmc1Δ* background, as the meiotic DSB levels resemble those in *dmc1Δ* cells (Figure 4.4 C). This is consistent with our previous suggestions that the *srs2-101* mutant allele may poison meiosis by accumulating non-functional complexes where repair pathways need to be cleared for further processing, whereas the pathways can be reconstituted by other mechanisms when having a null mutant. Spore viability in the *dmc1Δ srs2-101* and *dmc1Δ srs2Δ* double mutants remained at the similar levels as observed in the *dmc1Δ* single mutant (see Table 3.1, spore viability is undetermined because all these strains were unable to sporulate). These results imply that the *srs2-101* mutation does not cause increase in Rad51 recombinase activity in *dmc1Δ* cells, to repair the DSBs. This could be due to Rad51 molecules that are not removed from invading 3' ssDNA tails remaining inhibited by Hed1, so that meiotic DSB repair via strand invasion is blocked without both Dmc1 and Rad51 recombinase activities. Also, due to the lack of the Srs2 helicase activity, it is possible that excessive Rad51 that is unable to carry out strand invasion, which

could accumulate and form deleterious intermediates and result in the *dmc1Δ srs2-101* double mutant to have more breaks unrepaired. Alternatively, a higher level of unrepaired DSBs observed in the *dmc1 srs2-101* double mutant than the *dmc1* single mutant may imply that there is some repair within the *dmc1Δ* cells which may be dependent on Srs2 helicase activity.

4.5 Srs2 helicase/translocase activity is required for meiotic DSB repair and spore viability when both *DMC1* and *HED1* are absent

Removal of *HED1* in a *dmc1Δ* mutant substantially rescues meiotic defects such as DSB repair, sporulation and spore viability (Figure 4.3 and Table 3.1, spore viability is 79.90%). This has been proposed by the findings that Rad51 catalytic activity plays an essential role in the suppression of these defects in *dmc1Δ* cells (Tsubouchi and Roeder, 2003). We then hypothesised that if Srs2 is responsible for dismantling Rad51 activity, mutations in the Srs2 helicase domain or the *SRS2* null mutant would suppress meiotic defects of *dmc1* cells, allowing more Rad51 activity in place of Dmc1 for strand invasion. As shown in previous sections, neither meiotic DSB repair (Figure 4.4, 4.5) nor the sporulation efficiency was improved in *dmc1Δ* by *srs2-101* or *srs2Δ* (see Table 3.1). Furthermore, a major reduction in spore viability in *hed1Δ srs2-101* and *hed1Δ srs2Δ* double mutants was also observed (Figure 4.2 E), implying that instead of promoting Rad51-dependent repair, *srs2* might create more defective Rad51 nucleofilaments during recombination. Because in *dmc1Δ hed1Δ* cells there would be only Rad51 for strand exchange, so if mutation or deletion of *SRS2* could result in accumulating defective Rad51 filament, then the meiotic phenotype of *dmc1Δ hed1Δ* would be exacerbated. To test this possibility, we monitored the *ARE1*-DSB in *dmc1Δ hed1Δ*,
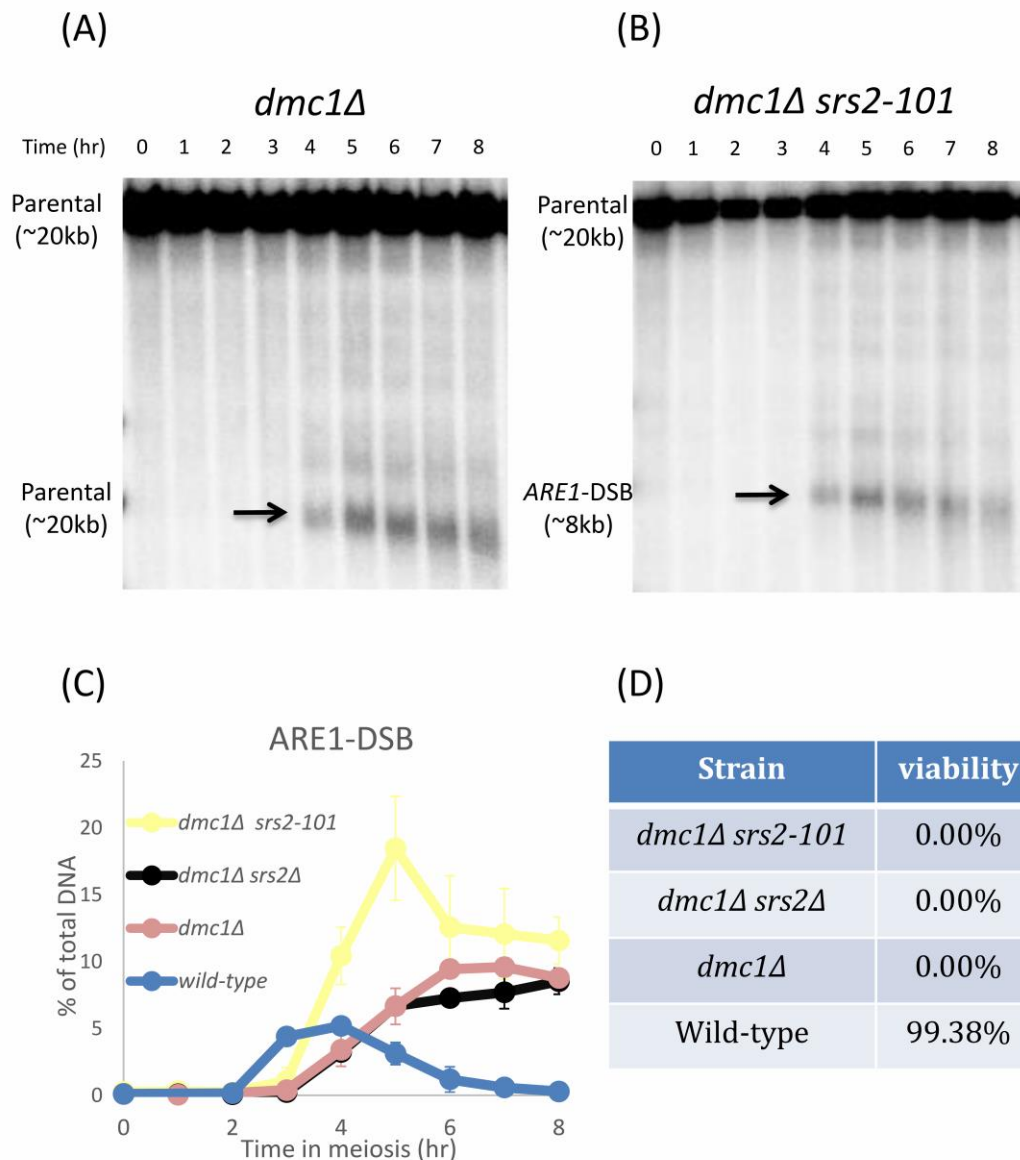
Figure 4.4. *srs2-101* exacerbates *dmc1Δ* defect in DSB repair

Synchronous meiotic time course DNA of *dmc1Δ* (A) and *dmc1Δ srs2-101* (B) were extracted and visualised by Southern blotting. Arrows indicate Spo11-DSBs. (C) Cumulative-DSB levels of *dmc1Δ* (pink), *dmc1Δ srs2-101* (yellow) and *dmc1Δ srs2Δ* (black) are shown. Two independent experiments for *dmc1Δ* and *dmc1Δ srs2-101* were used. Error bars indicate standard deviation. (D) Spore viability of *dmc1Δ srs2-101*, *dmc1Δ srs2Δ*, *dmc1Δ* and wild-type is shown. Mutation of *SRS2* at its helicase consensus sequence in the absence of *DMC1* results in higher cumulative-DSB levels compared with *dmc1Δ* counterpart.
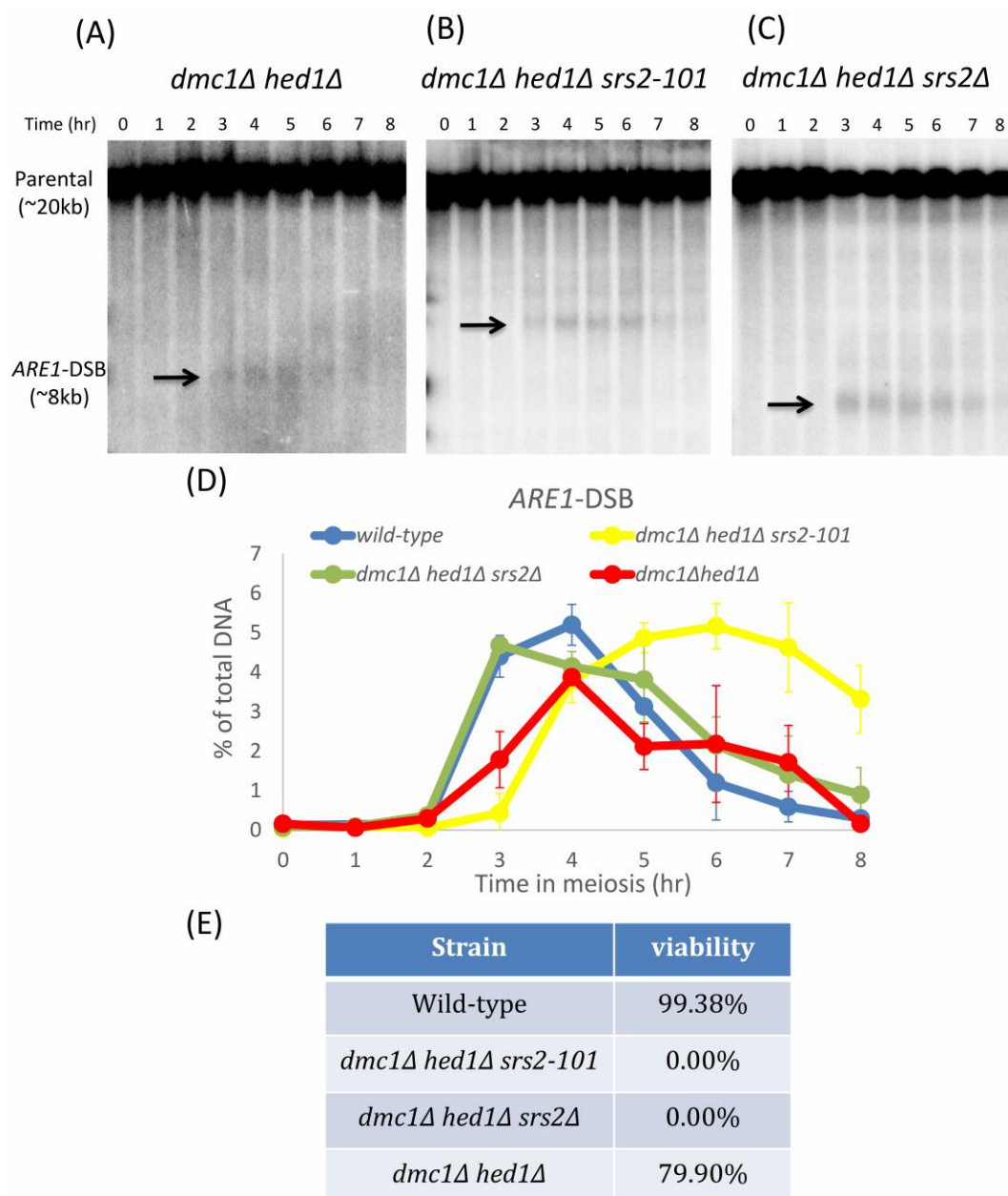
Figure 4.5. *srs2-101* significantly delays DSB repair in *dmc1Δ hed1Δ* but deletion of *SRS2* in *dmc1Δ hed1Δ* resembles wild-type in DSB repair

Visualisation of meiotic DSB by Southern blotting from *dmc1Δ hed1Δ* (A), *dmc1Δ hed1Δ srs2-101* (B) and *dmc1Δ hed1Δ srs2Δ* (C). Arrows indicate Spo11-DSBs. Time for synchronous time course and parental DNA are also indicated. (D) Quantification of *ARE1-DSB* form the Southern blots are shown (blue: wild-type, yellow: *dmc1Δ hed1Δ srs2-101*, green: *dmc1Δ hed1Δ srs2Δ* and red: *dmc1Δ hed1Δ*). Two independent experiments are carried out for the three mutants and three independent experiments for wild-type. Error bars indicate standard deviation. (E) Spore viability of each strain is shown. DSB levels in *dmc1Δ hed1Δ srs2-101* persisted going up until 6h of meiosis, showing a significant delay in DSB turnover compared with other mutants, whereas DSB levels in *dmc1Δ hed1Δ srs2Δ* resemble those of wild-type cells.
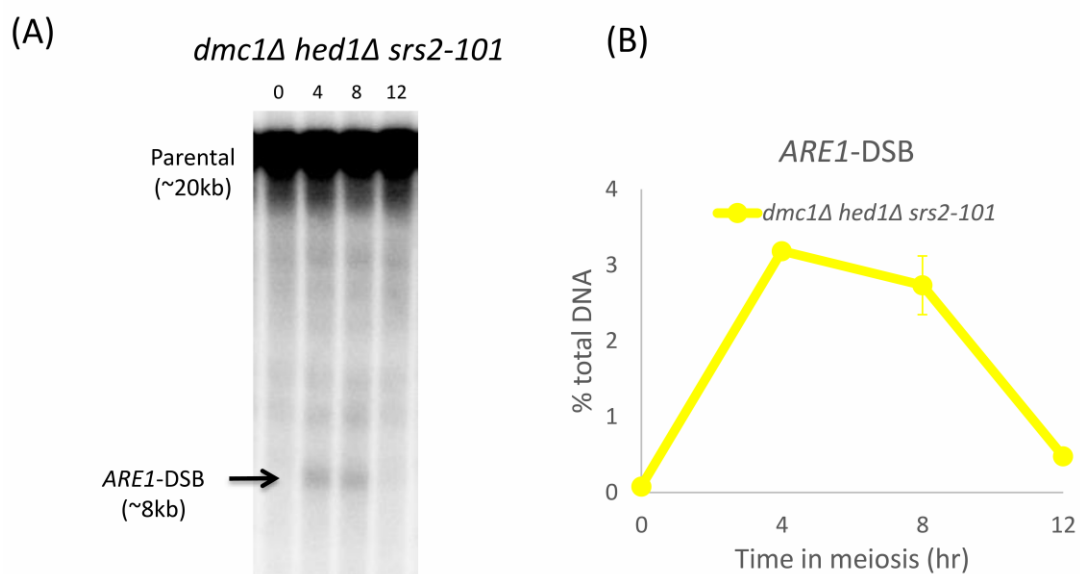
(A)

dmc1Δ hed1Δ srs2-101

0   4   8   12

Parental
(~20kb)

ARE1-DSB
(~8kb)

(B)

ARE1-DSB

dmc1Δ hed1Δ srs2-101

% total DNA

Time in meiosis (hr)

Figure 4.6. Meiotic DSBs in *dmc1Δ hed1Δ srs2-101* are rapidly repaired during late meiosis

(A) Visualisation of meiotic DSB by Southern blotting from *dmc1Δ hed1Δ srs2-101*Arrows indicate parental DNA and Spo11-DSBs. Time for synchronous time course (4h interval) and parental DNA are also indicated. (B) Quantification of *ARE1*-DSB form the Southern blots are shown. . Two independent experiments were carried out. Error bars indicate standard deviation. DSB levels are substantially reduced from 8h to 12h of meiosis.

dmc1Δ hed1Δ srs2-101 and *dmc1Δ hed1Δ srs2Δ* mutants. *srs2-101* has a major impact on DSB repair when both *DMC1* and *HED1* are eliminated, where the formation and repair of DSBs were significantly delayed in comparison to the *dmc1Δ hed1Δ* or *dmc1Δ hed1Δ srs2Δ* mutants (Figure 4.5 D, yellow curve). However, the *ARE1*-DSB levels of *dmc1Δ hed1Δ srs2Δ* triple mutant are very similar to those observed in wild-type (Figure 4.5 D, green curve). To further investigate the delay in DSB repair in *dmc1Δ hed1Δ srs2-101*, we carried out meiotic synchronous time courses with elongated time frame up to 12 hours. In the 8h time frame experiments we found that after 6h of meiosis there is significant DSB repair in the triple mutant (Figure 4.5 D), and this is complete by 12h (Figure 4.6).

These results suggest that Srs2 plays a role in the *hed1* rescue of repair in *dmc1Δ* cells.   The difference in severity of phenotypes between *dmc1Δ hed1Δ srs2Δ* and *dmc1Δ hed1Δ srs2-101* could reflect the possibility raised earlier that the non-functional allele may occupy DNA so that all the other possible unknown repair pathway could not be faithfully executed.

4.6 Discussion

Physical analysis of DNA DSB repair using natural *ARE1*-DSB hotspot assay in the *srs2* mutants including the helicase defective *srs2-101* allele and *srs2Δ* allowed us to further investigate the role of Srs2 during meiotic DSB repair process. We wondered whether the increased repair efficiency in *srs2-101* cells could be due to excess Rad51 that carries out more strand invasion over Dmc1, we analysed the *ARE1*-DSB frequency of *hed1Δ* homozygote mutant, which failed to restrain Rad51-mediated strand invasion during meiosis. As shown in Figure 4.1 C, *hed1Δ* cells also show lower DSB levels similar to *srs2-101* cells, suggesting that *srs2-101*

may be acting like *hed1Δ* in increasing DSB repair efficiency by having more Rad51-mediated strand exchange during meiosis. Strong evidence of *hed1Δ* in increasing Rad51-mediated recombination is that when Dmc1 is absent, excess Rad51 nucleofilaments help suppress *dmc1Δ* defect in meiotic DSB repair (Figure 4.2 C), suggesting that Rad51 replaces Dmc1 function in meiotic DSB repair in the absence of Dmc1. Therefore, we expected that since both *srs2-101* and *hed1Δ* were theoretically promoting Rad51 activity, doubly mutating *SRS2* and *HED*1 could possibly further increase DSB repair efficiency, and the defects in meiotic DSB repair and spore lethality of *dmc1Δ* should be effectively suppressed. The repair efficiency of *hed1Δ srs2-101* is limited in comparison to its single mutant counterparts (Figure 3.2 D and Figure 4.1 C) and spore viability is significantly reduced (Figure 4.2 D). It has been reported that in the presence of Dmc1, the preference of recombination template choice of *hed1* single mutant is slightly altered from IH recombination to IS recombination, but the IH/IS ratio is dramatically decreased when both Dmc1 and Hed1 are absent, suggesting that Dmc1 inhibits Rad51-mediated strand invasion towards IS recombination (Lao et al., 2013). Therefore, even if Rad51 activity is increased in the absence of both Hed1 and Srs2, Dmc1 could prevent excessive Rad51-mediated IS recombination occurring. This could be the reason why the DSB turnover is restrained in *hed1 srs2* mutants. However, this does not account for the reduced spore viability observed in the *hed1 srs2* double mutants. A possible explanation could be that Dmc1 can only inhibit a certain quantity of activated Rad51 (e.g. *hed1* single mutant) but not in hyper-activated mutants such as *hed1 srs2* double mutants, so that proper IH/IS ratio is not established, subsequently leading to spore lethality. This suggestion indeed requires JM assessments for the double mutants.

Since wild-type level of sporulation efficiency and spore viability require proper balance between Rad51 and Dmc1, and Srs2 is needed for down-regulating unwanted Rad51 strand invasion events during recombination. Srs2 might influence both Rad51-dependent and Dmc1-independent repair pathways. To test this possibility, we performed *ARE1*-DSB analyses on *dmc1* mutants in *srs2* backgrounds. The loss of Srs2 helicase activity results in higher level of unrepaired DSB than other mutants such as *dmc1Δ* and *dmc1Δ srs2Δ* (Figure4.6). These results suggest that there is a Srs2-dependent repair pathway in a Dmc1-independent manner during meiosis. This could be because *srs2-101* allele potentially forms toxic complexes which block other repair pathways, while *srs2Δ*could be presumably rescued by these pathways. Nevertheless, sporulation efficiency and spore formation are defective in all *dmc1* mutants, confirming that regardless of presence of Srs2, Dmc1 is indeed essential for normal meiotic progression.

Importantly, loss of *HED1* suppresses *dmc1* defects in DSB repair by improving Rad51-Rad54 interaction. However, loss of Srs2 translocase activity or the absence of *SRS2* does not rescue *dmc1* phenotypes, despite the fact that *srs2* mutants presumably improve Rad51-dependent repair. It could be possible that Hed1 blocks the access of *srs2* cells in promoting Rad51-dependent repair in the absence of Dmc1. Therefore the *ARE1*-DSB frequency for *dmc1Δ hed1Δ srs2-101* and *dmc1Δ hed1Δ srs2Δ* was examined which was aimed to test whether Hed1 antagonises Srs2 in regulating Rad51 in the absence of Dmc1. From another point of view, these experiments could potentially reveal whether Rad51-dependent pathway can fully compensate Dmc1 in DNA repair in the absence of negative regulators such as Hed1 and Srs2. Our data indicate that mutation or deletion of *SRS2* negatively influences Dmc1-independent repair pathway while both *DMC1*

and *HED1* are deleted, in which *srs2-101* severely delays the repair in *dmc1Δ hed1Δ* background while DSB repair is slightly delayed in *dmc1Δ hed1Δ srs2Δ* (Figure 4.5). These data also suggest that *srs2* presumably creates defective Rad51 nucleofilaments for recombination, which might explain why there is an increase in spore lethality and inefficient sporulation in *hed1 srs2* and *dmc1 hed1 srs2* mutants.

Because *srs2-101* has high similarity with Hed1 in meiotic DSB repair, we then wondered if this was because there is more intersister repair. We then aimed to investigate JM formation during recombination using a recombination assay system. Also we worked on *srs2-101* in *mek1* background in which the dependency of Srs2 for Mek1-mediated inter-sister repair could be examined.

Chapter 5

The role of Srs2 in inter-sister recombination

5.1 Total JM formation is reduced but the ratio of multi-chromatid JM is increased in *srs2-101 ndt80Δ* cells

We previously found that *srs2-101* has more rapid meiotic DSB repair than wild-type, which is very similar to *hed1* mutant. Although the faster repair in *hed1* was not specifically mentioned (Tsubouchi and Roeder, 2006), we hypothesised that it could be due to increased intersister repair over interhomologue repair. To test this, we employed a recombination assay system which is specifically designed to monitor and distinguish the formation between IS JMs and IH JMs (Allers and Lichten, 2001). *SRS2* and *srs2-101* strains in *ndt80Δ* backgrounds were examined using the *URA3-arg4* construct where JMs formed by IS and IH recombination can be distinguished (Figure 5.1 A and B). In *srs2-101 ndt80Δ* cells, IH JMs started to form normally at 4h of meiosis and gradually accumulated to 9h (Figure 5.1 C, P2 x P1 lane) as in *SRS2 ndt80Δ* strain (Figure 5.1 D, P2 x P1 lane). However the majority of JMs in *srs2-101 ndt80Δ* were also formed between interhomologue chromosomes where IS JMs were not so obviously seen (Figure 5.1 C, P1 x P1 lane and P2 x P2 lane). The total JM formation was also calculated for *SRS2 ndt80Δ* and *srs2-101 ndt80Δ* strains. The overall JM formation level in *srs2-101 ndt80Δ* cells (Figure 5.1 E, light blue curve) was reduced compared with *SRS2 ndt80Δ* (Figure 5.1 E, dark blue curve).
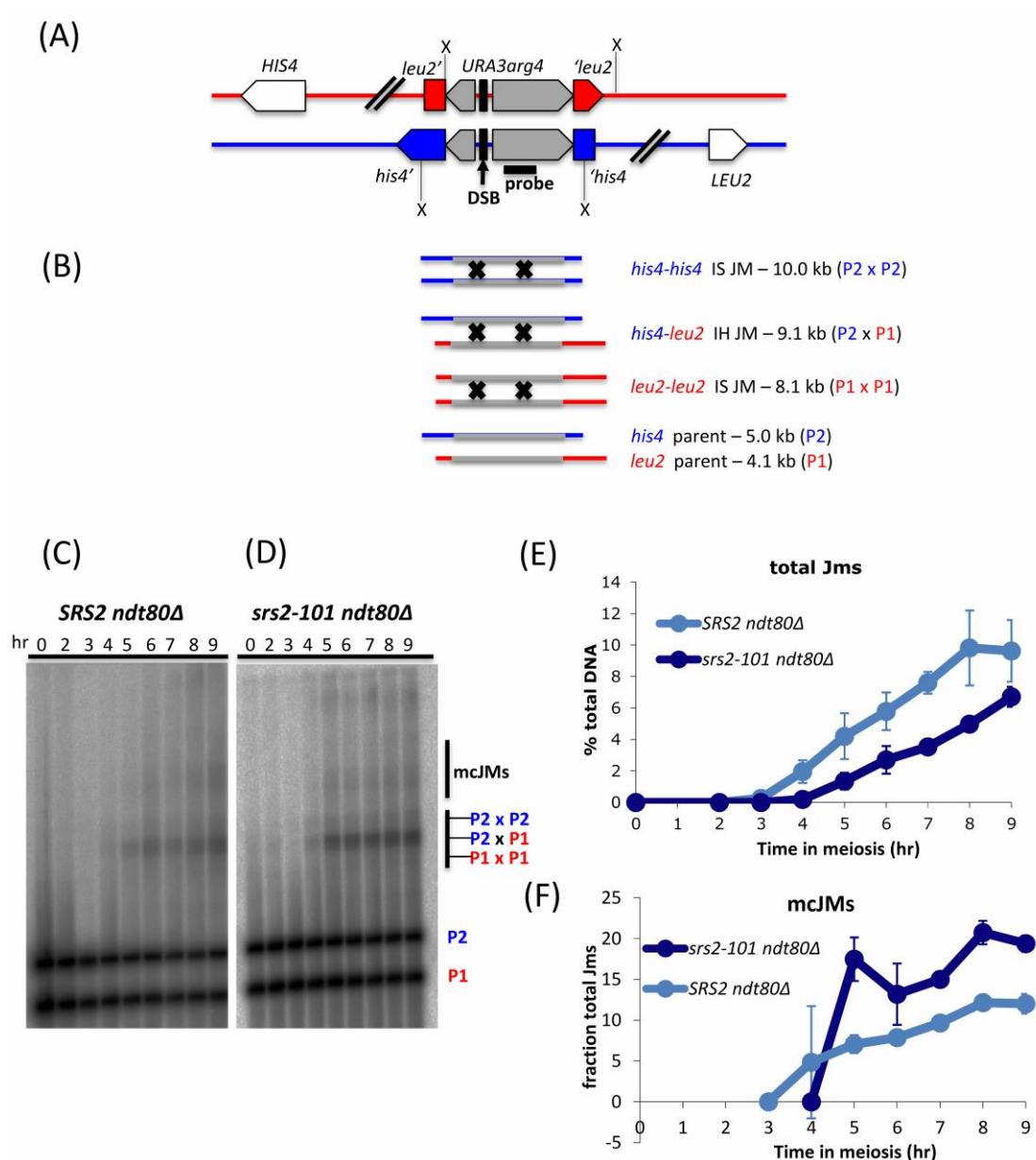
Figure 5.1. Detection of JMs using recombination assay system

(A) Schematic diagram of the recombination assay system used to distinguish IS and IH JMs. The *URA3-arg4* construct is inserted at *LEU2* at one homologue (red) and at *HIS4* on the other homologue (blue). Digestion with XmnI (X) produces various recombination products including IS JM and IH JM during recombination, which can be distinguished based on their electrophoretic mobility (B). Representative Southern blot of DNA from *SRS2 ndt80Δ* strain (C) and *srs2-101 ndt80Δ* strain (D) with *his4::URA3-arg4* and *leu2::URA3- arg4* inserts. Parental DNA and JMs are also depicted. (E) Frequencies of total JMs in *SRS2 ndt80Δ* and *srs2-101 ndt80Δ* strains. Error bars indicate standard deviation, two independent experiments. (F) Diagram of multi-chromatid JMs (mcJMs) in proportion to total JMs in *SRS2 ndt80Δ* and *srs2-101 ndt80Δ* strains.

When JM precursor is undergoing unregulated events such as in *sgs1* cells, strand exchange is prone to occur between sister chromatids and multi-chromatids to form off-pathway products (Jessop and Lichten, 2008). These products include elevated levels of IS JMs and multi-chromatid JMs (mcJMs). Here we focused on looking at the mcJM levels of both *SRS2 ndt80Δ* and *srs2-101 ndt80Δ* to see if *srs2-101* had impact on regulating normal JM formation. mcJMs were more frequently formed in *srs2-101 ndt80Δ* cells than in *SRS2 ndt80Δ* cells (Figure 5.1 F), raising the possibility that *srs2-101* may reduce recombination between homologues but increase abnormal recombination products to form during meiosis.

5.2 Mek1 is required for BSCR establishment

A strong bias of repairing meiotic DSB via homologous chromosomes over sister chromatids is established in *S. cerevisiae* during meiotic recombination. The mechanism is barrier to sister chromatid repair (BSCR) which prevents strand invasion of sister chromatids so that the use of homologues as a repair template becomes default. BSCR is created by a number of proteins that comprises of chromosome axial elements, including Red1, Hop1 and Mek1. Among these proteins, Mek1 directly interferes with Rad51 function by phosphorylating the Rad51 accessory protein Rad54, limiting Rad51 function in strand invasion specifically during meiosis. Rad51 and Dmc1 both colocalise to DSBs and act to facilitate meiotic recombination between homologues. Rad51 helps facilitate Dmc1 localise to break sites, but not vice versa, suggesting that Rad51 is not dispensable during meiotic recombination, regardless the fact that Rad51's recombinase activity is more specific to sister chromatids. Previous studies have indicated that *dmc1* cells arrest in meiosis prophase due to a failure to repair meiotic DSBs and that Mek1 function is responsible for the situation where repair

using sister chromatid is prevented, therefore triggering the meiotic recombination checkpoint so cell arrest takes place in cells lacking Dmc1 function. We previously found that the Rad51 strand exchange activity was not sufficient to compensate Dmc1's absence even when the Rad51 inhibitors such as *HED1* and *SRS2* were eliminated. What's more, the inability to repair meiotic DSB in the *dmc1Δ* was apparently exacerbated in the *dmc1Δ srs2-101* double mutant (see Figure 4.4), suggesting that there is a Srs2-dependent pathway for some repair in a Dmc1-independent manner, and this repair pathway possibly takes place between sister chromatids. Therefore, based on this suggestion, Srs2 might be required for DSB repair in *mek1* mutants because mutation of Mek1 removes the barrier to intersister repair, which allows DSB repair in *dmc1* background. To ask whether Srs2 is needed for Mek1-mediated inter-sister repair, an analogue sensitive allele of Mek1 (*mek1-as*) was used, whose kinase activity can be conditionally inhibited by adding the inhibitor 1-NM-PP1 (4-amino-1-(tert-butyl)-3-(10-naphthylmethyl) pyrazolo [3,4-d]pyrimidine) which allows inter-sister repair in the absence of Dmc1.

5.3 Meiotic defects in *dmc1* are effectively suppressed by the addition of 1-NM-PP1 inhibitor to the *mek1-as* cells

It has been reported that Mek1 kinase activity is required for establishing a barrier to Dmc1 independent repair pathway (Niu et al., 2005). In other words, loss of Mek1 kinase activity could allow meiotic DSB repair in the absence of Dmc1, thereby promoting Rad51 mediated inter-sister repair. Here, repair at the *ARE1*-DSB hot spot was examined with or without the addition of 1-NM-PP1 in the *mek1-as dmc1Δ* cells (hereafter *mek1-as dmc1Δ −I, mek1-as dmc1Δ +I*, respectively). All *mek1-as* strains were tested under the premise that Mek1 function is unaffected

by the presence or the absence of the inhibitor (Wan et al., 2004). Mek1 still retained its kinase function to inhibit Dmc1 independent repair pathway in the absence of the inhibitor (Fig 5.2 A purple curve), as meiotic DSBs accumulated over the period of meiotic time course, displaying *dmc1Δ* mutant defect in meiotic DSB repair phenotype as expected. In contrast, DSB levels in the *mek1-as dmc1Δ +I* strain were substantially reduced, implying that DSBs were significantly more rapidly repaired (Figure 5.2 A brown curve). DAPI staining also revealed that sporulation was retarded in *mek1-as dmc1Δ –I*, as only 5% of the cells went through MI and MII (Figure 5.2 B purple curve and Figure 5.2 C). This defect in meiotic progression was significantly suppressed by the loss of Mek1 activity (Figure 5.2 B brown curve and Figure 5.1 C). In consistence with published data, our results confirmed that Mek1 activity is a key role that causes meiotic arrest in the absence of Dmc1 (Niu et al., 2005).

5.4 Confirmation that Mek1 function dominates over Hed1 in regulating Dmc1-independent repair pathway

Hed1 is also known to participate in creating BSCR by directly inhibiting Rad51 during strand invasion, ensuring that inter-homologue bias is properly established. Previous studies have shown that loss of Mek1 or Hed1 function in *dmc1* cells allows meiotic DSBs to be repaired via inter-sister recombination, implying that activation of Rad51 activity leads to efficient meiotic DSB repair in the absence of Dmc1 (Tsubouchi and Roeder, 2006). Therefore, to ask whether Mek1 and Hed1 could act synergistically to inhibit Rad51-mediated repair in the absence of Dmc1, we again examined meiotic DSB dynamics at *ARE1* hot spot in *mek1-as dmc1Δ hed1Δ* with or without the addition of the inhibitor (hereafter *mek1-as dmc1Δ hed1Δ +I* or *mek1-as dmc1Δ hed1Δ –I*, respectively). Without the
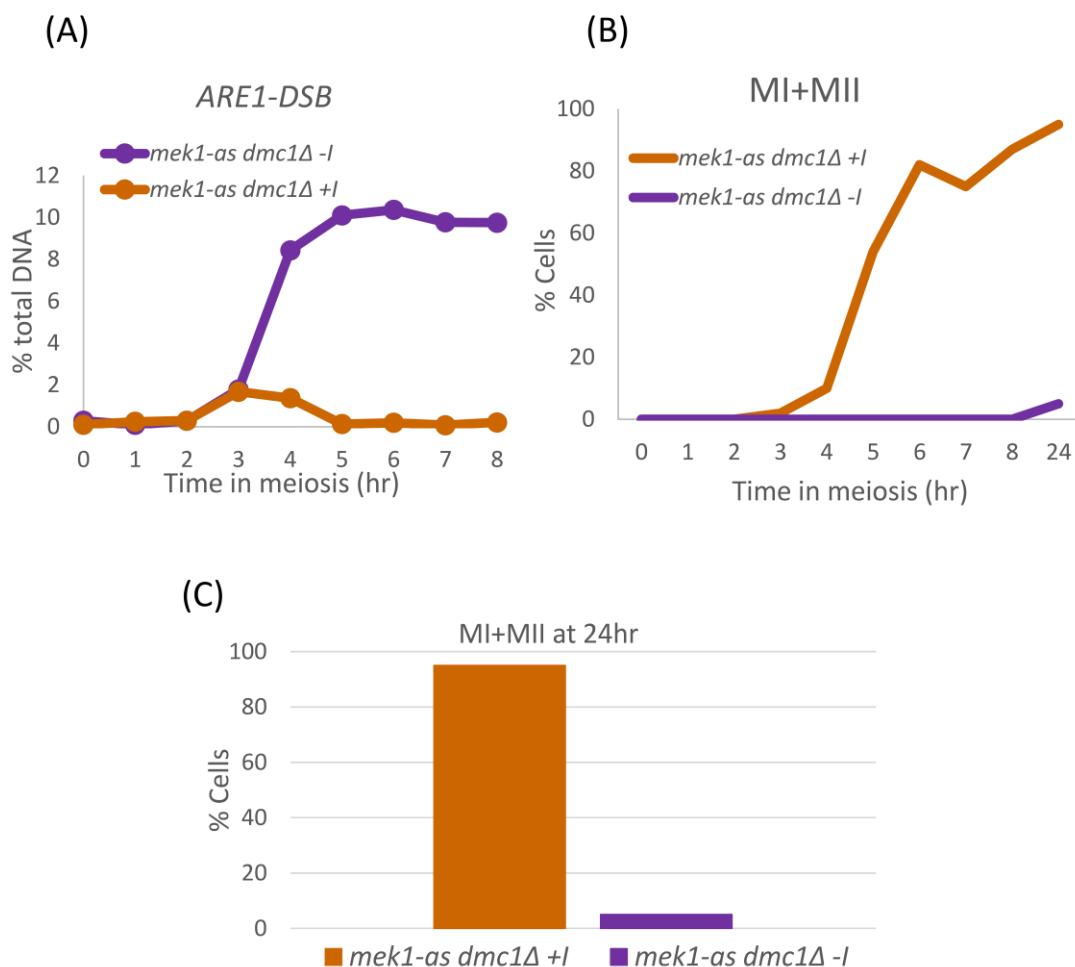
Figure 5.2. Loss of Mek1 activity effectively rescues dmc1 defects in DSB repair and meiotic progression

(A) Quantification of meiotic DSB from synchronous time courses of the mek1-as dmc1Δ strain. I: 1-NM-PP1 inhibitor. The inhibitor was added when meiotic time course began. Without the presence of 1-NM-PP1 inhibitor, mek1-as dmc1Δ accumulated meiotic DSB the same way as dmc1Δ (purple curve, also see figure 3.8), whereas Mek1 activity is fully inactivated by the addition of the inhibitor, effectively rescuing dmc1Δ in DSB repair as most of the DSB was rapidly and efficiently repaired (brown curve). (B) Meiotic progression in the mek1-as dmc1Δ strain with and without the presence of the inhibitor. The addition of the inhibitor significantly suppressed dmc1Δ defect in sporulation (brown curve compared with purple curve). (C) Sporulation frequencies of the mek1-as dmc1Δ strain at 24 hour of meiosis are indicated in the bar chart. Frequencies were scored by summing up DAPI bodies with two, three and four nuclei in 100 cells.
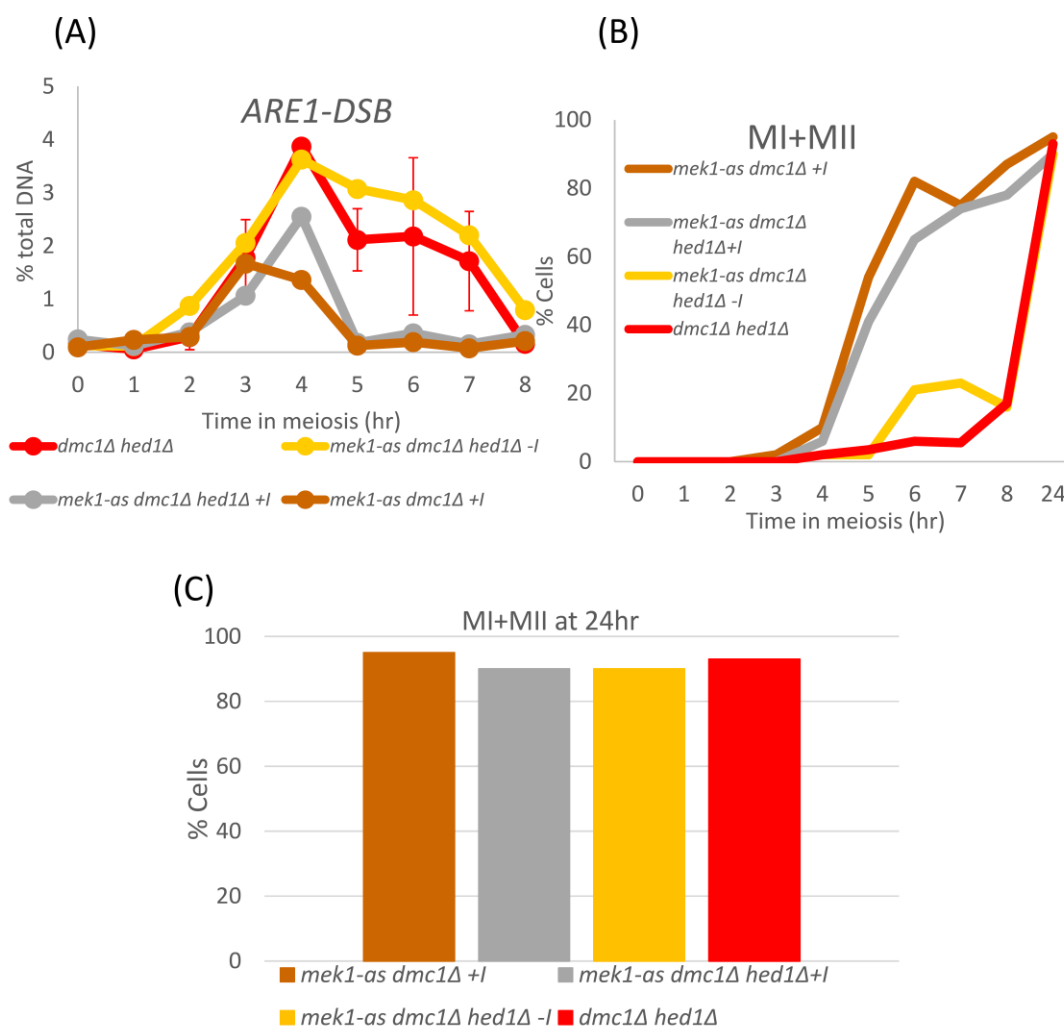
Figure 5.3. Mek1 function dominates over Hed1 in meiotic DSB repair and meiotic progression

(A) Quantitative analysis of meiotic DSB from *mek1-as* strains and *dmc1Δ hed1Δ*.   Mutant strains with or without *HED1* in the absence of Mek1 activity (grey: *mek1-as dmc1Δ hed1Δ* +I, brown: *mek1-as dmc1Δ* +I, I: 1-NM-PP1 inhibitor) result in more rapid DSB turnover than the others (yellow: *mek1-as dmc1Δ hed1Δ* –I, red: *dmc1Δ hed1Δ*). Error bars indicate standard deviation. (B) Quantification of nuclear division during meioiss. Mutants with full Mek1 function (red and yellow curves) have a significant delay in meiotic progression both in MI and MII than those strains with limited Mek1 function (grey and brown curves). (C) Sporulation frequencies of the four mutants at 24hr of meiosis are indicated in the bar chart. Sporulation frequencies were scored by summing up DAPI bodies with two, three and four nuclei in 100 cells.

inhibitor's presence, DSB levels of *mek1-as dmc1Δ hed1Δ* were not significantly changed compared with the *dmc1Δ hed1Δ* strain, suggesting that the *mek1-as* allele has no effects on meiotic DSB kinetics (Figure 5.3 A, yellow and red curves). DSB levels were decreased by 35% at the peak (4h) in *mek1-as dmc1Δ hed1Δ +I* (Figure 5.3, grey curve) compared to the *dmc1Δ hed1Δ* (Figure 5.3 A, red curve) and *mek1-as dmc1Δ hed1Δ –I* cells (Figure 5.3 A, yellow curve). Moreover, most of the breaks were repaired by 6-hour of meiosis, whereas the majority of the breaks in both *dmc1Δ hed1Δ* and *mek1-as dmc1Δ hed1Δ –I* cells were not repaired until 8-hour of meiosis, indicating that meiotic DSBs were more efficiently repaired in the *mek1-as dmc1Δ hed1Δ +I* cells and the improved repair efficiency is due to the lack of Mek1 activity which facilitates Dmc1-independent repair pathway. However, to our surprise, DSB levels in *mek1-as dmc1Δ +I* cells (Figure 5.3 A, brown curve) resembled those in *mek1-as dmc1Δ hed1Δ +I* cells (Figure 5.3 A, grey curve), suggesting that Mek1 activity dominates over Hed1 activity in regulating Dmc1-indepedndent pathway. We also examined meiosis progression by DAPI staining to assess this suggestion. As shown in Figure 5.3 B and C, most of the *mek1-as dmc1Δ–I* cells arrested at MI and only 5% of the cells went through MI and MII. Despite the fact that over 90% of the *dmc1Δ hed1Δ* and *mek1-as dmc1Δ hed1Δ –I* cells executed MI (Figure 5.3 B red curve and yellow curve, respectively), a severe delay in meiotic progression was observed in these mutants compared to *mek1-as dmc1Δ hed1Δ +I* and *mek1-as dmc1Δ +I* cells (Figure 5.3 B grey curve and brown curve, respectively). Our data suggest that in the absence of *DMC1*, deletion of *HED1* relives some repair but Mek1 function is still a main barrier for DSB repair.

5.5 Srs2 is required for normal meiotic progression in the absence of Mek1

We measured the *ARE1*-DSB in *mek1-as dmc1Δ* and *mek1-as dmc1Δ srs2-101* in the presence of the inhibitor (hereafter *mek1-as dmc1Δ +I* and *mek1-as dmc1Δ srs2-101 +I*, respectively) to block out Mek1 activity during meiosis in order to see if *srs2-101* accelerates DSB repair by increasing sister recombination. As previously shown, meiotic DSBs were efficiently repaired in *mek1-as dmc1Δ +I* (Figure 5.4 A brown curve). The *mek1-as dmc1Δ srs2-101 +I* strain, on the other hand, showed nearly identical DSB pattern with *mek1-as dmc1Δ +I* from the beginning to 4h of meiosis, then with a delay in repair later on until 8h of meiosis (Figure 5.4 A purple curve). Despite the fact that the repair efficiency of *mek1-as dmc1Δ srs2-101 +I* was decreased from 4h, the final unrepaired DSB level at 8h (0.43%) was still two times higher than that of *mek1-as dmc1Δ +I* (0.21%), indicating that Mek1-independent repair could not effectively repair meiotic DSBs without Srs2 helicase activity. Furthermore, because the DSB assays for the two strains were assessed in the absence of Dmc1, where the sister chromatids became the more preferable repair template for homologous recombination, the possibility of *srs2-101/DMC1* accelerates DSB repair by increasing sister recombination becomes less likely. Interestingly, by examining meiotic progression, a reduction of 25% of cells underwent first and second meiotic divisions in *mek1-as dmc1Δ srs2-101 +I* (Figure 5.4 C purple curve) in comparison to *mek1-as dmc1Δ +I* (Figure 5.4 C brown curve) was observed, suggesting that *srs2-101* does have some impact on Mek1-independent pathway in meiotic progression. We also examined DSB repair kinetics in *mek1-as dmc1Δ hed1Δ +I* and *mek1-as dmc1Δ hed1Δ srs2-101 +I* in order to look deeper into whether the presence of Hed1 could influence the requirements of Srs2 for Mek1-independent pathway. The overall DSB profile of

the quadruple mutant has an hour delay in repair (Figure 5.4, green curve) compared with its triple mutant counterpart (Figure 5.4B, grey curve). This result indicates that Hed1 is not necessarily required for Mek1-independent DSB repair pathway and again shows that loss of Mek1 activity dominates in rescuing Dmc1-independent repair over Hed1. DAPI bodies of *mek1-as dmc1Δ hed1Δ srs2-101 +I* with two to four nuclei were reduced by 29% at 24h of meiosis (Figure 5.4 C, green curve, and Figure 5.4 D, green bar) compared to *mek1-as dmc1Δ hed1Δ +I* (Figure 5.4 C, grey curve, and Figure 5.4 D, grey bar). These data are consistent with the DAPI staining for *mek1-as dmc1Δ srs2-101 +I* and *mek1-as dmc1Δ+I* (Figure 5.3 D, orange and purple bars), in which the lack of Srs2 activity results in a significant decrease in completing MI and MII.
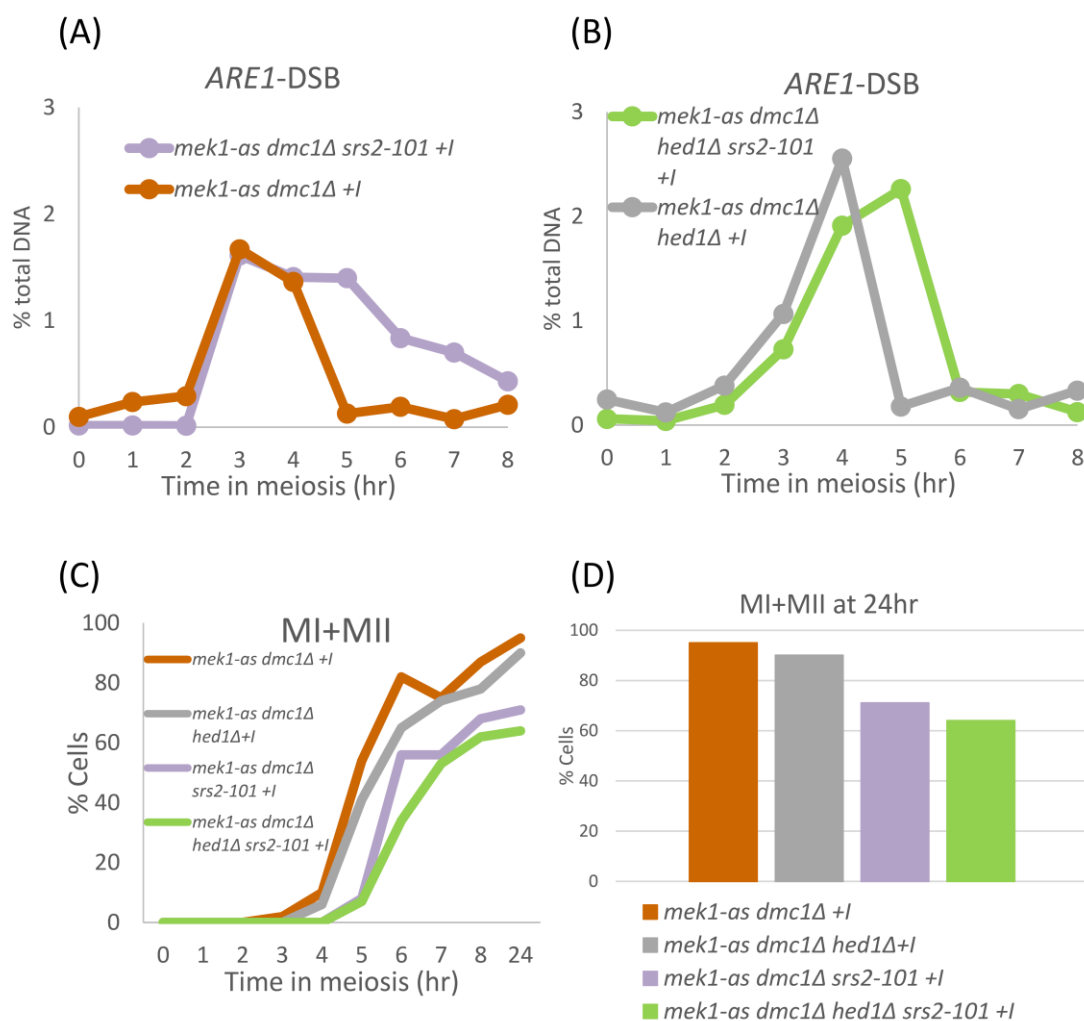
Figure 5.4. Srs2 is not required for Mek1-independent DSB repair pathway but needed for normal meiotic progression

(A) Quantitative analysis of meiotic DSB from *mek1-as dmc1Δ srs2-101 +I* and *mek1-as dmc1Δ +I* (purple: *mek1-as dmc1Δ srs2-101 +I*, brown: *mek1-as dmc1Δ +I*, I: 1-NM-PP1 inhibitor). (B) Quantitative analysis of meiotic DSB from *mek1-as dmc1Δ hed1Δ srs2-101 +I* and *mek1-as dmc1Δ hed1Δ +I* (green: *mek1-as dmc1Δ srs2-101 +I*, grey: *mek1-as dmc1Δ hed1Δ +I*). An hour delay in DSB turnover was observed in the quadruple mutant. (C) Meiotic progression of the four mutants are indicated. Percentage of cells that underwent MI and MII were scored by summing up DAPI bodies with two to four nuclei at the time point indicated. (D) Sporulation of each strain at 24h of meiosis is specifically indicated by the bar chart. Strains with *srs2-101* mutant allele show reduced level of meiotic progression at 24h than those *SRS2* strains.

5.6 Discussion

When examining JMs during meiosis we found that the overall JMs levels in *srs2-101 ndt80Δ* cells were generally lower than those in *SRS2 ndt80Δ* cells (Figure 5.1 E). Like Sgs1's role in limiting intersister and multi-chromatid JMs formation during wild-type meiosis (Jessop and Lichten, 2008), Srs2 seems to regulate and inhibit these abnormal recombination products to form. However in the absence of Sgs1, timing of DSB appearance and disappearance, DSB levels and timing of meiotic divisions did not differ substantially among wild-type (Jessop et al., 2006) where *srs2-101* strain has greater impact on these categories. In addition, the lack of Sgs1 activity results in increased total JM formation (Jessop and Lichten, 2008), but *srs2-101* strain oppositely reduces total JM levels (Figure 5.1 E). The reason for the increase of total JM maybe because recombination events requires orientation from Sgs1 activity since Sgs1 is responsible for directing JMs towards ZMM-dependent and NCO pathways, therefore the outcome of lacking Sgs1 activity would be accumulating more JMs than wild-type cells during recombination; whereas Srs2 could be acting cooperatively with Sgs1 where the precursor of JMs could be directed by Srs2 so that when *srs2-101* accumulates and forms complexes, this orientation may be lost, resulting in a barrier to form normal JMs or increasing the possibility to form unregulated mcJMs. Whether these JMs are properly resolved to form COs or NCOs requires further investigation.

Mutations on Mek1 remove BSCR, which allows DSB repair to occur more efficiently even without Dmc1. This suggests that *mek1* mutants repair DNA DSBs with increased level of IS recombination. In *srs2-101* mutant, meiotic DSB is more efficiently repaired and this could be also due to elevated recombination between

sister chromatids (Figure 3.2 D). A Mek1 mutant allele *mek1-as* which is sensitive to the inhibitor 1-NM-PP1, was used for analyses for DSB repair in various mutants in the absence of Dmc1 in order to specifically focus on intersister repair in these mutants. The *ARE1*-DSB analyses reveal that DSB repair profile is an hour delayed in *mek1-as dmc1Δ srs2-101 +I* compared with *mek1-as dmc1Δ +I* (Figure 5.4 A). Furthermore, Hed1 could influence the requirements of Srs2 for Mek1-independent pathway, we again assessed *ARE1*-DSB analyses for *mek1-as dmc1Δ hed1Δ +I* and *mek1-as dmc1Δ hed1Δ srs2-101 +I* strains, which again showed similar overall DSB profiles between each other (Figure 5.4 B). *srs2-101* may decrease meiosis efficiency by creating defective Rad51 nucleofilaments for recombination, because the *ARE1*-DSB repair is delayed in both *mek1-as dmc1Δ hed1Δ srs2-101 +I* and *mek1-as dmc1Δ srs2-101 +I*, in which DSB repair is mainly carried out by Rad51-mediated recombination (Figure 5.4 A and B). This idea is even strengthened by the observation of DAPI staining for nuclear division. *mek1-as dmc1Δ srs2-101 +I* and *mek1-as dmc1Δ hed1Δ srs2-101 +I* show 25% and 29% reduction in cells complete MI and MII at 24-hour in comparison to their non-*srs2-101* counterparts *mek1-as dmc1Δ +I* and *mek1-as dmc1Δ hed1Δ +I* (Figure 5.4 D).

Chapter 6

Cytological analysis of *Saccharomyces cerevisiae srs2* mutants during meiosis

Introduction

The *srs2-101* diploid mutant has been reported to have approximately a 10-fold increase in UV sensitivity compared to the wild-type strain (Rong et al. 1991). However, although the *srs2-101* homozygous diploids strains undergo normal commitment to meiotic recombination, this event was found to be delayed by several hours in the mutant strains and the strains appear to stall in the progression from meiosis I to meiosis II (Palladino and Klein 1992). The delay in meiotic progression was associated with a 4-fold increase in meiotic recombination rate and the level of sporulation was 75% of the isogenic wild type level and spore viability was reduced to 60% of the wild type. Moreover, only 16% of the tetrads dissected gave four viable spores, in comparison to 81 % for the isogenic wild type strain (Palladino and Klein 1992). Based on the DAPI analysis of sporulated strain, Palladino and Klein have previously analysed the meiotic progression in *srs2-101*. However more cytological and molecular analysis are needed to clarify and understand the reason of the delay of meiotic progression.

One of the functions of Srs2 is thought to be constraining HR at specific times and to particular cellular locations (Burgess et al., 2009). In this regard, Srs2 is suggested to use its anti-recombinase to disrupt Rad51 nucleofilaments during

recombination processes (Van Komen et al., 2003). It has been reported that the deletion of *SRS2*, as well as helicase defective *srs2-K41A* leads to recombination foci accumulation including increases Rad51 and Rad54 foci during mitosis (Burgess et al., 2009). However, how Srs2 influences Rad51 foci in meiosis is less well known compared to mitosis. Shinohara and colleagues have shown evidence that Srs2 specifically dismantles Rad51 nucleofilament in meiosis by the observations that over-expression of Srs2 leads to reduced levels of Rad51 foci but Dmc1 remain unaffected (Sasanuma et al., 2013). In other words, since Srs2 specifically regulates Rad51 filaments, it is expected that when Srs2 is absent or defective, Rad51 foci should persist longer than wild-type cells during meiosis.

Here we have used Zip1, a protein, which is localised to the central region of the SC, tagging with green fluorescent protein (GFP) to monitor if SC formation pattern was altered in *srs2-101* diploid mutants. We made the use of Zip1-GFP, tubulin tagged with GFP (TUB1-GFP) and spindle pole body (SPB) tagged with mCherry to further investigate SC formation and meiotic progression in *srs2-101* mutant during meiosis I and meiosis II. In addition, we used immunostaining approaches to address whether Rad51 foci persist in the *srs2* mutants during meiosis.

Results

6.1 Delay in the transition of meiosis I to meiosis II in *srs2* cells

Our DAPI data indicate that DAPI bodies with two nuclei of *srs2* mutants stay longer than wild-type cells even up to 24h of meiosis. The viability pattern of *srs2* mutants also shows that the amount of 1-2 viable spores in *srs2-101* mutant is much higher than that of wild-type (Figure 3.1 I). This might be due to inefficient

chromosome segregation from meiosis I to meiosis II, which causes a delay in triggering second meiotic division and spore lethality. To test this possibility, we made the use of tubulin tagged with GFP and SPB tagged with mCherry to monitor the dynamics of chromosome segregation from meiosis I to meiosis II. The red signal of SPB formation was scored as an indication of meiotic progression in both wild-type and *srs2-101* during meiosis (Figure 6.1). Cells with only one red dot were scored as "single cell", and cells with 2, 3 and 4 SPBs were scored MI 2SPB (MI stands for meiosis I), MII 3SPB (MII stands for meiosis II) and MII 4SPB, respectively. Finally, when meiosis was completed and four spores were formed, no SPB and tubulin signal was detected, the tetrad was then scored as 4 cells. Strikingly, the percentage of single cell and MI 2SPB of *srs2-101* cells after 8h in SPM are both twice as much as that of wild-type. This suggests there is a deficiency in the progression through meiosis II as signals for MI 2SPB, MII 3SPB and MII 4SPB in *srs2-101* cells are significantly reduced compared to wild-type.
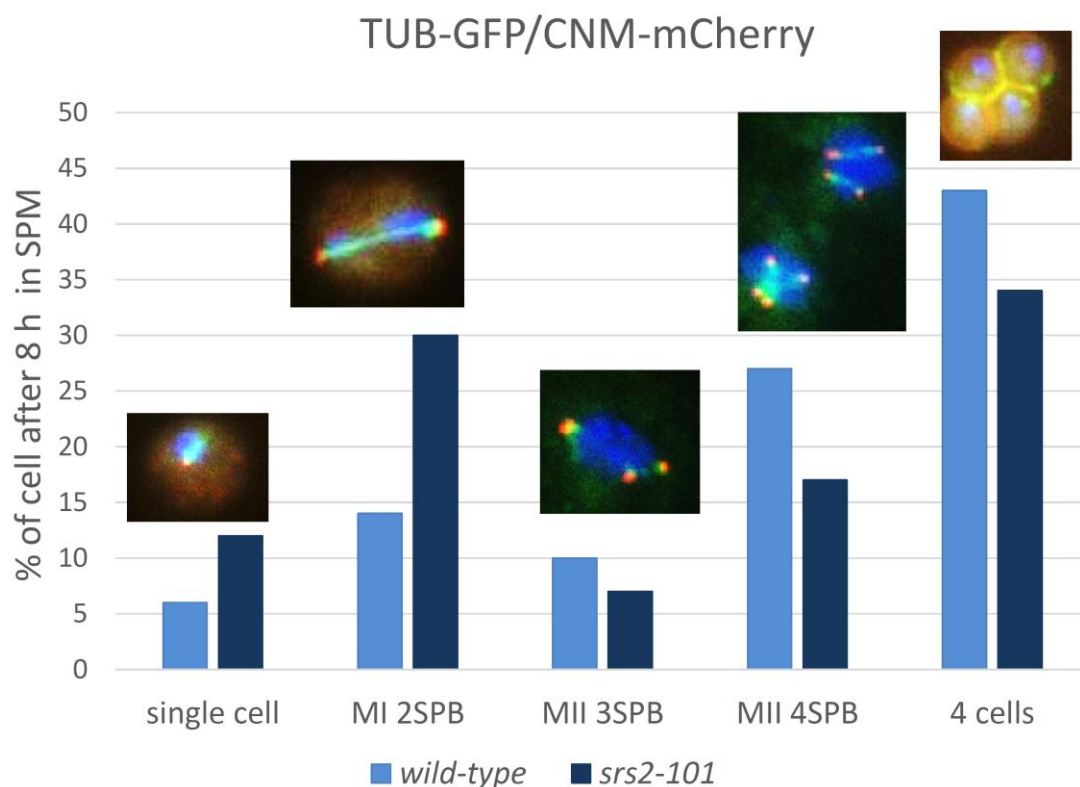
Figure 6.1. The progression from meiosis I to meiosis II is delayed in the *srs2-101* diploids

The meiotic progression for wild-type and *srs2-101* is determined by scoring mCherry tagged SPB during meiosis. Cells at different stages of meiosis are classified as single cell, MI 2SPB, MII 3SPB, MII 4SPB and 4 cells, respectively. Representative SPB signal of wild-type for each stage are shown above the bar charts. Two independent experiments for wild-type and *srs2-101* were used, only the average of each strain is shown.

6.2 Delay in progression of meiotic recombination in *srs2-101* mutant

As determined by DAPI staining and fluorescence microscopy, the kinetics of the meiotic nuclear divisions was delayed in *srs2-101*. Moreover, the sporulation and spore viability were reduced (Figure 3.1). Since genetic analyses were unable to fully explain these phenomena, we were then interested in examining the progression of these diploid strains through meiosis and during meiotic recombination using Zip1 tagged strains. In wild-type cells the SC started to appear approximately at 3h after meiosis was induced (data not shown); by 9h most of the SC had disappeared with ~95% of no SC signal cells (Figure 6.2A). However in *srs2-101* cells, cells remain higher levels of class I, II and III SC especially at later time points of meiosis (Figure 6.2B, C and D). The observation that fewer *srs2-101* cells had no SC detected compared to wild-type cells may result from higher levels of SC unresolved, raising the possibility that the SC may be persisted in *srs2-101* cells.

6.3 Rad51 foci accumulate in the *srs2-101* mutant and persist at pachytene

The recruitment of recombination factors can be visualised cytologically as proteins involved in recombination and checkpoint localise to discrete foci at DSB sites (Lisby et al., 2001). It has previously been reported that *srs2* strains including null and helicase defective mutants cause recombination foci accumulation including increased Rad51 and Rad54 foci during mitosis (Burgess et al., 2009). We then wanted to address whether mutation of *SRS2* in meiosis was also linked to accumulation of Rad51 foci that lead to formation of non-functional Rad51 filaments and caused further meiotic defects. We performed immunofluorescence

staining to visualise Rad51 foci in both wild-type and *srs2-101* mutant during meiosis. From 5h of meiosis we started to count Rad51 foci because the majority of DNA starts to be cleaved by Spo11, where the break ends can be bound by Rad51. In wild-type cells there is a significant decrease in Rad51 foci from 7h (7.8 foci per cell) to 9h (1.2 foci per cell) of meiosis (Figure 6.3C light blue bars), whereas the Rad51 foci of *srs2-101* cells remained high at this stage (4.5 foci per cell, Figure 6.3A dark blue bars). This indicates that *srs2-101* cells have difficulties to remove Rad51 timely. We also found that the persistence of Rad51 foci seemed to be highly correlated with a delay in SC dissolution in meiosis I as these foci were observed and persisted in *srs2-101* cells that remained at zygotene or pachytene stage after 9h of meiosis (Zip1-GFP signal in Figure 6.3 A). However, only a few Rad51 foci were observed as most of the wild-type cells exited pachytene stage by 9h in SPM (Figure 6.3 B, wild-type 9h).
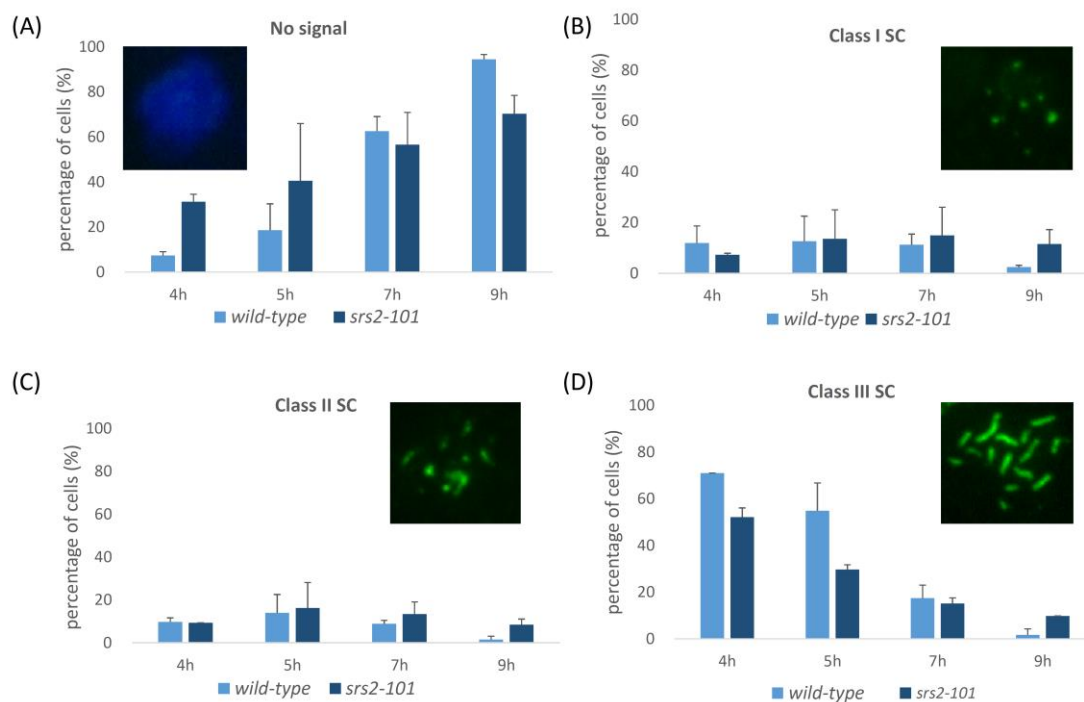
Figure 6.2. SC dissolution is delayed in *srs2-101* cells relative to the wild-type.
Panel A-D indicate discrete SC status (no signal, Class I, Class II and Class III, respectively) scored by GFP tagging of Zip1 in wild-type and *srs2-101* mutant. Representative SC images of wild-type are shown in each panel.
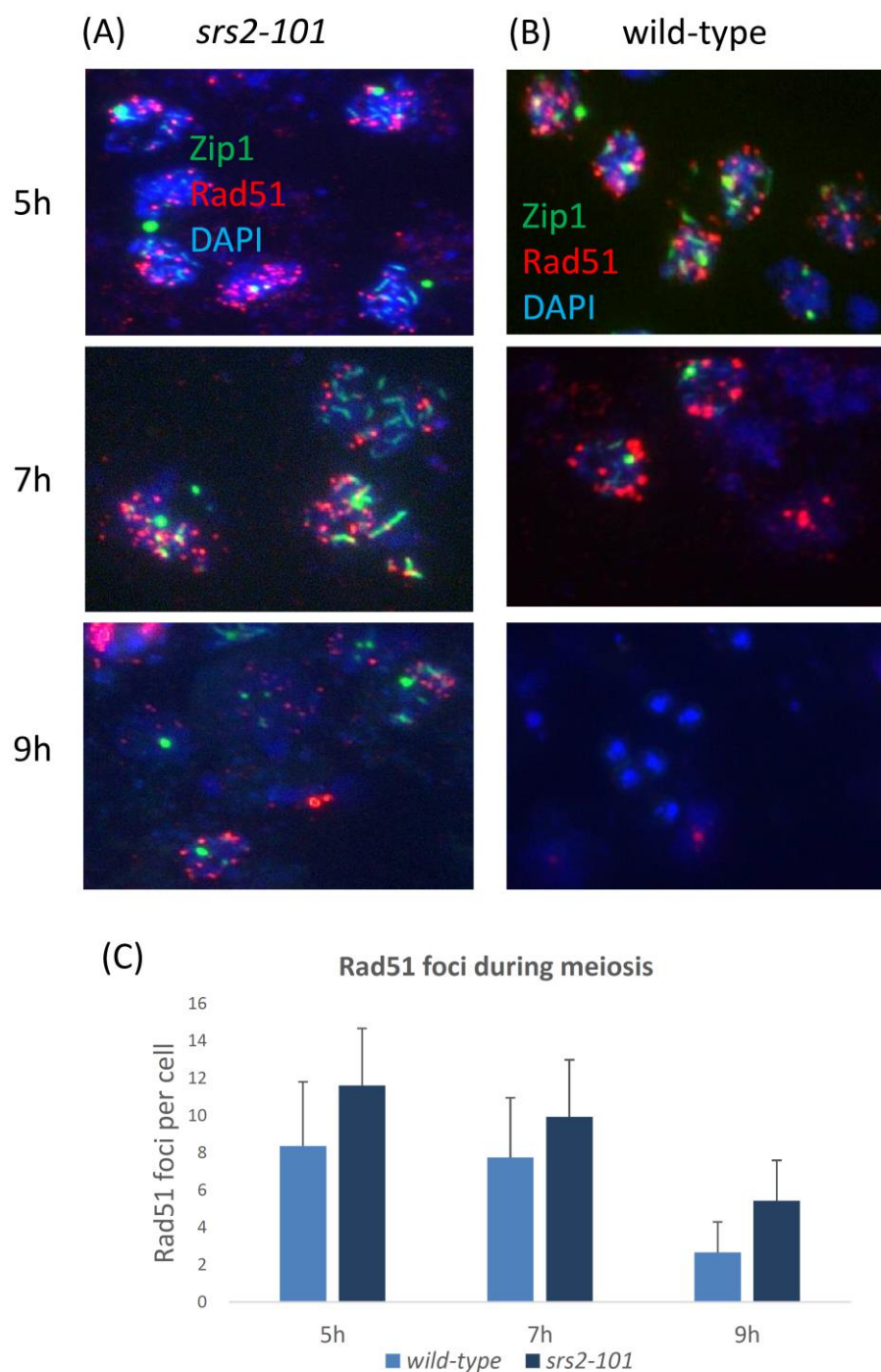
Figure 6.3. Rad51 foci accumulate at pachytene stage in *srs2-101* cells

Rad51 foci are visualised using immunofluorescence staining against Rad51 in both *srs2-101* mutant (A) and wild-type (B). Specific time points examined for Rad51 foci are indicated above the photos. The green signals indicate the SC component Zip1, Rad51 signals are shown in red and blue signals are DAPI staining bodies. Rad51 foci as well as Zip1 signal still exist at 9h of meiosis in *srs2-101* cells (A), where most of the Rad51 and Zip1 signals have disappeared (B). (C) Quantification of Rad51 foci in wild-type (light blue bars) and *srs2-101* cells (dark blue bars). Error bars indicate standard deviation.
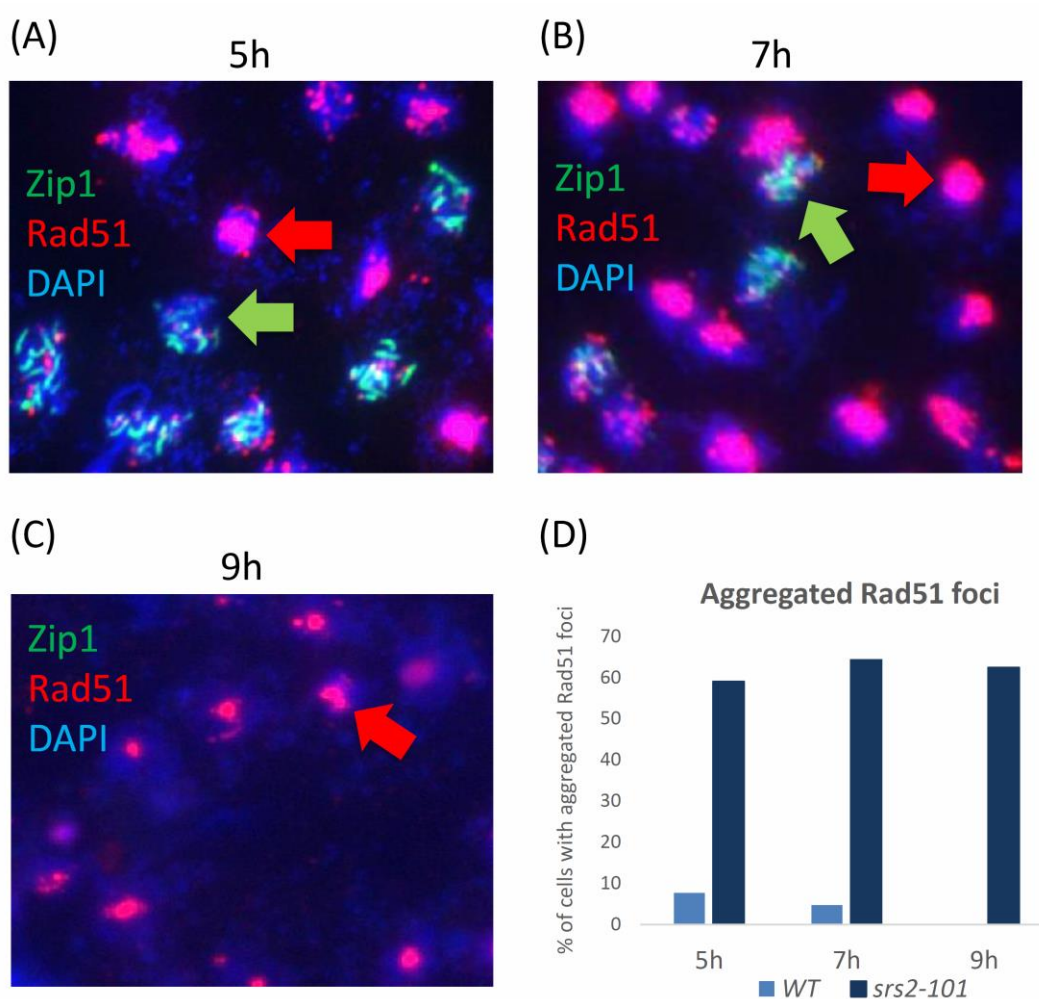
Figure 6.4. Rad51 foci are aggregated in a large amount of *srs2-101* cells with full SC dissolution

The red arrow indicates aggregated Rad51 foci in *srs2-101* cells, and cells with full length SC and persisted Rad51 foci are pointed by the green arrow. At 3h of meiosis the big aggregate of Rad51 foci have not appeared (A), but the aggregates start to appear by 5h of meiosis (B), and the cell population with Rad51 aggregates increases later on (C). (D)Quantitative data for Rada51 aggregation in wild-type and *srs2-101* cells.

6.4 A fraction of *srs2-101* cells have Rad51 foci aggregation with SC dissolution

In the previous test we found that ~15% of *srs2-101* cells have full length SC with Rad51 foci persisted at 9h after meiosis has been initiated (Figure 6.3 C), where wild-type has very little amount of population that still remained at the same stage. Here, we studied the correlation between SC formation/dissolution and Rad51 foci appearance/disappearance in wild-type and *srs2-101* cells using immunostaining techniques. In wild-type cells, 70% of the whole population had formed full length SC by 4h of meiosis, and by 9h most SC had disappeared (Figure 6.2 D). Rad51 foci in wild-type cells was first detected at 5h of meiosis in our test, and most of Rad51 foci as well as SC in wild-type cells started to disappear by 7h of meiosis. In *srs2-101* cells there were a fraction of cells had similar SC formation pattern but with a delay in disappearance of SC (Figure 6.2). However, 60% of *srs2-101* cells aggregated Rad51 foci with no SC signals by 5h of meiosis (Figure 6.4 D). On the other hand, SCs were fully formed with scattered Rad51 foci in the rest of *srs2-101* cell population (Figure 6.4 B, green arrow). This phenomenon is even more obvious in late meiosis (Figure6.4 C), where most of the aggregated Rad51 foci remained in a large fraction of cells without SC signals.

6.5 Discussion

Several biochemical studies have confirmed that Srs2 possesses anti-recombinase activity that dislodges Rad51 from ssDNA both *in vitro* and *in vivo* (Burgess et al., 2009; Colavito et al., 2009; Van Komen et al., 2003). In this study, the lack of Srs2 activity *srs2-101* allele, as well as *srs2* null mutants demonstrate that meiotic progression is delayed, which consequently leads to spore lethality (Figure 3.1). Since genetic analyses could not fully address the delay in meiotic progression, we

then intended to cytologically monitor it by several approaches, including GFP tagged Zip1 for SC formation/dissolution, mCherry tagged SPB for meiotic division and Rad51 immunostaining for monitoring how Srs2 affects Rad51 foci during meiosis.

After 9h in SPM, about one-third of *srs2-101* cells remain at zygotene stage (class I and II SC), whereas only 3.9% for wild-type cells at the same stage (Figure 6.2 B and C). Moreover, these mutants also show much higher percentages of class III SC than wild-type (Figure 6.2 D). These results indicate that most of the wild-type cells have gone through meiosis I properly but a significant delay occurred in the SC dissolution in the *srs2-101* mutant. These results do not necessarily address the possibility that whether the delay in SC dissolution is due to an inefficiency of chromosome segregation in *srs2-101* mutant during meiosis. Also, by DAPI staining and viability pattern test (see Figure 3.1) we wondered if the delay was caused by inefficient chromosome segregation from meiosis I to meiosis II. Therefore we made the use of mCherry tagged SPB to effectively monitor the dynamics of chromosome segregation. As shown in Figure 6.1, 30% of *srs2-101* cells remain at MI 2SPB after 8h in SPM, whereas only 14% of wild-type cells are at the same stage, demonstrating a two-fold higher amount of the *srs2-101* mutant cells that are stalled at meiosis I than wild-type. This delay might further influence meiosis II as less mCherry signal for MII 3SPB, MII 4SPB and 4 cells in the mutant is detected in the *srs2-101* diploid cells than wild-type. These results suggest that the delay in meiotic progression in *srs2-101* strain is due to an inefficiency of progression from meiosis I to meiosis II.

We then looked deeper into Rad51 foci localisation in both wild-type and *srs2-101* cells during meiosis to better understand what would be the cause of *srs2-101* induced meiotic defects including the delay in SC dissolution and inefficiency of progression from meiosis I to meiosis II. Our findings show that there is a fraction of *srs2-101* cells that have Rad51 aggregates with full SC dissolution (Figure 6.4, red arrow). These cells could possibly process SC dissolution more rapidly than cells with persisted Rad51 foci and full length SC (Figure 6.4, green arrow).

It has been reported that overexpression of Srs2 during meiosis reduces Rad51-containing foci to a level that's significantly lower than a non-overexpression strain (Sasanuma et al., 2013). Our data show higher levels of Rad51 foci in *srs2-101* mutant during late meiosis, suggesting that this result is in congruence with the idea that Srs2 specifically removes Rad51 foci during meiosis and the dismantling function of Srs2 lies in its helicase activity (Sasanuma et al., 2013). Interestingly, overexpression of Srs2 during meiosis also causes a delay in meiosis I, defective SC formation and inviable spore formation as seen in *srs2-101* strains. Despite the fact that Srs2 overexpression reduces Rad51 foci, it also delays the turnover of these foci as they could still be detected during late meiosis. This is also been observed in our *srs2-101* strains (Figure 6.3, *srs2-101* 9h). As suggested by Sasanuma et al. that meiotic overexpression of Srs2 results in dosage-dependent toxicity, it is possible that *srs2-101* mutant allele could also lead to formation of complexes that eventually results in a similar phenotype. Therefore, efficient meiotic progression indeed requires a specific quantity and quality of Srs2.

Chapter 7

General discussion

7.1 Srs2 is required for normal meiotic progression

Meiosis is a specialised cell division in which one diploid parent cell divides producing four haploid daughter cells, and this process requires recombination between homologous chromosomes that is initiated by DNA–double–strand breaks (DSBs) mediated by the Spo11 protein. During the breakage of DNA, helicases are potentially important for unwinding duplex DNA so that the broken DNA molecules can be repaired by the recombination machinery. The DNA helicase Srs2 is our main target helicase to be investigated in this study because it has been shown that it is required for normal meiotic progression and, more importantly, spore viability (Palladino and Klein, 1992).

We took the advantage of using a helicase/translocase defective mutant allele *srs2-101* because it is known that the loss of this activity causes several mitotic as well as meiosis defects. This suggests that Srs2's helicase/translocase does play a role in both mitosis and meiosis. In addition, we also made the use of *srs2Δ* mutant in order to see if the non-functional *srs2-101* allele caused different outcomes compared to the delete mutant.

We analysed meiotic progression by counting DAPI bodies and testing spore viability for both *srs2* mutants. As shown in Figure 3.1, both *srs2-101* and *srs2Δ*

show delayed meiotic progression and reduced spore viability. Despite these two mutants share these trait of meiotic defects, there is some differences between them. When analysing the spore viability pattern for the two mutants, *srs2-101* cells seem to have two viable spores (see Figure 3.1 G and I), whereas *srs2Δ* cells have more 3 or 4 viable spores as well as 0 viable (see Figure 3.1 H and I). This could imply that *srs2-101* may be accumulating to block any other repair pathways which *srs2Δ* cells do not. This hypothesis could be backed up by the suggestion that overexpresses Srs2 during meiosis results in dosage-dependent toxicity (Sasanuma et al., 2013), where *srs2-101* mutant allele could also lead to accumulation of complexes that eventually results in a similar phenotype.

Meiotic DSB analyses also reveal differences between the two *srs2* mutants. In a previous study (Lydia Hulme, 2008 ,unpublished data) as well as in this study, *srs2-101* cells generally show faster DSB turn-over rate than *srs2Δ* cells and wild-type cells (Figure 3.2), this leads us towards the thoughts of increased inter-sister chromatid repair in *srs2-101* cells.

7.2 Inter-sister repair is not necessarily increased by *srs2-101*

There are two recombinases involved in homologous recombination pathway, which are Rad51 and Dmc1. Rad51 expresses and functions in both mitosis and meiosis, and the Rad51-mediated repair pathway is biased towards sister chromatids; whereas Dmc1 only expresses in meiosis and is thought to direct strand invasion towards homologous chromosomes. If Srs2 is required for removing Rad51 from DSB sites, the absence of Srs2 may consequently lead repair towards Rad51-mediated inter-sister repair rather than inter-homologue repair

during meiosis. We have used several approaches in order to determine whether

this hypothesis is true.

In *hed1Δ* mutant, meiotic DSB levels are reduced compared to wild-type cells

(Tsubouchi and Roeder, 2006 and this study), and this is also thought to be that

DSBs are directed towards IS repair during meiosis. Because Hed1 effectively

blocks Rad51-mediated repair which resembles what Srs2 does, we carried out an

epistasis analysis to determine whether the rapid repair of *srs2-101* could be due

to an increase in Rad51 activity as seen in *hed1Δ* cells and if Hed1 and Srs2 are in

the same pathways in regulating Rad51 during meiosis. From our epistasis

analysis, we conclude that Srs2 is epistatic to Hed1, and the phenotypes of DSB-

turnover and spore viability Srs2 and Hed1 are separable because mutation or

deletion of Srs2 does not significantly alter DSB turnover rate in the absence of

Hed1, but these mutants show a huge reduction in spore viability compared to

hed1Δ and wild-type and are very similar to *srs2* single mutants (Figure 4.2). Lao

et al. suggest that the repair template choice in *hed1Δ* is slightly altered to inter-

sister chromatids. This subtle change could be due to the presence of Dmc1 which

inhibits Rad51-mediated strand invasion towards IS recombination, therefore

when both Dmc1 and Hed1 are absent the IH/IS ratio is dramatically decreased

(Lao et al., 2013). This might explain the restrained DSB turnover in *hed1 srs2*

mutants because Dmc1 is still inhibiting Rad51-mediated IS repair (Figure 4.2).

Therefore, in theory, this inhibition of IS repair could be eliminated once Dmc1 is

absent in *srs2* or *hed1* mutant backgrounds. It has been reported that defects in

meiotic DSB repair and spore viability are effectively rescued in *dmc1Δ hed1Δ*

double mutant (Tsubouchi and Roeder, 2003, 2006, this study, see Figure 4.3 C

and Table 3.1), suggesting that in the absence of Dmc1 the inhibition to IS repair

is dismissed. However the mutant allele *srs2-101* seems to exacerbate the DSB repair defect in *dmc1Δ* background (Figure 4.4) which implies that there is a potential repair pathway that is dependent on or cooperative with fully functional Srs2. Furthermore, when analysing meiotic DSB frequency in *dmc1Δ hed1Δ srs2-101* we found there is a delay in repair, but this delay in repair is not so obviously seen in *dmc1Δ hed1Δ srs2Δ* (Figure 4.5), again implying that *srs2-101* cells could form toxic complexes that block Dmc1-independent repair. All of these experiments were to use *hed1Δ* or *dmc1Δ* as a model to reflect if *srs2-101* could influence the preference of template choice. Clearly these results could not fully address why *srs2-101* cells repair meiotic DSB more rapidly and yet whether these cells prefer using intersister chromatids as repair templates.

We made the use of a recombination assay system (Allers and Lichten, 2001, Figure 5.1), a more straightforward method for detecting recombination intermediates between intersister chromatids and interhomologue chromosomes. In addition, in order to monitor the recombination intermediates more clearly, JM levels were measured in *ndt80Δ* background where JMs could not be resolved but accumulated after meiosis had been initiated. Unregulated recombination intermediates such as multi-chromatid JMs (mcJMs) could also be detected using this method. In *srs2-101 ndt80Δ* cells there is a 30% decrease in total JM levels but a 60% increase in mcJM fractions compared to SRS2 *ndt80Δ* cells (Figure 5.1). This suggests that neither IS JM levels nor IH JM levels are significantly increased in *srs2-101 ndt80Δ* cells, and a big fraction of the recombination intermediates become unregulated mcJMs. To be able to better understand the mechanisms of recombination intermediates orientation, we take another helicase Sgs1 for an example of mediating recombination intermediates to compare with Srs2. Sgs1 is

thought to be responsible for directing most of JMs towards ZMM-dependent and a small proportion of NCO pathways (Jessop et al., 2006), therefore once Sgs1 activity is lost, resolution of these recombination intermediates is then stalled and thus causes accumulation of JMs (Jessop and Lichten, 2008) as well as mcJMs (De Muyt et al., 2012). However, according to our results, *srs2-101* allele seems to raise the turnover of the intermediates towards mcJMs (Figure 5.1 D). This implies that Sgs1 and Srs2 work cooperatively to regulate normal JM formation which ensures proper ratio of CO/NCO during recombination (Figure 7.1). This suggestion could be consistent with a previous finding that in the absence of both Sgs1 and Srs2 leads to cell lethality, indicating that *sgs1Δ srs2Δ* mutants may create excessive toxic recombination intermediates normally dismantled by Srs2 or Sgs1 (Gangloff et al., 2000; Ira et al., 2003). Based on our results, the idea of *srs2-101* increases IS recombination becomes less likely.

Mutation of Mek1 is another example of increased level of IS recombination, however, we found an hour delay in repair (Figure 5.4 A) and a 20% reduction in finishing meiosis I and II (Figure 5.4 C and D) when Srs2 helicase activity is lost, suggesting that *mek1* mutants do require Srs2 to maintain its normal meiotic progression. This may imply that when barrier to sister chromatids is lost (e.g. *mek1* mutants), Srs2 may be required to direct recombination intermediates towards CO products.
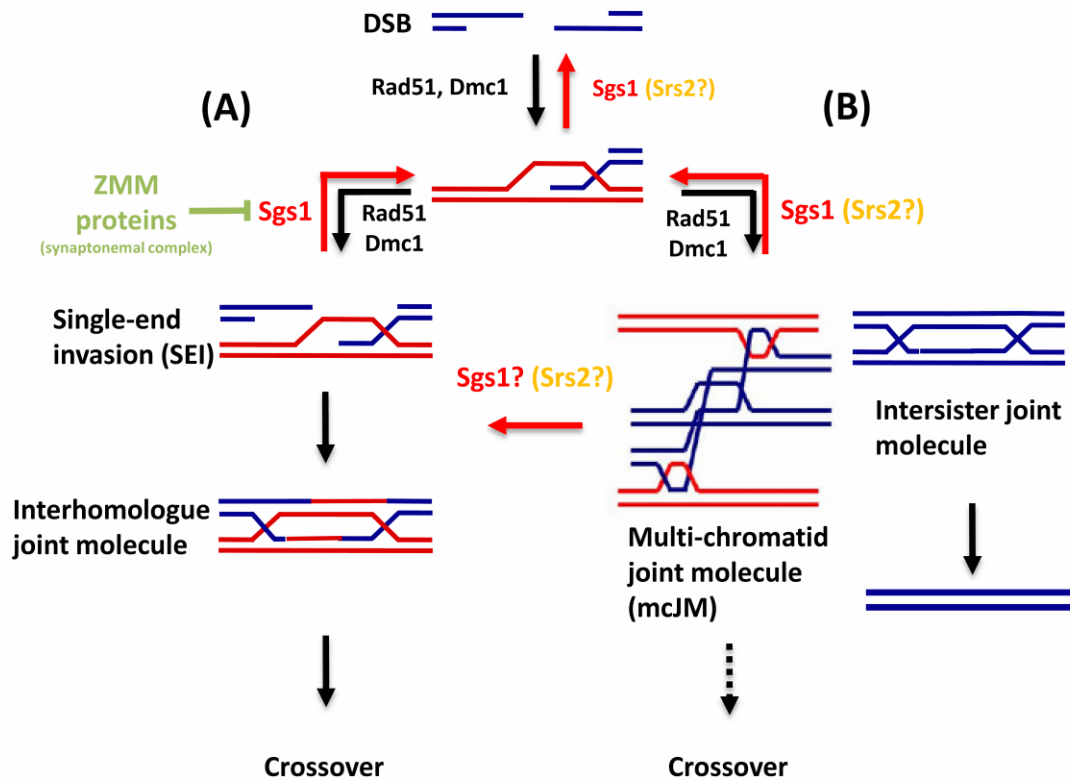
Figure 7.1. Model of regulation of interhomologue recombination by Sgs1-Srs2

Sgs1 (and presumably Srs2) disassociates strand invasion activity mediated by Rad51/Dmc1 in order to regulate an appropriate timing for recombination to occur. (A) Synaptonemal complex-associated proteins (ZMMs) protect strand invasion intermediate disassociation from Sgs1 which coordinate it towards crossover products (Jessop and Lichten, 2008). However, strand invasion activity may escape from the protection by ZMMs (B), which leads to the formation of either unregulated joint molecules (mcJMs) or intersister joint molecules. Sgs1 or Srs2 could provide second opportunity to disassemble mcJMs to form COs or return mcJMs to the recombination precusors. This figure is adopted from Jessop and Lichten, 2008.

7.3 *srs2-101* specifically delays the meiotic progression from MI to MII

Several evidence has indicated that both *srs2-101* negatively influence meiosis, including delaying meiotic progression (Figure 3.1 E), raising spore lethality (Figure 3.1 I). These phenotypes could be due to failure to segregate chromosomes during meiosis. By cytological approaches, we managed to monitor SC formation and dissolution. In *S. cerevisiae* the formation and dissolution of SC is an important indication of meiotic progression as several recombination events are tightly correlated to the SC, including single-end invasion, formation of double-Holliday Junction and crossover formation (Figure 1.2). Therefore investigating the SC formation and dissolution would help better understand meiotic progression in *S. cerevisiae*. Our cytological work reveals that a proportion of *srs2-101* cells have greater levels of all classes of SC and lower levels of no SC signal at late meiosis compared with wild-type (Figure 6.2), suggesting that these cells cause delay in formation and dissolution of SC during meiosis. Interestingly, our direct monitoring of chromosome segregation by visualising spindle-pole body (SPB) and tubulin show that *srs2-101* cells have greater impact on the transition from MI to MII as a big population of *srs2-101* cells were found at MI with 2-SPB (Figure 6.1). *srs2-101* cells with delayed SC formation/dissolution may eventually undergo MI to MII and successfully generate four spores, however, a fraction of cells form huge Rad51 foci with very little SC formation at early stage of meiosis(Figure 6.4). These cells may process meiotic progression more rapidly than wild-type cells because a faster turnover of SC dissolution was observed.

7.4 The quantity of Rad51 recombinase activity is vital for meiosis

Interestingly, when testing if *srs2-101* phenotype is dependent on Rad51 recombinase activity using recombinase-defective *rad51-II3A* (Cloud et al, 2012), we also found two types of cells when undergoing meiosis (data not shown). A fraction of cells undergo meiosis at extremely fast frequency and form wild-type level viable spores, whereas the other fraction of the cells fail to sporulate and remain diploids. It is possible that the cells with faster meiotic progression could resemble those Rad51-aggregated cells, and the other population of the cells could be like the cells with delayed SC formation/dissolution. However we previously hypothesise that faster recombination may lead to cell death, which is apparently not the case in *rad51-II3A srs2-101* cells with faster sporulation. Cloud et al. suggest that Dmc1 requires Rad51 as an accessary protein to help it process strand exchange and is Rad51 recombinase activity independent (Cloud et al, 2012). This raises the possibility that in *rad51-II3A srs2-101* cells even though Rad51 may accumulate due to lack of Srs2 activity and Rad51 strand exchange activity is lost, Dmc1 is still helped by Rad51 binding activity, carrying out processing of normal meiosis. However in Rad51 *srs2-101* there is too much Rad51 recombinase activity, which may destroy the Rad51/Dmc1 balance for repair template choice. Therefore controlling of Rad51 recombinase activity plays a vital role in regulating normal meiosis.

7.5 Conclusions and future work

In this study, we have found a few phenomena which have not been fully addressed, these are: 1. *srs2-101* mutant cells process meiotic DSBs more rapidly than wild-type cells, but resemble those observed in *hed1Δ* cells, 2. Rad51 foci persisted throughout meiosis and aggregated in *srs2-101* mutant cells and 3. A fraction of *srs2-101* cells undergo SC dissolution more quickly than wild-type cells with normal Rad51 disassociation during meiosis. By the recombination assay system we found that IS recombination is not increased in *srs2-101* cells as we previously hypothesised. Therefore the increased meiotic DSB repair of *srs2-101* mutant is concluded to have no correlation with increasing IS recombination. However, the reasons for formation of two types of *srs2-101* cells during the observation of SC formation/dissolution and Rad51 foci remain elusive because it requires strong evidence of whether faster kinetics of SC/Rad51 aggregation dissolution leads to meiotic defects and normal kinetics of SC dissolution/delayed Rad51 foci disappearance contributes to normal meiosis. Thus our future work will be based on these findings, using live-cell imaging system to carefully observe the correlation between SC formation/dissolution and Rad51 foci formation/disappearance (or aggregation) throughout meiosis. Meanwhile, further investigation for CO/NCO ratio using recombination assay cassettes and/or 2-D electrophoresis to identify DNA intermediates during meiotic recombination is also required so that the role of Srs2 during meiosis could be more clearly addressed.

References

Agarwal, S., and Roeder, G.S. (2000). Zip3 provides a link between recombination enzymes and synaptonemal complex proteins. Cell *102*, 245–255.

Alani, E., Padmore, R., and Kleckner, N. (1990). Analysis of wild-type and rad50 mutants of yeast suggests an intimate relationship between meiotic chromosome synapsis and recombination. Cell *61*, 419–436.

Allers, T., and Lichten, M. (2001). Differential timing and control of noncrossover and crossover recombination during meiosis. Cell *106*, 47–57.

Bae SH, Choi E, Lee KH, Park JS, Lee SH, Seo YS. (1998). Dna2 of *Saccharomyces cerevisiae* possesses a single-stranded DNA-specific endonuclease activity that is able to act on double-stranded DNA in the presence of ATP. J Biol Chem. 41, 26880-90.

Bailis, J.M., and Roeder, G.S. (1998). Synaptonemal complex morphogenesis and sister-chromatid cohesion require Mek1-dependent phosphorylation of a meiotic chromosomal protein. Genes Dev. 12, 3551–3563.

Bernstein, K., Gangloff, S., and Rothstein, R. (2010). The RecQ DNA helicases in DNA repair. Annu. Rev. Genet. 393–417.

Bernstein, K. a, Reid, R.J.D., Sunjevaric, I., Demuth, K., Burgess, R.C., and Rothstein, R. (2011). The Shu complex, which contains Rad51 paralogues, promotes DNA repair through inhibition of the Srs2 anti-recombinase. Mol. Biol. Cell *22*, 1599–1607.

Bishop, D.K., and Zickler, D. (2004). Early Decision : Meiotic Crossover Interference prior to Stable Strand Exchange and Synapsis Review. *117*, 9–15.

Bishop, D.K., Nikolski, Y., Oshiro, J., Chon, J., Shinohara, M., and Chen, X. (1999). High copy number suppression of the meiotic arrest caused by a dmc1 mutation: REC114 imposes an early recombination block and RAD54 promotes a DMC1-independent DSB repair pathway. Genes Cells *4*, 425–444.

Börner, G.V., Kleckner, N., and Hunter, N. (2004). Crossover/noncrossover differentiation, synaptonemal complex formation, and regulatory surveillance at the leptotene/zygotene transition of meiosis. Cell *117*, 29–45.

Budd, M.E., and Campbell, J.L. (2009). Interplay of Mre11 nuclease with Dna2 plus Sgs1 in Rad51-dependent recombinational repair. PLoS One *4*, e4267.

Burgess, R.C., Lisby, M., Altmannova, V., Krejci, L., Sung, P., and Rothstein, R. (2009). Localization of recombination proteins and Srs2 reveals anti-recombinase function in vivo. J. Cell Biol. *185*, 969–981.

Busygina, V., Sehorn, M.G., Shi, I.Y., Tsubouchi, H., Roeder, G.S., and Sung, P. (2008). Hed1 regulates Rad51-mediated recombination via a novel mechanism. Genes Dev. *22*, 786–795.

Busygina, V., Saro, D., Williams, G., Leung, W., Say, A.F., Sehorn, M.G., Sung, P., Tsubouchi, H., Haven, N., Berkeley, L., et al. (2012). Novel Attributes of Hed1 Affect Dynamics and Activity of the Rad51 Presynaptic Filament during Meiotic Recombination. J. Biol. Chem. *287*, 1566–1575.

Cao, L., Alani, E., and Kleckner, N. (1990). A pathway for generation and processing of double-strand breaks during meiotic recombination in *S. cerevisiae*. Cell *61*, 1089–1101.

Chanet, R., Heude, M., Adjiri, a, Maloisel, L., and Fabre, F. (1996). Semidominant mutations in the yeast Rad51 protein and their relationships with the Srs2 helicase. Mol. Cell. Biol. *16*, 4782–4789.

Chen, Q., Pearlman, R.E., and Moens, P.B. (1992). Isolation and characterization of a cDNA encoding a synaptonemal complex protein. Biochem. Cell Biol. *70*, 1030–1038.

Chiolo, I., Carotenuto, W., Maffioletti, G., Petrini, J.H.J., Foiani, M., and Liberi, G. (2005). Srs2 and Sgs1 DNA Helicases Associate with Mre11 in Different Subcomplexes following Checkpoint Activation and CDK1 mediated Srs2 phosphorylation. American Society for Microbiology *25*, 5738–5751.

Chiolo, I., Saponaro, M., Baryshnikova, A., Kim, J.-H., Seo, Y.-S., and Liberi, G. (2007). The human F-Box DNA helicase FBH1 faces *Saccharomyces cerevisiae* Srs2 and postreplication repair pathway roles. Mol. Cell. Biol. *27*, 7439–7450.

Chua, P.R., and Roeder, G.S. (1998). Zip2, a meiosis-specific protein required for the initiation of chromosome synapsis. Cell *93*, 349–359.

Colavito, S., Macris-Kiss, M., Seong, C., Gleeson, O., Greene, E.C., Klein, H.L., Krejci, L., and Sung, P. (2009). Functional significance of the Rad51-Srs2 complex in Rad51 presynaptic filament disruption. Nucleic Acids Res. *37*, 6754–6764.

De Muyt, A., Jessop, L., Kolar, E., Sourirajan, A., Chen, J., Dayani, Y., and Lichten, M. (2012). BLM Helicase Ortholog Sgs1 Is a Central Regulator of Meiotic Recombination Intermediate Metabolism. Mol. Cell *46*, 43–53.

Dernburg, a F., McDonald, K., Moulder, G., Barstead, R., Dresser, M., and Villeneuve, a M. (1998). Meiotic recombination in C. elegans initiates by a conserved mechanism and is dispensable for homologous chromosome synapsis. Cell *94*, 387–398.

Dobson, M.J., Pearlman, R.E., Karaiskakis, a, Spyropoulos, B., and Moens, P.B. (1994). Synaptonemal complex proteins: occurrence, epitope mapping and chromosome disjunction. J. Cell Sci. *107* 2749–2760.

Dupaigne, P., Le Breton, C., Fabre, F., Gangloff, S., Le Cam, E., and Veaute, X. (2008). The Srs2 helicase activity is stimulated by Rad51 filaments on dsDNA: implications for crossover incidence during mitotic recombination. Mol. Cell *29*, 243–254.

Fiorentini, P., Huang, K.N., Tishkoff, D.X., Kolodner, R.D., and Symington, L.S. (1997). Exonuclease I of *Saccharomyces cerevisiae* functions in mitotic recombination in vivo and in vitro. Mol Cell 1997 May; 17(5):2764-73

Fung, J.C., Rockmill, B., Odell, M., and Roeder, G.S. (2004). Imposition of crossover interference through the nonrandom distribution of synapsis initiation complexes. Cell *116*, 795–802.

Gangloff, S., Soustelle, C., and Fabre, F. (2000). Homologous recombination is responsible for cell death in the absence of the Sgs1 and Srs2 helicases. Nat. Genet. *25*, 192–194.

Gasior, S.L., Wong, a. K., Kora, Y., Shinohara, a., and Bishop, D.K. (1998). Rad52 associates with RPA and functions with Rad55 and Rad57 to assemble meiotic recombination complexes. Genes Dev. *12*, 2208–2221.

Gasior, S.L., Olivares, H., Ear, U., Hari, D.M., Weichselbaum, R., and Bishop, D.K. (2001). Assembly of RecA-like recombinases: distinct roles for mediator proteins in mitosis and meiosis. Proc. Natl. Acad. Sci. U. S. A. *98*, 8411–8418.

Gerton, J.L., Derisi, J., Shroff, R., Lichten, M., Brown, P.O., and Petes, T.D. (2000). Global mapping of meiotic recombination hotspots and coldspots in the yeast *Saccharomyces cerevisiae*. Proc. Natl. Acad. Sci. U. S. A. 97, 11383–11390

Goldfarb, T., and Lichten, M. (2010). Frequent and efficient use of the sister chromatid for DNA double-strand break repair during budding yeast meiosis. PLoS Biol. *8*, e1000520.

Hassold, T., and Hunt, P. (2001). To err (meiotically) is human: the genesis of human aneuploidy. Nat. Rev. Genet. *2*, 280–291.

Heyer, W.-D., Li, X., Rolfsmeier, M., and Zhang, X.-P. (2006). Rad54: the Swiss Army knife of homologous recombination Nucleic Acids Res. *34*, 4115–4125.

Hollingsworth, N.M. (2010). Phosphorylation and the creation of interhomolog bias during meiosis in yeast. Cell Cycle *9*, 436–437.

Hollingsworth, N.M., and Byers, B. (1989). HOP1: a yeast meiotic pairing gene. Genetics *121*, 445–462.

Hollingsworth, N.M., and Ponte, L. (1997). Genetic interactions between HOP1, RED1 and MEK1 suggest that MEK1 regulates assembly of axial element components during meiosis in the yeast *Saccharomyces cerevisiae*. Genetics. 1997 Sep;147(1):33-42.

Hollingsworth, N.M., Ponte, L., and Halsey, C. (1995). MSH5, a novel MutS homolog, facilitates meiotic reciprocal recombination between homologs in *Saccharomyces cerevisiae* but not mismatch repair. Genes Dev. *9*, 1728–1739.

Hong, S., Sung, Y., Yu, M., Lee, M., Kleckner, N., and Kim, K.P. (2013). The logic and mechanism of homologous recombination partner choice. Mol. Cell *51*, 440–453.

Hunter, N., and Kleckner, N. (2001). The single-end invasion: an asymmetric intermediate at the double-strand break to double-holliday junction transition of meiotic recombination. Cell *106*, 59–70.

Ira, G., Malkova, A., Liberi, G., Foiani, M., and Haber, J.E. (2003). Srs2 and Sgs1-Top3 suppress crossovers during double-strand break repair in yeast. Cell *115*, 401–411.

Jessop, L., and Lichten, M. (2008). Mus81/Mms4 endonuclease and Sgs1 helicase collaborate to ensure proper recombination intermediate metabolism during meiosis. Mol. Cell *31*, 313–323.

Jessop, L., Rockmill, B., Roeder, G.S., and Lichten, M. (2006). Meiotic chromosome synapsis-promoting proteins antagonize the anti-crossover activity of sgs1. PLoS Genet. *2*, e155.

Johnson, R.D., and Symington, L.S. (1995). Functional differences and interactions among the putative RecA homologs Rad51, Rad55, and Rad57. Mol. Cell. Biol. *15*, 4843–4850.

Keeney, S., Giroux, C.N., and Kleckner, N. (1997). Meiosis-specific DNA double-strand breaks are catalyzed by Spo11, a member of a widely conserved protein family. Cell *88*, 375–384.

Klein, H.L. (2001). Mutations in recombinational repair and in checkpoint control genes suppress the lethal combination of srs2Delta with other DNA repair genes in *Saccharomyces cerevisiae*. Genetics *157*, 557–565.

Koehler; K.E.; C.L Boulton; H. E.Collins; R. L. French; K.C. Herman; S. M. Lacefield; L. D. Madden; C. D. Shuetz and R. S. (1996). Spontaneous X chromosome MI and MII nondisjunction events in Drosophila melanogaster oocytes have different recombination histories. Nat. Genet. *14*, 406–414.

Van Komen, S., Reddy, M.S., Krejci, L., Klein, H., and Sung, P. (2003). ATPase and DNA helicase activities of the *Saccharomyces cerevisiae* anti-recombinase Srs2. J. Biol. Chem. *278*, 44331–44337.

Krejci, L., Macris, M., Li, Y., Van Komen, S., Villemain, J., Ellenberger, T., Klein, H., and Sung, P. (2004). Role of ATP hydrolysis in the antirecombinase function of *Saccharomyces cerevisiae* Srs2 protein. J. Biol. Chem. *279*, 23193–23199.

Krogh, B.O., and Symington, L.S. (2004). Recombination proteins in yeast. Annu. Rev. Genet. *38*, 233–271.

Lao, J.P., Cloud, V., Huang, C.-C., Grubb, J., Thacker, D., Lee, C.-Y., Dresser, M.E., Hunter, N., and Bishop, D.K. (2013). Meiotic crossover control by concerted action of Rad51-Dmc1 in homolog template bias and robust homeostatic regulation. PLoS Genet. *9*, e1003978.

Lee, S.E., Bressan, D. a, Petrini, J.H.J., and Haber, J.E. (2002). Complementation between N-terminal *Saccharomyces cerevisiae* mre11 alleles in DNA repair and telomere length maintenance. DNA Repair (Amst). *1*, 27–40.

Lengsfeld, B.M., Rattray, A.J., Bhaskara, V., Ghirlando, R., and Paull, T.T. (2007). Sae2 is an endonuclease that processes hairpin DNA cooperatively with the Mre11/Rad50/Xrs2 complex. Mol. Cell *28*, 638–651.

Leu, J.Y., Chua, P.R., and Roeder, G.S. (1998). The meiosis-specific Hop2 protein of *S. cerevisiae* ensures synapsis between homologous chromosomes. Cell *94*, 375–386.

Lisby, M., Rothstein, R., and Mortensen, U.H. (2001). Rad52 forms DNA repair and recombination centers during S phase. Proc. Natl. Acad. Sci. U. S. A. *98*, 8276–8282.

Liu, J., Renault, L., Veaute, X., Fabre, F., Stahlberg, H., and Heyer, W.-D. (2011). Rad51 paralogues Rad55–Rad57 balance the antirecombinase Srs2 in Rad51 filament formation. Nature 479(7372):245-8.

Loidl, J., Klein, F., and Scherthan, H. (1994). Homologous pairing is reduced but not abolished in asynaptic mutants of yeast. J. Cell Biol. *125*, 1191–1200.

Longhese, M.P., Bonetti, D., Guerini, I., Manfrini, N., and Clerici, M. (2009). DNA double-strand breaks in meiosis: checking their formation, processing and repair. DNA Repair (Amst). *8*, 1127–1138.

Lui, D.Y., Peoples-Holst, T.L., Mell, J.C., Wu, H.-Y., Dean, E.W., and Burgess, S.M. (2006). Analysis of close stable homolog juxtaposition during meiosis in mutants of *Saccharomyces cerevisiae*. Genetics *173*, 1207–1222.

Lynn, A., Soucek, R., and Börner, G.V. (2007). ZMM proteins during meiosis: crossover artists at work. Chromosome Res. *15*, 591–605.

Mankouri, H.W., and Hickson, I.D. (2007). The RecQ helicase-topoisomerase III-Rmi1 complex: a DNA structure-specific "dissolvasome"? Trends Biochem. Sci. *32*, 538–546.

Marini, V., and Krejci, L. (2010). Srs2: the "Odd-Job Man" in DNA repair. DNA Repair (Amst). *9*, 268–275.

Mary Sym and G. S. Roeder (1995). Zip1-induced Changes in Synaptonemal Complex Structure and polycomplex Assembly. J Cell Biol. *128*, 455–466.

Mazin, A. V, Alexeev, A. a, and Kowalczykowski, S.C. (2003). A novel function of Rad54 protein. Stabilization of the Rad51 nucleoprotein filament. J. Biol. Chem. *278*, 14029–14036.

McKim, K.S. (1998). Meiotic Synapsis in the Absence of Recombination. Science *279*, 876–878.

Milne, G.T., Ho, T., and Weaver, D.T. (1995). Modulation of *Saccaromyces cerevisiae* DNA double-strand repair by SRS2 and RAD51. Genetics. 139:1189-1199

Mimitou, E.P., and Symington, L.S. (2009a). Nucleases and helicases take center stage in homologous recombination. Trends Biochem. Sci. *34*, 264–272.

Mimitou, E.P., and Symington, L.S. (2009b). DNA end resection: many nucleases make light work. DNA Repair (Amst). *8*, 983–995.

Mimitou, E.P., and Symington, L.S. (2010). Ku prevents Exo1 and Sgs1-dependent resection of DNA ends in the absence of a functional MRX complex or Sae2. EMBO J. *29*, 3358–3369.

Miyazaki, T., Bressan, D. a, Shinohara, M., Haber, J.E., and Shinohara, A. (2004). In vivo assembly and disassembly of Rad51 and Rad52 complexes during double-strand break repair. EMBO J. *23*, 939–949.

Moreau, S., Morgan, E. a, and Symington, L.S. (2001). Overlapping functions of the *Saccharomyces cerevisiae* Mre11, Exo1 and Rad27 nucleases in DNA metabolism. Genetics *159*, 1423–1433.

Moses, M.J. (1968). The synaptinemal complex. Annu. Rev. Genet. *2*, 363–412.

Neale, M.J., and Keeney, S. (2006). Clarifying the mechanics of DNA strand exchange in meiotic recombination. Nature *442*, 153–158.

Neale, M.J., Ramachandran, M., Trelles-Sticken, E., Scherthan, H., and Goldman, A.S.H. (2002). Wild-type levels of Spo11-induced DSBs are required for normal single-strand resection during meiosis. Mol. Cell *9*, 835–846.

Neale, M.J., Pan, J., and Keeney, S. (2005). Endonucleolytic processing of covalent protein-linked DNA double-strand breaks. Nature *436*, 1053–1057.

Niu, H., Wan, L., Baumgartner, B., Schaefer, D., Loidl, J., and Hollingsworth, N.M. (2005). Partner Choice during Meiosis Is Regulated by Hop1-promoted Dimerization of Mek1. Mol. Biol. Cell *16*, 5804–5818.

Niu, H., Li, X., Job, E., Park, C., Moazed, D., Gygi, S.P., and Hollingsworth, N.M. (2007). Mek1 kinase is regulated to suppress double-strand break repair between sister chromatids during budding yeast meiosis. Mol. Cell. Biol. *27*, 5456–5467.

Niu, H., Wan, L., Busygina, V., Kwon, Y., Allen, J. a, Li, X., Kunz, R.C., Kubota, K., Wang, B., Sung, P., et al. (2009). Regulation of meiotic recombination via Mek1-mediated Rad54 phosphorylation. Mol. Cell *36*, 393–404.

Padmore, R., Cao, L., and Kleckner, N. (1991). Temporal comparison of recombination and synaptonemal complex formation during meiosis in *S. cerevisiae*. Cell *66*, 1239–1256.

Palladino, F., and Klein, H.L. (1992). Analysis of Mitotic and Meiotic Defects in *Saccharomyces cerevisiae* Srs2 DNA Helicase Mutants. Genetics. 132(1): 23–37

Papouli, E., Chen, S., Davies, A. a, Huttner, D., Krejci, L., Sung, P., and Ulrich, H.D. (2005). Crosstalk between SUMO and ubiquitin on PCNA is mediated by recruitment of the helicase Srs2p. Mol. Cell *19*, 123–133.

Rockmill, B., and Roeder, G.S. (1990). Meiosis in asynaptic yeast. Genetics *126*, 563–574.

Rockmill, B., and Roeder, G.S. (1991). A meiosis-specific protein kinase homolog required for chromosome synapsis and recombination. Genes Dev. *5*, 2392–2404.

Rockmill, B., Fung, J.C., Branda, S.S., and Roeder, G.S. (2003). The Sgs1 Helicase Regulates Chromosome Synapsis and Meiotic Crossing Over. Curr. Biol. *13*, 1954–1962.

San Filippo, J., Sung, P., and Klein, H. (2008). Mechanism of eukaryotic homologous recombination. Annu. Rev. Biochem. *77*, 229–257.

Sasanuma, H., Furihata, Y., Shinohara, M., and Shinohara, A. (2013). Remodeling of the Rad51 DNA strand-exchange protein by the Srs2 helicase. Genetics *194*, 859–872.

Schiestl, R.H., Prakash, S., and Prakash, L. (1990). The *SRS2* suppressor of *rad6* mutations of *Saccharomyces cerevisiae* acts by channelling DNA lesions into the *RAD52* DNA repair pathway. Genetics, 124, 817–831.

Schmekel, K., and Daneholt, B. (1995). The central region of the synaptonemal complex revealed in three dimensions. Trends Cell Biol. *5*, 239–242.

Schwacha, a, and Kleckner, N. (1995). Identification of double Holliday junctions as intermediates in meiotic recombination. Cell *83*, 783–791.

Sears, D.D., Hegemann, J.H., and Hieter, P. (1992). Meiotic recombination and segregation of human-derived artificial chromosomes in *Saccharomyces cerevisiae*. Proc. Natl. Acad. Sci. U. S. A. *89*, 5296–5300.

Seong, C., Colavito, S., Kwon, Y., Sung, P., and Krejci, L. (2009). Regulation of Rad51 recombinase presynaptic filament assembly via interactions with the Rad52 mediator and the Srs2 anti-recombinase. J. Biol. Chem. *284*, 24363–24371.

Sheridan, S., and Bishop, D.K. (2006). Red1-Hed1 regulation: recombinase Rad51, though capable of playing the leading role, may be relegated to supporting Dmc1 in budding yeast meiosis. Genes Dev. *20*, 1685–1691.

Shinohara, a, Ogawa, H., and Ogawa, T. (1992). Rad51 protein involved in repair and recombination in S. *cerevisiae* is a RecA-like protein. Cell *69*, 457–470.

Shinohara, a, Gasior, S., Ogawa, T., Kleckner, N., and Bishop, D.K. (1997). Saccharomyces *cerevisiae* recA homologues RAD51 and DMC1 have both distinct and overlapping roles in meiotic recombination. Genes Cells *2*, 615–629.

Shinohara, M., Gasior, S.L., Bishop, D.K., and Shinohara, A. (2000). Tid1/Rdh54 promotes colocalization of Rad51 and Dmc1 during meiotic recombination. Proc. Natl. Acad. Sci. U. S. A. 97, 10814-9.

Smith, a, and Benavente, R. (1992). Identification of a structural protein component of rat synaptonemal complexes. Exp. Cell Res. *198*, 291–297.

Smith, a V, and Roeder, G.S. (1997). The yeast Red1 protein localizes to the cores of meiotic chromosomes. J. Cell Biol. *136*, 957–967.

Solinger, J. a, Kiianitsa, K., and Heyer, W.-D. (2002). Rad54, a Swi2/Snf2-like recombinational repair protein, disassembles Rad51:dsDNA filaments. Mol. Cell *10*, 1175–1188.

Song, B., and Sung, P. (2000). Functional interactions among yeast Rad51 recombinase, Rad52 mediator, and replication protein A in DNA strand exchange. J. Biol. Chem. *275*, 15895–15904.

Storlazzi, A., Gargano, S., Ruprich-Robert, G., Falque, M., David, M., Kleckner, N., and Zickler, D. (2010). Recombination proteins mediate meiotic spatial chromosome organization and pairing. Cell *141*, 94–106.

Sugawara, N., Wang, X., and Haber, J.E. (2003). In vivo roles of Rad52, Rad54, and Rad55 proteins in Rad51-mediated recombination. Mol. Cell *12*, 209–219.

Sun, W., Lorenz, A., Osman, F., and Whitby, M.C. (2011). A failure of meiotic chromosome segregation in a *fbh1Δ* mutant correlates with persistent Rad51-DNA associations. Nucleic Acids Res. *39*, 1718–1731.

Sung, P. (1997). Yeast Rad55 and Rad57 proteins form a heterodimer that functions with replication protein A to promote DNA strand exchange by Rad51 recombinase. Genes Dev. *11*, 1111–1121.

Sung, P., and Klein, H. (2006). Mechanism of homologous recombination : mediators and helicases take on regulatory functions. *Nature Reviews Molecular Cell Biology* 7, 739-750

Sym M, Engebrecht JA, Roeder GS. ZIP1 is a synaptonemal complex protein required for meiotic chromosome synapsis. Cell. 1993 Feb 12;72(3):365–378.

Terentyev, Y., Johnson, R., Neale, M.J., Khisroon, M., Bishop-Bailey, A., and Goldman, A.S.H. (2010). Evidence that MEK1 positively promotes interhomologue double-strand break repair. Nucleic Acids Res. *38*, 4349–4360.

Tran, P.T., Erdeniz, N., Symington, L.S., and Liskay, R.M. (2004). EXO1-A multi-tasking eukaryotic nuclease. DNA Repair (Amst). *3*, 1549–1559.

Tsubouchi, H., and Roeder, G.S. (2002). The Mnd1 Protein Forms a Complex with Hop2 To Promote Homologous Chromosome Pairing and Meiotic Double-Strand Break Repair. Mol. Cell. Biol. vol. 22 no. 9. 3078-3088

Tsubouchi, H., and Roeder, G.S. (2003). The importance of genetic recombination for fidelity of chromosome pairing in meiosis. Dev. Cell *5*, 915–925.

Tsubouchi, H., and Roeder, G.S. (2004). The budding yeast Mei5 and Sae3 proteins act together with dmc1 during meiotic recombination. Genetics *168*, 1219–1230.

Tsubouchi, H., and Roeder, G.S. (2006). Budding yeast Hed1 down-regulates the mitotic recombination machinery when meiotic recombination is impaired. Genes Dev. *20*, 1766–1775.

Veronica Cloud, Yuen-Ling Chan, Jennifer Grubb, Brian Budke, D.B. (2012). Rad51 Is an Accessory Factor for Dmc1-Mediated Joint Molecule Formation During Meiosis. Science. *337*, 1222–1224.

Wan, L., Santos, T.D.L., Zhang, C., Shokat, K., and Hollingsworth, N.M. (2004). Mek1 Kinase Activity Functions Downstream of RED1 in the Regulation of Meiotic Double Strand Break Repair in Budding Yeast. *15*, 11–23.

Xu, L., Weiner, B.M., and Kleckner, N. (1997). Meiotic cells monitor the status of the interhomolog recombination complex. Genes Dev. *11*, 106–118.

Zhu, Z., Chung, W.-H., Shim, E.Y., Lee, S.E., and Ira, G. (2008). Sgs1 helicase and two nucleases Dna2 and Exo1 resect DNA double-strand break ends. Cell *134*, 981–994.

Zickler, D., and Kleckner, N. (1999). Integrating Structure and Function. Annu Rev Genet *33*, 603–754.